AD-A189 576 THEORY OF LASER COOLING AND SPECTROSCOPY OF HARMONICALLY TRAPPED SINGLE ATOMS(U) AIR FORCE INST OF TECH WRIGHT-PATTERSON AFB OH SCHOOL OF ENGINEERING A L WELLS DEC 87 AFIT/DS/PH/87-5 1/2

UNCLASSIFIED F/G 7/4 NL

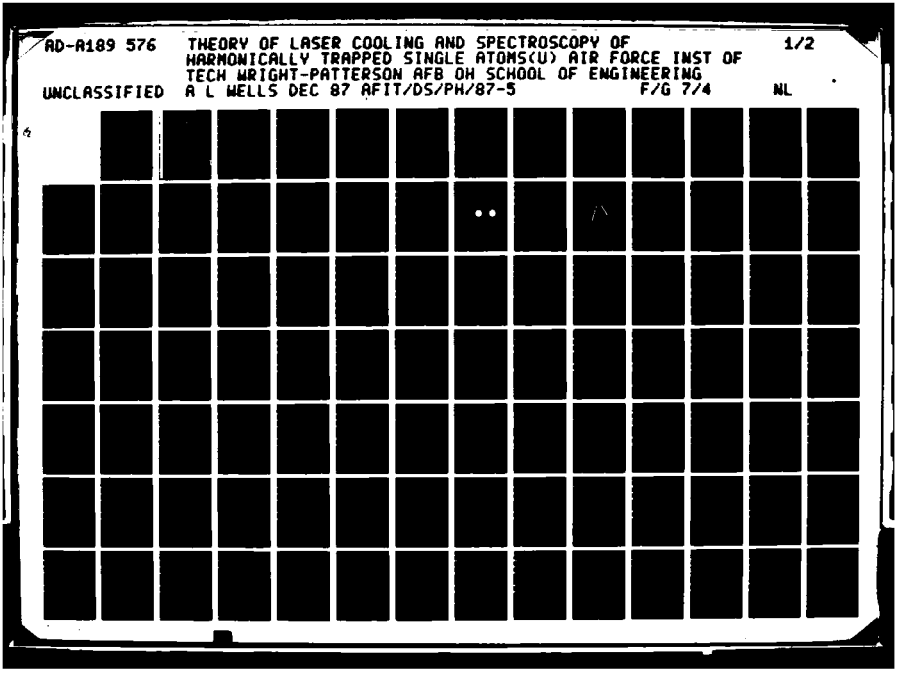

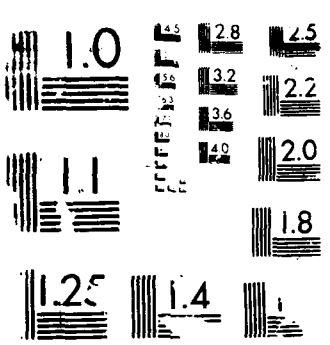
1.0
1.1
1.25
1.4
2.8
3.2
3.6
4.0
2.5
2.2
2.0
1.8

DTIC FILE COPY

AD-A189 576

THEORY OF LASER COOLING AND SPECTROSCOPY OF HARMONICALLY TRAPPED SINGLE ATOMS

DISSERTATION

DTIC
ELECTE
MAR 0 2 1988
S H

DEPARTMENT OF THE AIR FORCE
AIR UNIVERSITY
AIR FORCE INSTITUTE OF TECHNOLOGY

Wright-Patterson Air Force Base, Ohio

DISTRIBUTION STATEMENT A
Approved for public release;
Distribution Unlimited

88 3 1 193

AFIT/DS/PH/87-5

THEORY OF LASER COOLING AND SPECTROSCOPY OF HARMONICALLY TRAPPED SINGLE ATOMS

DISSERTATION

AFIT/DS/PH/87-5 Ann Laurie Wells
Capt USAF

Approved for public release; distribution unlimited

DTIC

AFIT/DS/PH/87-5

THEORY OF LASER COOLING AND SPECTROSCOPY OF HARMONICALLY TRAPPED SINGLE ATOMS

DISSERTATION

Presented to the Faculty of the School of Engineering

of the Air Force Institute of Technology

Air University

In Partial Fulfillment of the

Requirements for the Degree of

Doctor of Philosophy

Ann Laurie Wells, B.S., M.S.

Captain, USAF

December 1987

Approved for public release; distribution unlimited

AFIT/DS/PH/87-5

THEORY OF LASER COOLING AND SPECTROSCOPY OF HARMONICALLY TRAPPED SINGLE ATOMS

Ann Laurie Wells, B.S., M.S.

Captain, USAF

Approved:

Richard J. Cook, Maj USAF, Chairman — 27 NOV 87

Won B. Roh — 30 Nov 87

Dennis W. Quinn — 30 NOV 87

James A. Lupo, Maj USAF — 1 Dec 87

Accepted:

J. S. Przemieniecki — 1 Dec. 87

J. S. Przemieniecki
Dean, School of Engineering

Acknowledgements

The author wishes to thank her research advisor Maj Richard J. Cook for many enlightening conversations and constant encouragement. To my fellow DS students and their families, I offer my thanks for helping to put me back together when I fell apart. I also must thank my husband and children for making many sacrifices so that I could finish this work.

ANN LAURIE WELLS

DTIC
COPY
INSPECTED

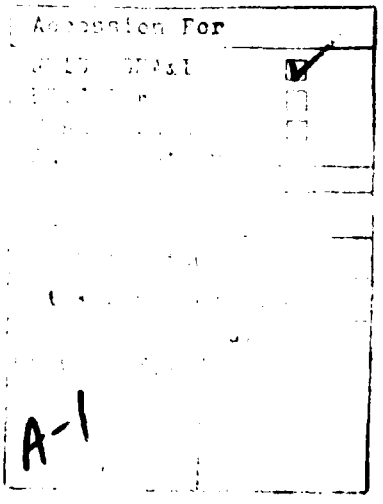

Table of Contents

List of Figures

Abstract

The problem of laser cooling of a single ion or atom in a harmonic trap was considered. A simple theory of sideband cooling has been developed. In the limit that the particle's secular motion can be treated semiclassically, the theory allows the calculation of a logarithmic cooling rate either numerically or, for two special cases, analytically. The theory could be used to optimize the parameters of a cooling experiment.

The spectroscopy of a single atom in the ladder configuration has been treated theoretically. A dressed atom approach was used to provide qualitative information about the system. The optical Bloch equations for the four level system in the rotating wave approximation were developed and solved for steady state. The Bloch equations were also solved in the adiabatic approximation and upward and downward transition rates were extracted from this treatment.

I. Introduction

A. Motivation

Breakthroughs in the trapping and cooling of ions have made it possible to perform spectroscopic experiments on a single ion trapped indefinitely in a volume with μm dimensions (31). Recent developments in the trapping and cooling of clouds of neutral atoms (26) indicate that confining a single neutral atom is feasible. Trapped, cooled atoms will possibly provide the ultimate laser frequency standard. Alone in the trap, the spectral lines of the atom will not be collisionally broadened and if restricted to a region smaller than $\lambda/4$, the Doppler effect will be suppressed (12). It is also possible, using the "atom amplifier" technique first proposed by Dehmelt (13), to use extremely weak transitions, accessing states with extremely long lifetimes and consequently narrow natural linewidths.

The theory of laser cooling in a harmonic trap has been developed by several researchers using different methods (10), (11), (18), (19), (20), (21), (29), (36), (38), (39), (40). Most of these theories are cumbersome and involved. A simple theory that displays the physical mechanisms of laser cooling and is numerically correct in regions of interest is desirable.

It is possible to observe effects in the spectroscopy of a single atom that are masked when the spectroscopic sample contains many atoms. One of the most interesting examples of this which has been observed is the phenomenon of "electron shelving" (3), (26), (33). In an electron shelving experiment (also known as an atom amplifier experiment), a single trapped atom is used to detect a single

quantum jump. A simple example of such an experiment uses the "V" configuation, shown in Figure 1. Two lasers are focused on the atom, one exciting a strong transition (Einstein coefficient $A \approx 10^8 s^{-1}$), and one exciting a weak transition (Einstein coefficient $A \approx 1 s^{-1}$). The transitions share a common lower level. Ordinarily the strong transition scatters about 10^8 photons per second, which can be observed with a photodetector. If, however, the atom makes the transition to the upper state of the weak transition (state 2), then the atom would stop scattering photons on the strong transition until the atom decayed back into the lower state (state 0). Thus single quantum jumps on a very weak transition can be observed. Other configurations of the atoms energy level structure have been considered theoretically. Some examples are the "Λ" configuration which is an inverted "V" (22), (32) and various three-level cascades (32).

One configuration which has not previously been considered, but which provides some interesting details is a four-level cascade in which two strong transitions are coupled by a weak transition. This ladder configuration is illustrated in Figure 2. One of the debates about the experiments involving three-level electron shelving schemes such as the "V" configuration has to do with quantum measurement theory. Currently accepted interpretations of quantum theory hold that quantum systems do not exist in any particular quantum state until a measurement projects them into some state. The question is whether a period of darkness, the absence of a fluorescence signal, constitutes a measurement which projects the atom into the metastable state, state 2 of Figure 1. For the ladder configuration there are no periods of darkness, instead the fluorescence alternates between wavelength ω_1 when the weak transition is not excited, and wavelength ω_3 when the weak transition is excited. A change in the wavelength of the fluorescence, which is a positive signal, as opposed to the absence of a signal for three-

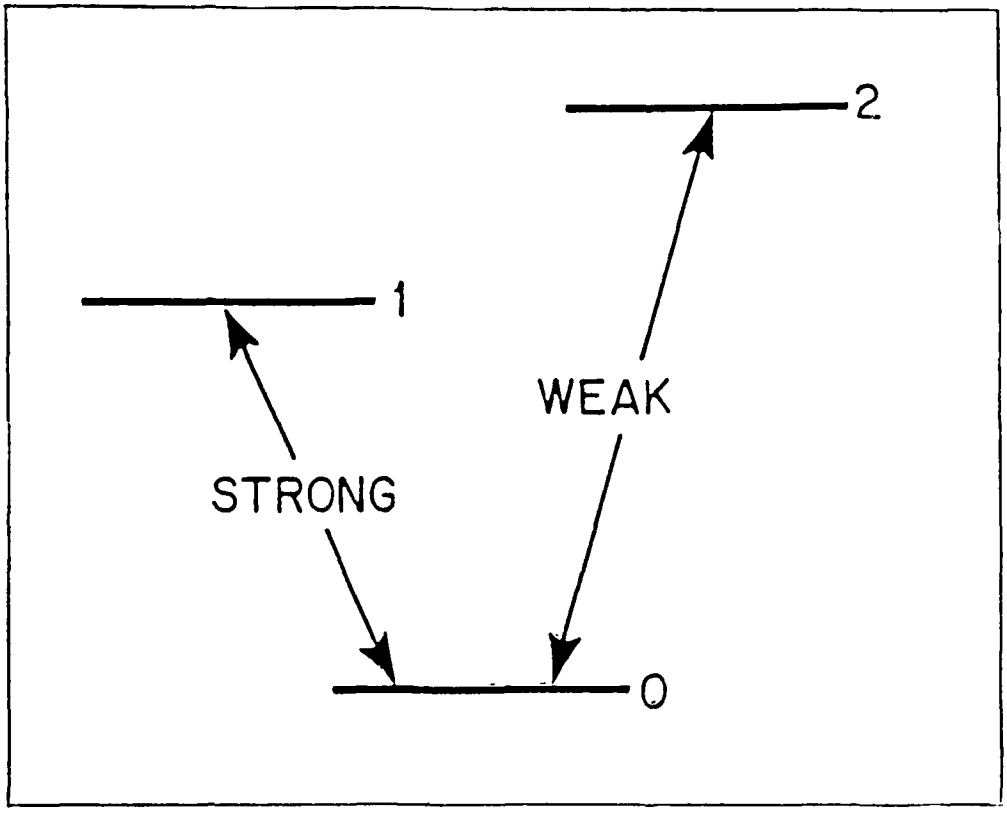

Figure 1. "V" Configuration.

level schemes, indicates a quantum jump. Thus an experiment using the ladder configuration could resolve whether what is being observed is indeed a single quantum event.

B. Problem Statement and Approach

The purpose of this research is twofold. First, in Chapter III, a simple theory of sideband cooling, in the limit that the amplitude of the ion's motion is less than the wavelength of the cooling light (the Lamb-Dicke limit), is developed. This is accomplished by first defining the operators which describe a two level atom in a harmonic trap and writing the Heisenberg equations of motion for these operators. The underlying assumption that makes it possible to simplify the theory is then made. This assumption is that the atom is "well localized", i.e., the uncertainty in the expectation value of the operator corresponding to the particle's position vector, $\vec{r}$, is small compared to the wavelength of the cooling laser, so that $\vec{r}$ can be replaced by its expectation value, $<\vec{r}>$, when taking expectation values of operators that are functions of $\vec{r}$. The equations of motion for the expectation values of all the pertinent operators then follow directly from the Heisenberg equations of motion for the operators. It is then possible to derive three simple, first order Bloch equations for the two-level atom in a harmonic trap. For one dimensional cooling, a dimensionless displacement described by a second order differential equation is defined. The problem is thus reduced to a set of four coupled, nonlinear differential equations, one of which is second order.

For two special cases these equations are solved analytically. The first case is the weak field case, in which the cooling radiation is taken to be sufficiently low in intensity that the probability that the atom is in the ground is very nearly unity. This eliminates one of the four coupled differential equations and reduces the

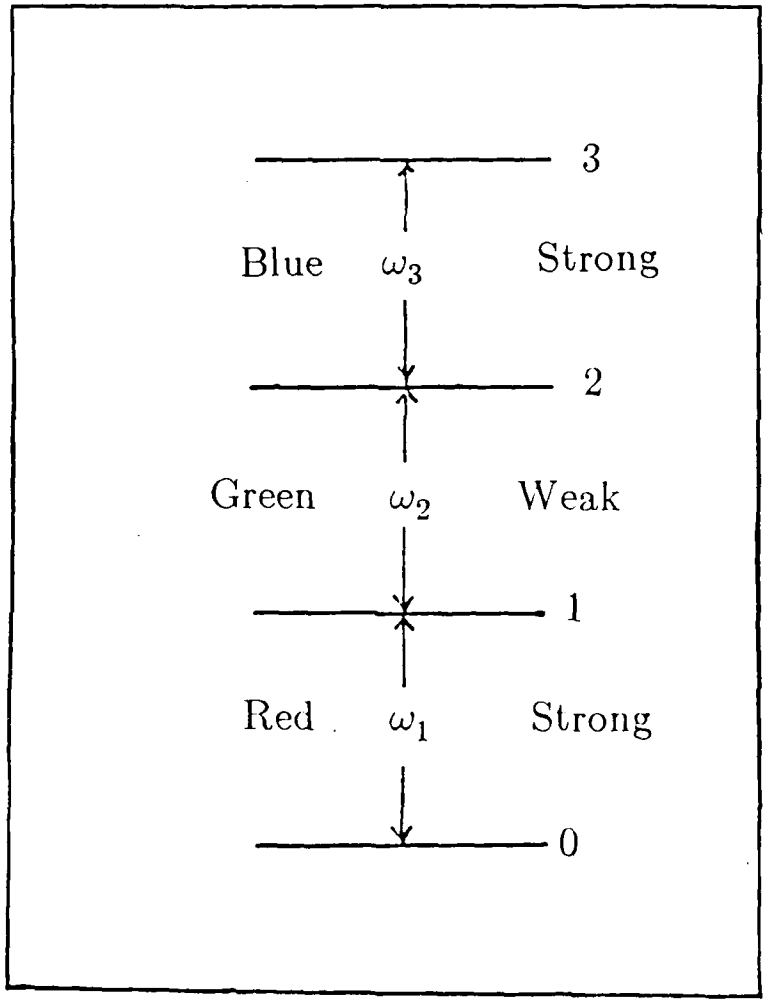

Figure 2. Ladder Configuration.

complexity of the remaining three. An analytical solution can then be derived.

The second case solved analytically makes use of an adiabatic approximation. Such an approximation is useful when trying to solve a coupled set of differential equations that can be divided into two groups. The first group consists of equations that have "large" self relaxation terms. The equations in the second group represent variables that change more slowly than the variables described by the equations in group one. If one is interested only in processes having time constants much smaller than the coefficients of the large self relaxation terms, then it is an excellent approximation to assume that the first group of variables adiabatically follow the more slowly varying second group. One can then use the steady state values of the first group of variables in the equations for the more slowly varying second group. This once again reduces the number and complexity of equations. For both special cases considered, it is shown that the amplitude of the dimensionless displacement decays exponentially and an analytical expression for the decay constant is presented. Decay of this amplitude corresponds to decreasing the atoms translational energy, which is what is meant by cooling.

The four original equations are solved numerically using a fourth order Runge-Kutta method, and the validity of each of the two analytical models is tested by comparing it to the numerical results. Exponential decay is observed for all the numerical cases considered, and a decay constant is calculated. Good agreement between the numerical and analytical results is seen in regions where the approximations used in deriving the analytical results are valid. Plots of the decay constant as a function of the various parameters of the four coupled equations can be easily generated, and some representative examples of such plots are presented.

In the second part of the research, contained in Chapter IV, the fluorescence signal of a single atom for the ladder configuration is analyzed theoretically. It is expected that the fluorescence will alternate between two wavelengths, ω_1 and ω_3. A splitting of the weak transition similar to the Autler-Townes doublet seen in the "V" configuration (23) is expected. A dressed atom approach is used to obtain qualitative information about this splitting.

The statistics of fluorescence are determined from deriving optical Bloch equations for the four-level system. The equations of motion for the density-matrix of a coherently excited, multi-level system, in the electric dipole approximation are taken from the literature (27). The on diagonal elements of the density matrix, ρ_{nn}, are just the probabilities to be in the state n. Only three of four probabilities are independent since the total probability must equal unity. The off diagonal elements of the density matrix, the coherences, oscillate at the transition frequencies between the two states that they correspond to, in this case optical frequencies. Since oscillations at such high frequencies have little effect on the probabilities, slowly varying coherences are defined so that the rotating wave approximation can be made. In the rotating wave approximation functions oscillating at optical frequencies are replaced by their time averaged values.

The resulting equations of motion are solved first in steady state. The steady state solution is compared with the qualitive results obtained from the dressed atom approach. Finally, the Bloch equations for the four-level atom are solved in an adiabatic approximation. The adiabatic approximation is appropriate here because the Einstein A coefficients appear in self relaxation terms for both the probabilities and the slowly varying coherences. We have specifically chosen transitions so that two of the A coefficients involved are very much larger than the third. It is shown that eventually all of the variables can be eliminated

adiabatically except one. The remaining variable corresponds to an inversion on an effective two level system driven by a rate process. The theory of two level systems driven by rate processes is well understood (9), (23), and the statistics of fluorescence for the ladder configuration follow directly from previous work (9), (23).

II. Background

A. Laser Cooling

1. Experiments

In 1980 Neuhauser, et al reported trapping a single barium ion in a Paul radio frequency quadrupole trap using laser cooling, and holding it in a volume with dimensions of $2\mu m$ (31). The Paul trap consists of three electrodes: two cap electrodes, shaped like hyperbolas, with a ring electrode between them. An oscillating electric field is applied to the electrodes. The trap is illustrated in Figure 3. The potential created in the trap space is

$$V(\vec{R},t)=v(\vec{R})\cos\Omega t=V_0(X^2+Y^2-2Z^2)\cos\Omega_{rf}\,t \tag{2.1}$$

where V is the electric potential, V_0 is a constant, and Ω_{rf} is the frequency of oscillation of the electric field (11). The origin of coordinates is at the center of the ring electrode with the z-axis running between the two cap electrodes, perpendicular to the plane of the ring electrode.

A Paul trap, which has an oscillating electric field, was used instead of a trap with a static electric field, such as a Penning trap, because static traps must use both an electric and magnetic field. The magnetic field causes a Zeeman effect which is undesirable for high resolution spectroscopy (11). It has been shown (10) that the time varying potential of the Paul trap is equivalent to a time indepen-

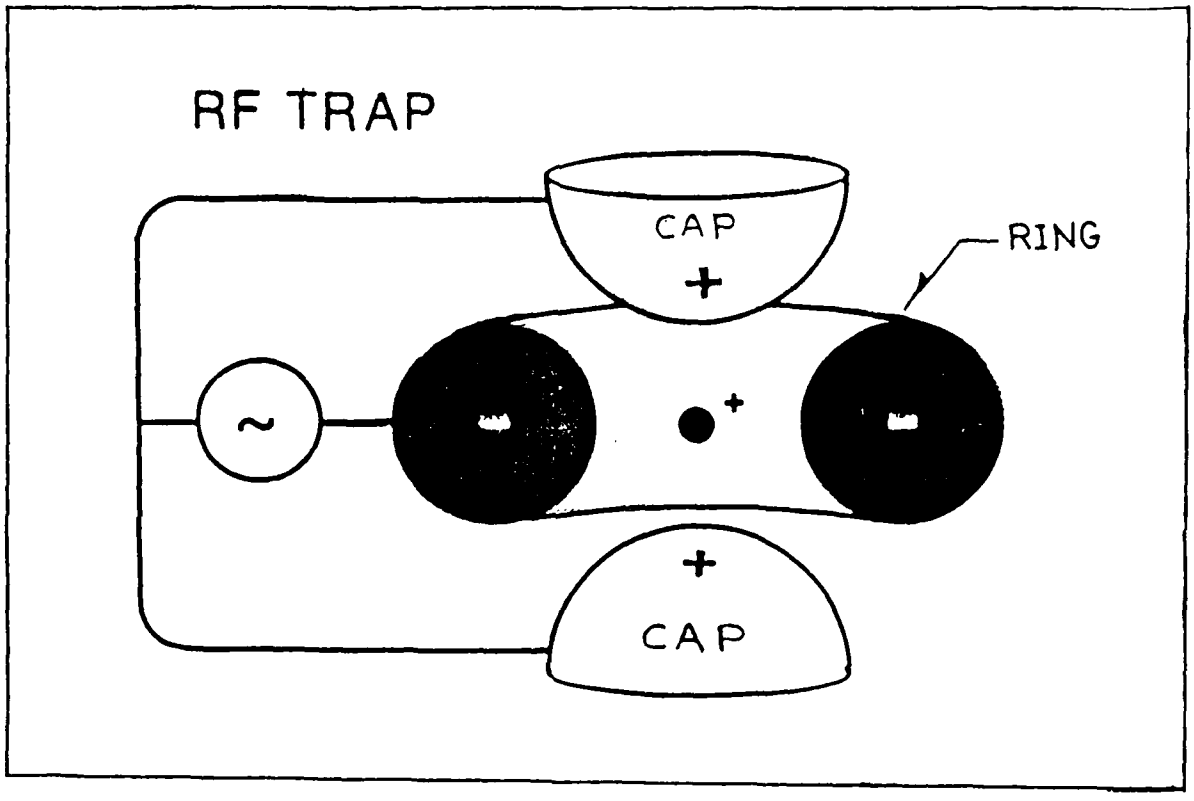

Figure 3. Radio Frequency Quadrupole Trap.

dent effective potential given by

$$V_{eff}(\vec{R}) = \frac{V_0^2}{m\Omega_{rf}^2}(X^2 + Y^2 + 4Z^2) \tag{2.2}$$

which is a harmonic potential. The angular frequencies of oscillation in the trap are given by

$$\nu_z = \nu_y = \tfrac{1}{2}\nu_z = \frac{2^{1/2} V_0}{m\Omega} \tag{2.3}$$

In the trap used by Neuhauser, et al the spacing between the two cap electrodes was 0.5 mm, and the inner diameter of the ring electrode was 0.75 mm. The frequency of oscillation of the electric field, Ω_{rf}, was 2π x 18MHz and the angular frequency of oscillation of the ion in the well, in the X and Y directions, ν_z, was 2π x 2.4MHz. A barium atomic beam was injected into the trap from an oven and ionized by an electron beam. The ion was thermalized by allowing helium buffer gas into the trap at a background pressure of $<10^{-4}$ Torr (30). A laser tuned to the Ba^+ line at 493.4 nm was shone on the trap, and when a barium ion was present in the trap it could be observed visually by fluorescence (31).

The 493.4 nm line for Ba^+ is a transition between the ground $6^2S_{1/2}$ state and an excited $6^2P_{1/2}$ state. For the purposes of cooling the ion, the laser was tuned to a frequency below the resonant frequency of the transition by an amount ν. One-third of the time, the ion spontaneously decayed to a $5^2D_{3/2}$ metastable excited state instead of back to the ground state. A second laser, tuned the $5^2D_{3/2}$–$6^2P_{1/2}$ transition at 649.9 nm kept the ion from sitting in the metastable state. An energy level diagram is shown in Figure 4. Both laser beams entered the trap between the ring electrode and one of the cap electrodes, at an angle of 45° to the z-axis.

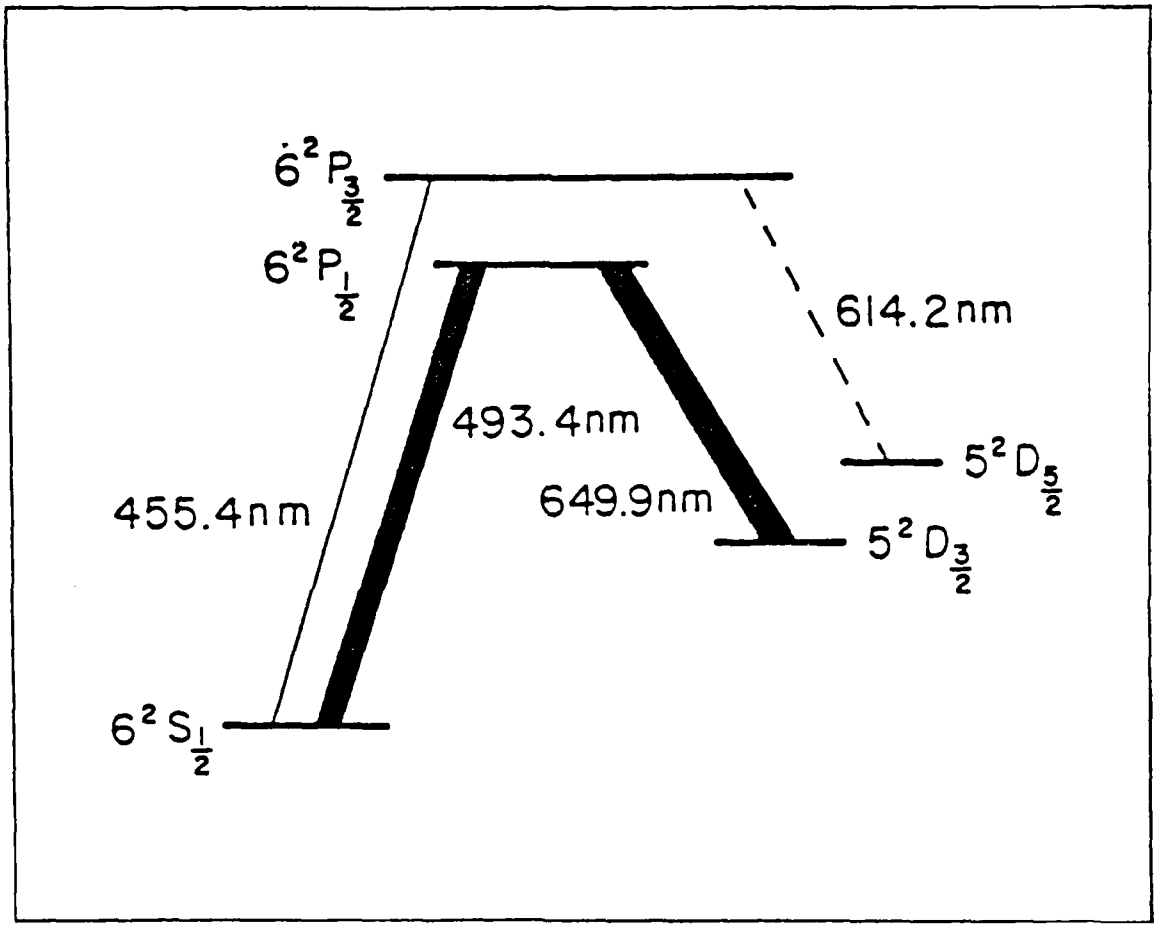

Figure 4. Energy Level Diagram For Nagourney, et al (28).

2. Laser Cooling Theories

The idea of using laser light tuned below resonance to cool atoms was first proposed by Hansch and Schawlow (17) for free atoms, and by Wineland and Dehmelt (38) for trapped ions. There is a fundamental difference between the laser cooling of free atoms and trapped atoms, at least in the Lamb-Dicke limit. Laser cooling of a free atom takes place because of the atom's Doppler shift (17). For a running wave laser field, when the laser is tuned to the lower half of the atom's Doppler spectrum, the atom is shifted into resonance when it moves toward the laser and out of resonance when it moves away from the laser. If the atom radiates spontaneously in three dimensions, then the net effect of absorbing photons as it moves toward the laser is to slow the atom, while the net effect of absorbing photons as it moves away from the laser is to speed the atom. Because of the Doppler shift, the atom absorbs more photons when it is moving toward the laser than away from it, so the atom is slowed. Laser cooling of free atoms and atoms in radiation traps has been treated extensively in the literature (2), (5), (6), (7), (8), (16), (25), and will not be discussed further here, except to note that in reference (8) Cook uses Ehrenfest's theorem and optical Bloch equations to deal with atomic motion in resonant radiation. The method used to come up with a simple theory of side-band cooling used in this work can be thought of as an extension of Cook's method to bound atoms.

A Doppler shift picture is a good physical description of the cooling of a trapped atom as long as the volume to which the atom is confined is large compared to the wavelength, λ, of the cooling laser. However, when an ion or atom is confined to a volume whose dimensions are smaller than $\lambda/4$ the Doppler shift is suppressed (12), so laser cooling of trapped ions in this limit, the Lamb-Dicke limit cannot be explained by the Doppler shift. Laser cooling in a trap, in the

Lamb-Dicke limit takes place via side-band cooling. The electronic levels of the ion are split by the energy levels in the trap. For a harmonic trap these levels are evenly spaced $\hbar\nu$ apart, where ν is the angular frequency of oscillation of the atom in the trap. Figure 5 is an energy level diagram for a two state atom split by the trap levels. The spectrum of the ion then looks like Figure 6, with the central peak at ω_0 and sidebands at $\omega_0 \pm m\nu$ where m is an integer. When the laser is tuned to a lower sideband ($\omega_0 - m\nu$), the ion is excited from the $|g,n>$ state (ground electronic state, nth harmonic oscillator level) to the $|e,n-m>$ state (excited electronic state, $n-m$ harmonic oscillator level) from which it decays to $|g,n-m>$. Thus, the net effect is to decrease the expectation value of the harmonic oscillator number operator, $<n>$, which corresponds to cooling the ion's secular motion.

The theory of cooling bound atoms, and specifically harmonically bound atoms has been treated by several groups. Stenholm, Javanainen, and Lindberg (19), (20), (21) have worked in this area both together and separately for many years. Reference (21) used a density matrix approach to deal with the final stages of laser cooling of harmonically trapped ions. This approach involved coupled equations for all the harmonic oscillator states which even in the Lamb-Dicke limit can mean hundreds of equations. These equations can be solved numerically for particular cases of interest. No attempt was made in this approach to determine a cooling rate. The parameter of interest to these authors was the minimum temperature achievable at the limits of cooling, which was plotted as a function of the detuning for one set of parameters (21). The minimum temperature was achieved for the detuning approximately equal to minus the angular frequency of oscillation in the trap. Stenholm has compiled a review of laser cooling theory (36) that contains an extensive bibliography.

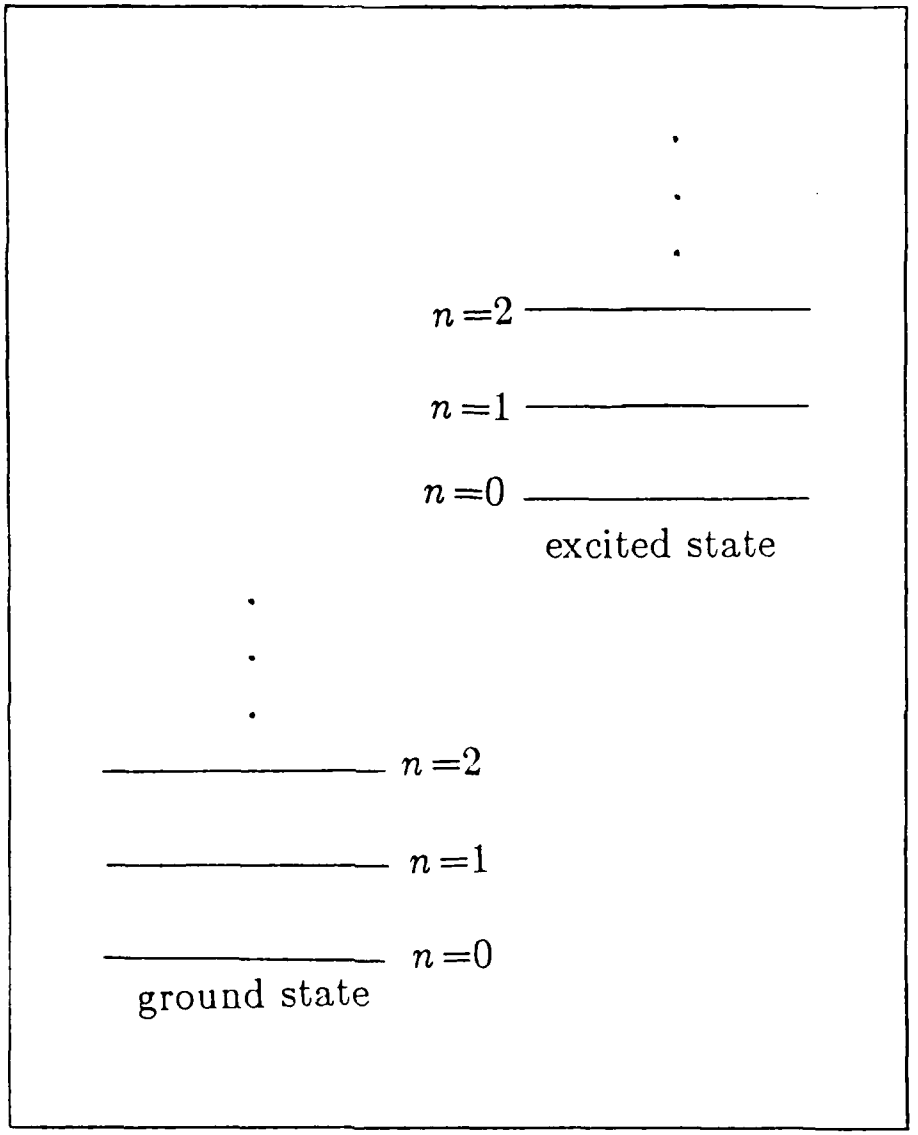

Figure 5. Energy Levels of Trapped Ion.

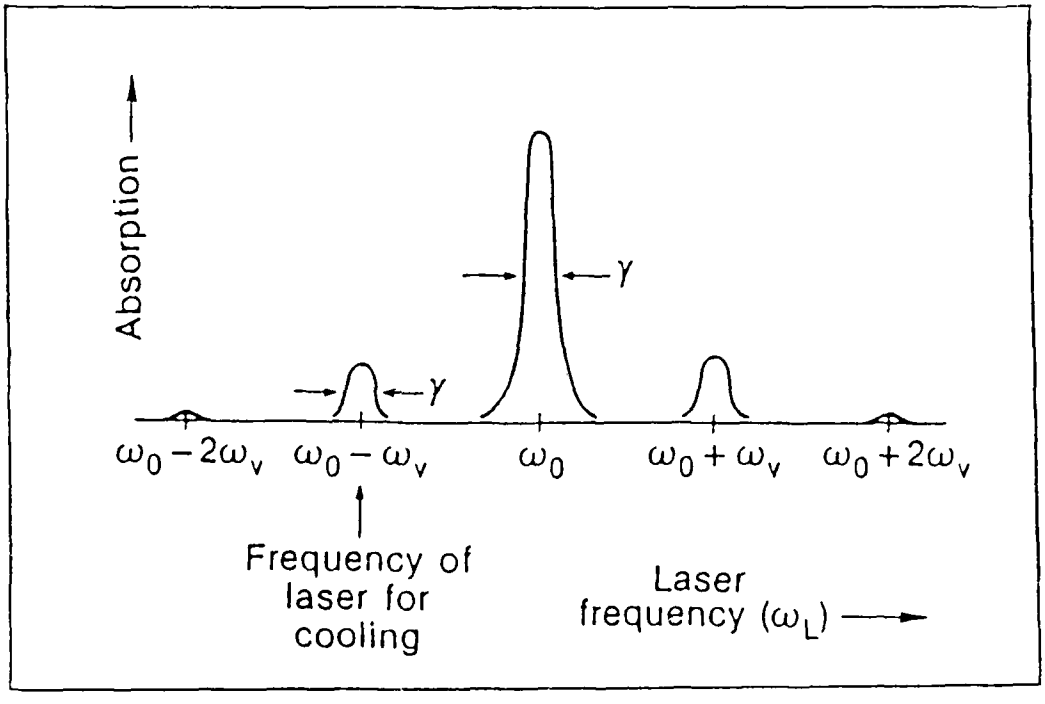

Figure 6. Spectrum of Trapped Ion (40).

Wineland and Itano (18), (29), (39) and, more recently, Wineland, Itano, Bergquist, and Hulet (40) have used both energy rate equations and quantum-mechanical perturbation theory to calculate minimum energies of cooling and dE_i/dt, where E_i is the energy of the secular motion along one of the harmonic oscillator axes. In references (18) and (39), the limiting assumption is made that the cooling transition is not saturated. These authors, like Stenholm, et al. are chiefly concerned with the minimum temperature achievable by laser cooling, and they do not calculate or plot rates of cooling as functions of the various parameters of the problem. However, where possible, the functional form of their expression for dE/dt will be compared to the cooling rates derived in Chapter III. References (39) and (40) deal with the limits of cooling in both radio-frequency quadrupole traps and Penning traps. The authors conclude that cooling to the zero point energy should be possible, that is, the expectation value of the harmonic oscillator number operator, $n=<\hat{n}>$, obeys the relationship, $n<<1$. They show quantitatively that it should be possible to detect when the ion has reached the ground state because the intensity from the lower sideband should vanish. A qualitative argument that this would be the case was made by Wells in reference (37).

B. Single Atom Spectroscopy

1. Theory of Electron Shelving

The idea of electron shelving was first suggested by Dehmelt in 1975 as a scheme for making more accurate atomic clocks (13). It was not until 1985 that Cook and Kimble (9) first theoretically treated the statistics of the proposed experiment. They considered the "V" configuration shown in Figure 1. The 1985

paper used rate equations and looked at the case of incoherent excitation. This paper predicted the fluorescence from the strong transition would flash on and off producing a random telegraph signal. The statistics of the fluorescence such as the distribution of on and off times and the two-time intensity correlation function were calculated. Schenzle, DeVoe, and Brewer (34) used a quantum statistical approach and calculated a second order correlation function of the fluorescence intensity to show that a single atom undergoes "large fluctuations between a state of full emission in the strong transition to a state of no emission."

Coherent excitation has been treated by many authors. Kimble, Cook, and Wells (23) showed that for the "V" configuration when the strong transition is highly saturated, the excitation of the weak transition can be treated as a rate process, so that much of the theory of reference (9) applies to the coherent case. Cohen-Tannoudji and Dalibard (4) also treated the "V" configuration. Using a dressed atom approach, they also showed that the strong transition fluorescence would have bright and dark periods and calculated the statistics of the fluorescence. Schenzle and Brewer (33) used photon counting statistics to arrive at the same conclusions. Javanainen (22) used the quantum regression theorem to calculate the photon-counting statistics for the "Λ" configuration. Pegg, Louden, and Knight (32) treated not only the "V" and "Λ" configurations but also two three-level cascades, one with the upper transition as the strong transition and one with the upper transition as the weak transition. They arrived at the erroneous conclusion that there would be no long dark periods. Arecchi, et al (1) showed that for the purposes of a frequency standard a pulsed excitation technique has some advantages over a cw scheme.

2. Exeperiments That Demonstrate Electron Shelving

Experimental verification of electron shelving has now been reported by three groups of researchers. Using the same experimental arrangements as for the 1980 Neuhauser, et al paper (31), Nagourney, Sandberg, and Dehmelt (28), have observed bright and dark periods in the fluorescence of a Ba^+ ion. The energy level diagram for this experiment is shown in Figure 4. The $6^2S_{1/2}$ is the ground state. The ion was cooled via the $6^2P_{1/2}$ to ground state transition by a stabilized, single frequency dye laser. As was mentioned in section II.A.1 there is a one in three chance that the ion will spontaneously decay to the metastable $5^2D_{3/2}$ state, so a second stabilized, single frequency dye laser was used to keep this level clear. The shelf level was the $5^2D_{5/2}$ level reached via the $6^2P_{3/2}$ level. The branching ratio for decay to the $5^2D_{5/2}$ level from the $6^2P_{3/2}$ level was 1 3. The light source used to excite the ion to the $6^2P_{3/2}$ level was a barium hollow cathode lamp, an incoherent source. Figure 7 is a plot of intensity versus time from reference (28). Note that when the ion is in the shelf state for this configuration, there is no resonant radiation driving the ion, so that the only way for the ion to leave the shelf state is by spontaneous emission. The length of the dark periods is distributed exponentially; making it possible to directly measure the spontaneous decay lifetime of the $5^2D_{5/2}$ state. The spontaneous decay lifetime measured for the $5^2D_{5/2}$ state was greater than 30 seconds.

Sauter, et al (33) have done a similar experiment with Ba^+ making use of a Λ configuration shown in Figure 8. Figure 9, from reference (33), is a plot of fluorescence versus time for a single trapped ion.

Bergquist, et al (3) have performed a very simular experiment using a mercury ion. Their experiment actually uses a "V" configuration. Figure 10 is an energy level diagram for this system. Figure 11 is a plot of intensity versus time

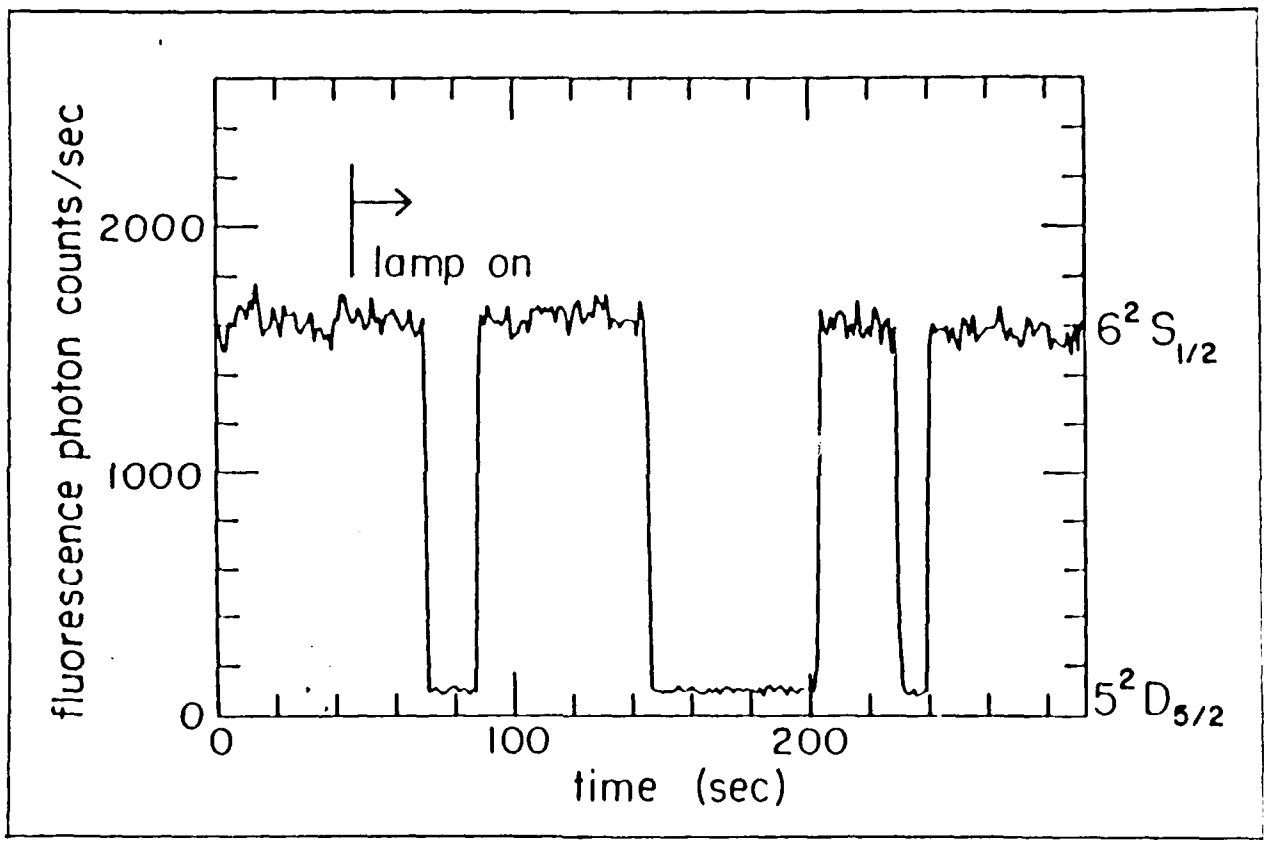

Figure 7. Intermittent Fluorescence from Nagourney, et al (28).

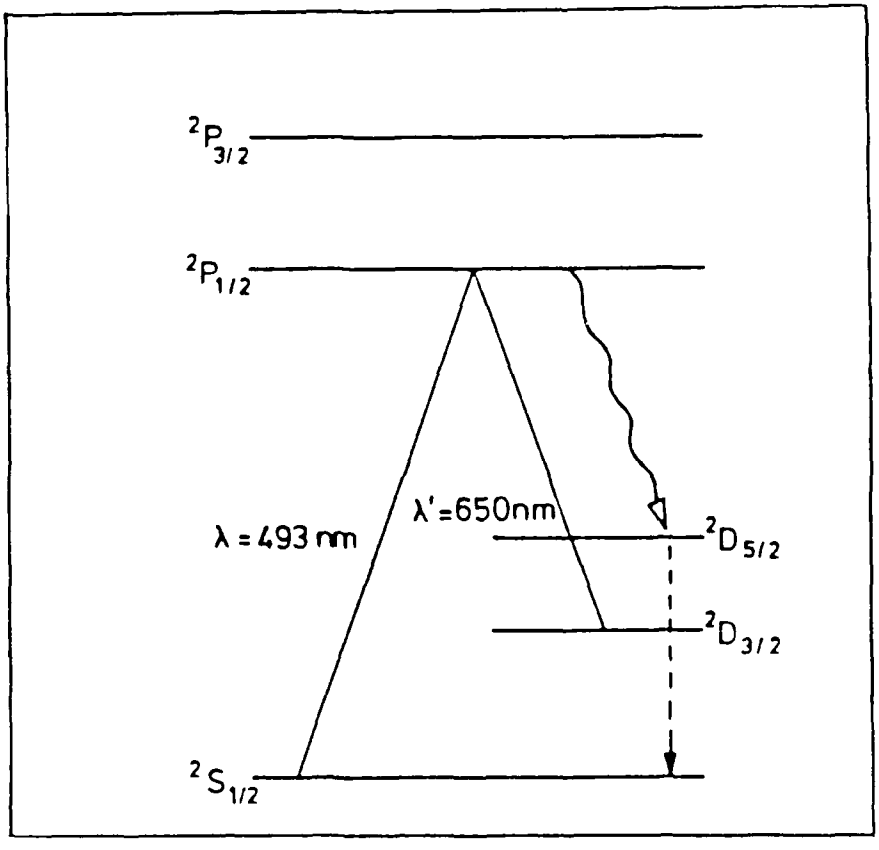

Figure 8. Energy Level Diagram from Sauter, et al (33).

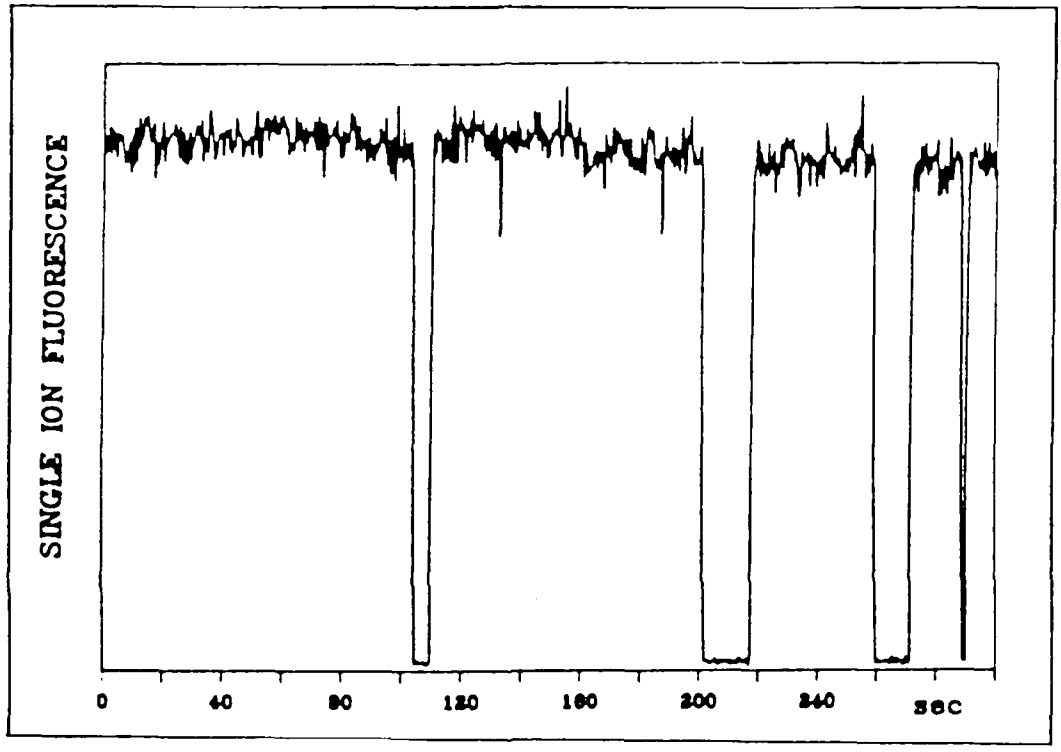

Figure 9. Intermittent Fluorescence from Sauter, et al (33).

from reference [3]. The lifetime of the shelving state is about 0.1 second, much shorter than for Nagourney, et al. Figure 11(a) is a plot of the fluorescence without the "shelving" laser turned on. The jumps in the flourescence are due to off resonance transitions caused by the "strong" transition laser. Figure 11(b) is a plot of the intensity for a single ion in the trap. Note that there are two levels of intensity, which correspond to the atom on and the atom off. Figure 11(c) is a plot of the intensity for two trapped ions. Note that there are three discernable levels of intensity, which correspond to both ions on; one ion on, one ion off; and both ions off.

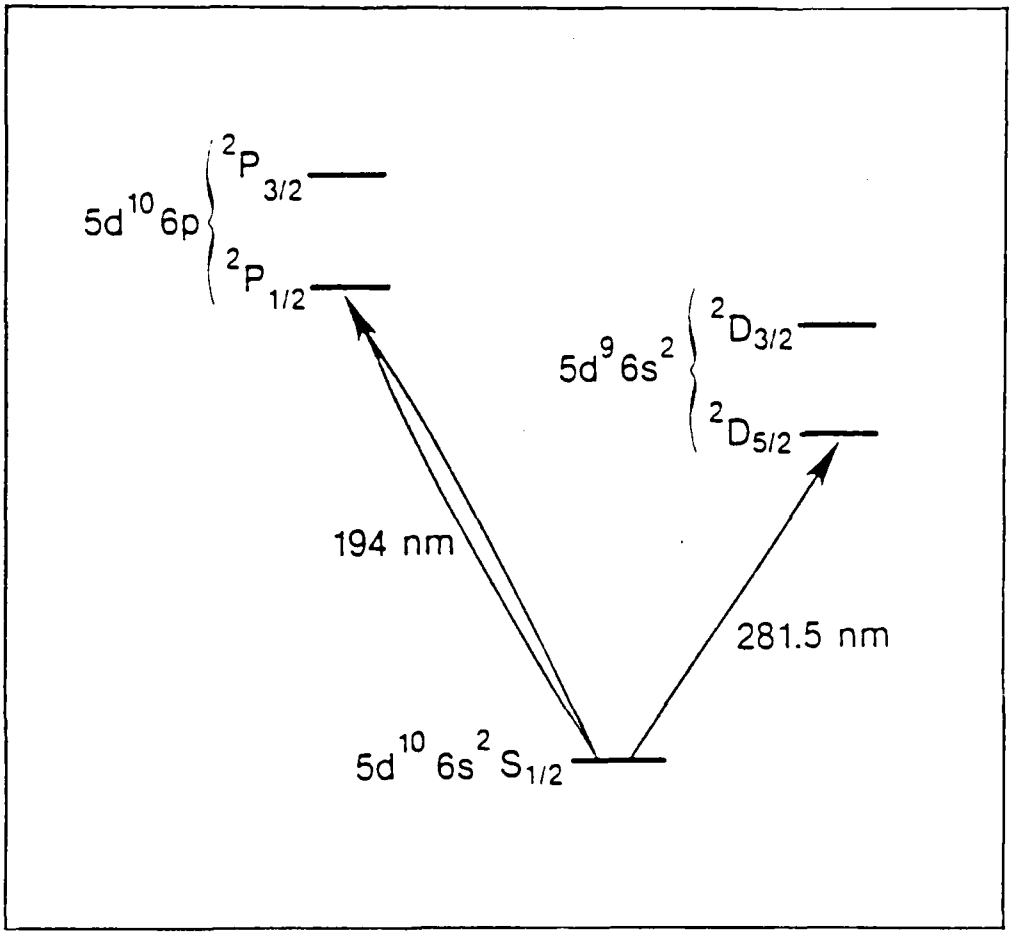

Figure 10. Energy Level Diagram from Bergquist, et al (3).

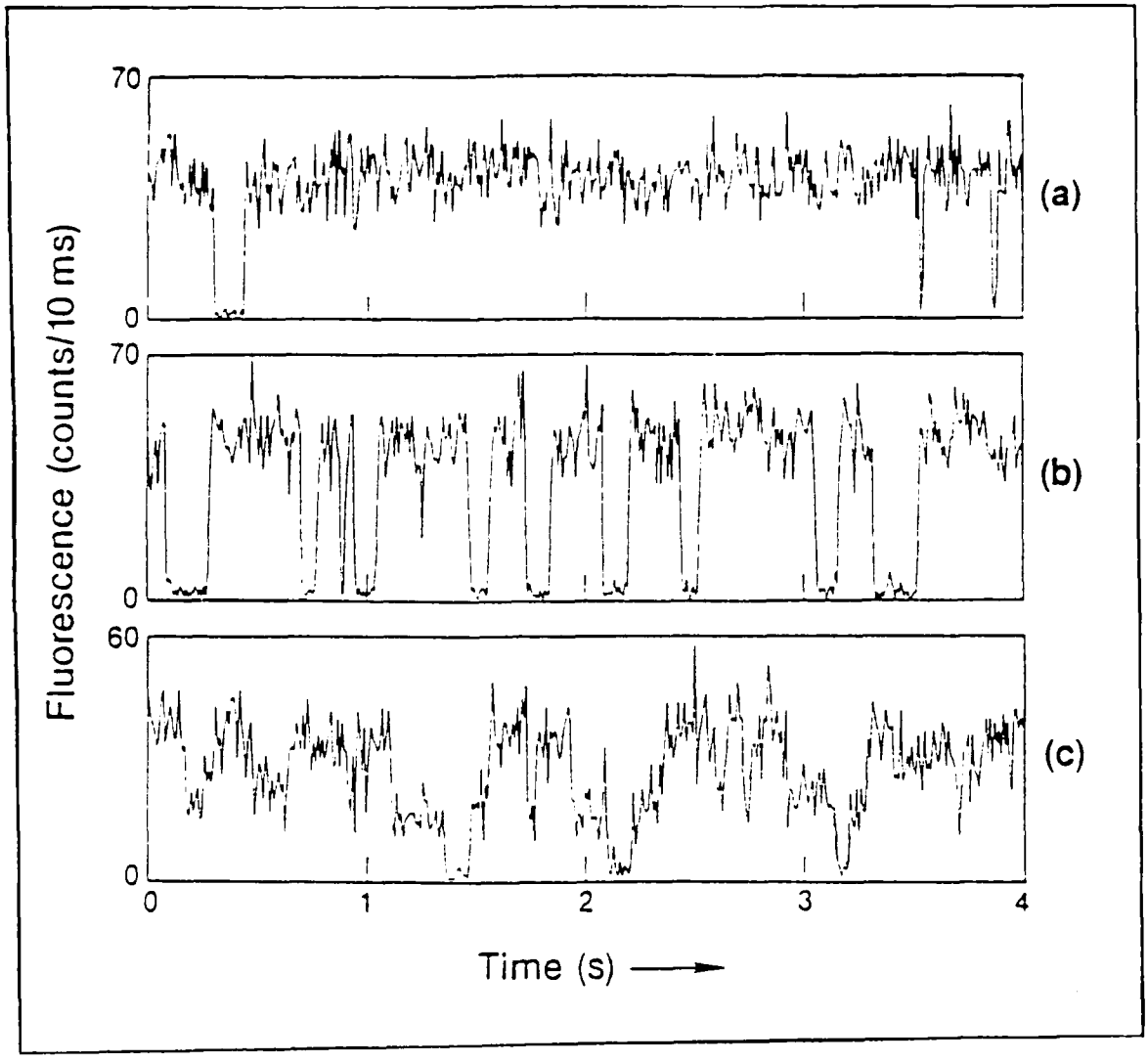

Figure 11. Intermittent Fluorescence from Bergquist, et al (3).

III. A Simple Theory of Sideband Cooling

A. Theory

The operators which describe a harmonically trapped, cooled, two-level ion can be divided into three groups. First there are the operators which describe the center of mass motion of the ion, $\vec{r}$ and $\vec{p}$. In the absence of any driving force, the equations of motion for these operators are determined by the unperturbed hamiltonian for the translational motion

$$\hat{H}_T=\frac{1}{2m}(\hat{p}_x^2+\hat{p}_y^2+\hat{p}_z^2)+\tfrac{1}{2}m(\nu_x^2\hat{x}^2+\nu_y^2\hat{y}^2+\nu_z^2\hat{z}^2), \tag{3.1}$$

where ν_x, ν_y, and ν_z are the frequencies of oscillation of the ion in the x, y, and z directions respectively. Next there are the operators which describe the internal motion of the ion. For an ion with only two states, $|1>$ and $|2>$, these operators may be taken to be

$$\hat{\sigma}=|1><2|, \tag{3.2a}$$

$$\hat{\sigma}^+=|2><1|, \tag{3.2b}$$

$$\hat{\sigma}_3=|2><2|-|1><1|. \tag{3.2c}$$

The hamiltonian for the unperturbed internal motion reads

$$H_I = \tfrac{1}{2}\hbar\omega_0\hat{\sigma}_3, \tag{3.3}$$

where ω_0 is the frequency of the transition between states $|2>$ and $|1>$. Finally, there is the interaction between the laser field and the ion. A classically prescribed field is assumed. For a classically prescribed field, in the electric dipole approximation the interaction hamiltonian is

$$H' = -\vec{\mu}\cdot\vec{E}(\vec{r},t). \tag{3.4}$$

Here $\vec{E}(\vec{r},t)$ is the applied electric field and $\vec{\mu}$ is the electric dipole operator for a two-level atom which may be written as

$$\vec{\mu} = \vec{\mu}(\hat{\sigma}^+ + \hat{\sigma}), \tag{3.5}$$

where $\vec{\mu} = <1|\vec{\mu}|2>$ is the dipole transition moment. For the purposes of this paper $\vec{\mu}$ is assumed to be real. For a running wave laser field, $\vec{E}(\vec{r},t)$ can be taken to be

$$\vec{E}(\vec{r},t) = \vec{e}_E E\cos(\vec{k}\cdot\vec{r} - \omega t), \tag{3.6}$$

where $\vec{e}_E$ is the unit polarization vector. If μ is defined as $\vec{\mu}\cdot\vec{e}_E$, then H' is given by

$$H' = -\mu E(\hat{\sigma}^+ + \hat{\sigma})\cos(\vec{k}\cdot\vec{r} - \omega t). \tag{3.7}$$

The total Hamiltonian of the system, H, is

$$H = H_T + H_I + H'. \tag{3.8}$$

The Heisenberg equations of motion for the operators $\vec{r}$, $\vec{p}$, $\hat{\sigma}$, and $\hat{\sigma}_3$ are

$$\frac{d\vec{r}}{dt}=\frac{\vec{r}\cdot H}{i\hbar}=\frac{\vec{p}}{m}, \tag{3.9a}$$

$$\frac{d\vec{p}}{dt}=-m(\nu_x^2 x\vec{e}_x+\nu_y^2 y\vec{e}_y+\nu_z^2 z\vec{e}_z)-\vec{k}\mu E(\hat{\sigma}^+ +\hat{\sigma})\sin(\vec{k}\cdot\vec{r}-\omega t), \tag{3.9b}$$

$$\frac{d\hat{\sigma}}{dt}=-i\omega_0\hat{\sigma}-i\frac{\mu E}{\hbar}\hat{\sigma}_3\cos(\vec{k}\cdot\vec{r}-\omega t), \tag{3.9c}$$

$$\frac{d\hat{\sigma}_3}{dt}=2i\frac{\mu E}{\hbar}(\hat{\sigma}^+ -\hat{\sigma})\cos(\vec{k}\cdot\vec{r}-\omega t). \tag{3.9d}$$

At this point the approximation is made that the atom is well localized, that is

$$\Delta r=\sqrt{|<\vec{r}>\cdot<\vec{r}>-<\vec{r}\cdot\vec{r}>|} \tag{3.10}$$

is small compared to the wavelength, $\lambda=2\pi/k$. This means that when taking expectation values $\vec{r}$ can be replaced by $<\vec{r}>$ in $\sin(\vec{k}\cdot\vec{r}-\omega t)$ and $\cos(\vec{k}\cdot\vec{r}-\omega t)$. The equations of motion for the pertinant expectation values become

$$\frac{d\vec{r}}{dt}=\frac{\vec{p}}{m}, \tag{3.11a}$$

$$\frac{d\vec{p}}{dt}=-m(\nu_x^2 x\vec{e}_x+\nu_y^2 y\vec{e}_y+\nu_z^2 z\vec{e}_z)-\vec{k}\mu E(\sigma^* +\sigma)\sin(\vec{k}\cdot\vec{r}-\omega t), \tag{3.11b}$$

$$\frac{d\sigma}{dt}=-(\beta+i\omega_0)\sigma-i\frac{\mu E}{\hbar}\sigma_3\cos(\vec{k}\cdot\vec{r}-\omega t), \tag{3.11c}$$

$$\frac{d\sigma_3}{dt}=2i\frac{\mu E}{\hbar}(\sigma^*-\sigma)\cos(\vec{k}\cdot\vec{r}-\omega t)-2\beta(\sigma_3-1). \tag{3.11d}$$

where $\vec{r}=<\vec{r}>$, $\vec{p}=<\vec{p}>$, $\sigma=<\dot{\sigma}>$, $\sigma_3=<\dot{\sigma}_3>$. Spontaneous emission has not been included in the Hamiltonian. Spontaneous is included by following the treatment of reference (27). Including spontaneous emission will change equations (3.11c) and (3.11d) to

$$\frac{d\sigma}{dt}=-(\beta+i\omega_0)\sigma-i\frac{\mu E}{\hbar}\sigma_3\cos(\vec{k}\cdot\vec{r}-\omega t) \tag{3.12a}$$

$$\frac{d\sigma_3}{dt}=2i\frac{\mu E}{\hbar}(\sigma^+-\sigma)\cos(\vec{k}\cdot\vec{r}-\omega t)-2\beta(\sigma_3+1) \tag{3.12b}$$

where β is half the Einstein A coefficient.

It is convenient to introduce slowly varying Bloch variables u, v, and w defined as

$$u=\sigma^* e^{-i\omega t}+\sigma e^{i\omega t}, \tag{3.13a}$$

$$v=-i(\sigma^* e^{-i\omega t}-\sigma e^{i\omega t}), \tag{3.13b}$$

$$w=\sigma_3. \tag{3.13c}$$

In the Lamb-Dicke limit ($\vec{k}\cdot\vec{r}<<1$) we may expand the trigonometric functions in equations (3.11) and (3.12) to first order in the small quantity $\vec{k}\cdot\vec{r}$.

$$\sin(\vec{k}\cdot\vec{r}-\omega t)=\sin(\vec{k}\cdot\vec{r})\cos\omega t-\cos(\vec{k}\cdot\vec{r})\sin\omega t\approx(\vec{k}\cdot\vec{r})\cos\omega t-\sin\omega t. \tag{3.14a}$$

$$\cos(\vec{k}\cdot\vec{r}-\omega t)=\sin(\vec{k}\cdot\vec{r})\sin\omega t-\cos(\vec{k}\cdot\vec{r})\cos\omega t\approx(\vec{k}\cdot\vec{r})\sin\omega t-\cos\omega t. \tag{3.14b}$$

The equations of motion for the Bloch variables and $\vec{p}$ become

$$\frac{du}{dt}=-\beta u+\Delta v+\Omega w(2\vec{k}\cdot\vec{r}\sin^2\omega t-\sin 2\omega t), \tag{3.15a}$$

$$\frac{dv}{dt}=-\Delta u-\beta v+\Omega(\vec{k}\cdot\vec{r}\sin 2\omega t+2\cos^2\omega t), \tag{3.15b}$$

$$\frac{dw}{dt}=-\Omega[2(\vec{k}\cdot\vec{r}u\sin^2\omega t+v\cos 2\omega t)+(u+\vec{k}\cdot\vec{r}v)\sin 2\omega t]-2\beta(w-1), \tag{3.15c}$$

$$\frac{d\vec{p}}{dt}=-m(\nu_x^2 x\vec{e}_x+\nu_y^2 y\vec{e}_y+\nu_z^2 z\vec{e}_z) \tag{3.15d}$$

$$-\vec{k}\hbar\Omega[\vec{k}\cdot\vec{r}u\cos^2\omega t+v\sin^2\omega t-\tfrac{1}{2}(u+\vec{k}\cdot\vec{r}v)\sin 2\omega t],$$

where $\Delta=\omega-\omega_0$ is the detuning and $\Omega=\mu E/\hbar$ is the Rabi frequency.

The terms $\sin^2\omega t$, $\cos^2\omega t$, $\sin 2\omega t$, and $\cos 2\omega t$ vary much faster than u, v, w, and $\vec{p}$ so that only their time averaged values have much effect. In the rotating wave approximation $\sin^2\omega t$ and $\cos^2\omega t$ are replaced by their time averaged values, ½. $\sin 2\omega t$ and $\cos 2\omega t$ average to 0. We consider cooling of the x degree of freedom, that is $\vec{k}$ is taken in the x direction ($k_x=k$, $k_y=k_z=0$ and $\nu_x=\nu$). The equations of motion are simplified by introducing the dimensionless displacement $s=kx$. The equations of motion become

$$\frac{du}{dt}=-\beta u+\Delta v+\Omega ws, \tag{3.16a}$$

$$\frac{dv}{dt}=-\Delta u-\beta v-\Omega w. \tag{3.16b}$$

$$\frac{dw}{dt}=-\Omega(su+v)-2\beta(w-1). \tag{3.16c}$$

$$\frac{d^2s}{dt^2}+\nu^2 s=-K(su+v). \tag{3.16d}$$

where $K=\hbar k^2\Omega/(2m)$. This set of four coupled, nonlinear differential equations describe the cooling process within the approximations given above.

The steady state solution of equations (3.16), u_0, v_0, w_0, and s_0, for small s_0 (Lamb-Dicke limit) is

$$u_0=-\frac{\Omega(\Delta+\beta s_0)}{\beta^2+\Delta^2+\frac{1}{2}\Omega^2}, \tag{3.17a}$$

$$v_0=-\frac{\Omega(\beta-\Delta s_0)}{\beta^2+\Delta^2+\frac{1}{2}\Omega^2}, \tag{3.17b}$$

$$w_0=-\frac{(\beta^2+\Delta^2)}{\beta^2+\Delta^2+\frac{1}{2}\Omega^2}, \tag{3.17c}$$

$$s_0=\frac{\hbar k^2\beta\Omega^2}{2m\nu^2(\beta^2+\Delta^2+\frac{1}{2}\Omega^2)}. \tag{3.17d}$$

Other solutions to equations (3.16) can be written in the form

$$f(t)=f_0+f_t(t), \tag{3.18}$$

where $f_t(t)$ has a steady value of zero. When solutions of this form are substi-

tuted into equation (3.16) we get

$$\frac{du_i}{dt}=-\gamma u_i-\Delta v_i-\Omega s_0 w_i-\Omega w_0 s_i-\Omega w_i s_i, \tag{3.19a}$$

$$\frac{dv_i}{dt}=-\Delta u_i-\gamma v_i+\Omega w_i, \tag{3.19b}$$

$$\frac{dw_i}{dt}=-\Omega(s_0 u_i+u_0 s_i+v_i)-2\gamma w_i-\Omega u_i s_i, \tag{3.19c}$$

$$\frac{d^2 s_i}{dt}+\nu^2 s_i=-K(s_0 u_i+u_0 s_i+v_i-s_i u_i). \tag{3.19d}$$

B. Special Cases

At this point certain special cases will be considered which can be solved analytically.

1. Weak Field Case, $\Omega<<\gamma,\nu$

For this case the atom remains near the ground state ($w=-1$) and we can set $w_0=-1$, $w_i=0$. The remaining equations are

$$\frac{du_i}{dt}=-\gamma u_i+\Delta v_i-\Omega s_i, \tag{3.20a}$$

$$\frac{dv_i}{dt}=-\Delta u_i-\gamma v_i, \tag{3.20b}$$

$$\frac{d^2 s_i}{dt^2} - (Ku_0 - \nu^2) s_i = -K(s_0 u_i - v_i). \tag{3.20c}$$

The terms on the right in equation (3.19d) are linear in Ω. ($K = \pi k^2 \Omega / 2m$). Also, since u_0 is linear in Ω, Ku_0 is quadratic in Ω. The dominant term in equation (3.20c) is $\nu^2 s_i$. A solution for s_i of the form

$$s_i = s_1(t)\cos\nu t + s_2(t)\sin\nu t \tag{3.21}$$

is assumed. If coefficients $s_1(t)$ and $s_2(t)$ vary much more slowly than $\cos\nu t$ and $\sin\nu t$ so that $d^2 s_1 / dt^2$ and $d^2 s_2 / dt^2$ can be neglected with respect to $2\nu ds_1 / dt$ and $2\nu ds_2 / dt$, then equation (3.20c) becomes

$$2\nu\left(\frac{ds_2}{dt}\cos\nu t - \frac{ds_1}{dt}\sin\nu t\right) = -K\left[s_0 u_i + v_i + u_0(s_1\cos\nu t + s_2\sin\nu t)\right]. \tag{3.22}$$

Defining $\xi = u_i - iv_i$, the equation for ξ is

$$\frac{d\xi}{dt} = -(\beta + i\Delta)\xi - \Omega s_i. \tag{3.23}$$

The solution of this equation is

$$\xi(t) = -\Omega \int_{-\infty}^{t_0 = t} e^{-(\beta + i\Delta)(t - t_0)} s_i(t_0)\, dt_0. \tag{3.24}$$

If $s_1(t)$ and $s_2(t)$ vary much more slowly than $e^{-\beta t}$, then they may be removed from the integral, which can then be evaluated. The result is

$$\begin{aligned}\xi(t) = -\tfrac{1}{2} s_1 \Omega \Bigg[& \frac{\beta\cos\nu t(1+i) + (\Delta+\nu)\sin\nu t(1-i)}{\beta^2 + (\Delta+\nu)^2} \\ & + \frac{\beta\cos\nu t(1-i) - (\Delta-\nu)\sin\nu t(1+i)}{\beta^2 + (\Delta-\nu)^2} \Bigg] \\ -\tfrac{1}{2} s_2 \Omega \Bigg[& \frac{\beta\sin\nu t(1-i) - (\Delta+\nu)\cos\nu t(1+i)}{\beta^2 + (\Delta+\nu)^2}\end{aligned} \tag{3.25}$$

$$+\frac{\mathcal{J}\sin\nu t(1-i)+(\Delta-\nu)\cos\nu t(1-i)}{\mathcal{J}^2+(\Delta-\nu)^2}\Bigg]$$

Noting that $\mathrm{Re}\{\xi\}=u_t$ and $\mathrm{Im}\{\xi\}=v_t$, substituting these expressions for u_t and v_t into equation (3.22), and equating the coefficients of $\sin\nu t$ and $\cos\nu t$, the equations for s_1 and s_2 are found to be

$$\frac{ds_1}{dt}=-\alpha s_1-\gamma s_2, \tag{3.26a}$$

$$\frac{ds_2}{dt}=-\alpha s_2-\gamma s_1, \tag{3.26b}$$

where α and γ are given by

$$\alpha=\frac{\pi k^2\Omega^2}{8m\nu}\left[\frac{\mathcal{J}+(\Delta-\nu)s_0}{\mathcal{J}^2+(\Delta-\nu)^2}+\frac{\mathcal{J}+(\Delta-\nu)s_0}{\mathcal{J}^2+(\Delta-\nu)^2}\right], \tag{3.27a}$$

$$\gamma=\frac{\pi k^2\Omega^2}{8m\nu}\left[\frac{\mathcal{J}s_0-(\Delta+\nu)}{\mathcal{J}^2+(\Delta+\nu)^2}+\frac{\mathcal{J}s_0-(\Delta-\nu)}{\mathcal{J}^2+(\Delta-\nu)^2}\right]+\frac{\pi k^2\Omega}{2m\nu}u_0. \tag{3.27b}$$

The solution of this two-equation system has the form

$$s_1(t)=e^{-\alpha t}(A\sin\nu t+B\cos\nu t), \tag{3.28a}$$

$$s_2(t)=e^{-\alpha t}(B\sin\nu t-A\cos\nu t), \tag{3.28b}$$

where $A=-s_2(0)$ and $B=s_1(0)$. Thus the equation for s_t, equation (3.21), becomes

$$s_t(t)=e^{-\alpha t}[A\sin(\gamma-\nu)t+B\cos(\gamma-\nu)t], \tag{3.29}$$

which is valid whenever: 1) $\mathcal{J}>>\alpha,\gamma$ so that the removal of s_1 and s_2 from the integral of equation (3.24) is valid: 2) $\nu>>\alpha,\gamma$ so that neglecting d^2s_1/dt^2 and d^2s_2/dt^2 in the derivation of equation (3.22) is valid: and 3) $\mathcal{J}>>\Omega$ so that w does not differ significantly from -1.

2. Adiabatic Approximation, β Is The Largest Frequency

A more general case which does not place as strong a condition on Ω and w is to assume that β is much larger than any of the other frequencies in the problem. The Bloch variables as well as s are assumed to have the form

$$f(t)=f_0+f_1(t)\cos\nu t+f_2(t)\sin\nu t \tag{3.30}$$

$$=f_0+\mathrm{Re}\left[F(t)e^{i\nu t}\right],$$

where

$$F(t)=f_1(t)-if_2(t). \tag{3.31}$$

When the second derivative of S as well as the nonlinear terms of equations (3.10) are negligible, the equations of motion for U, V, W, and S are

$$\frac{dU}{dt}=-(i\nu+\beta)U+\Delta V+\Omega s_0 W+\Omega w_0 S, \tag{3.32a}$$

$$\frac{dV}{dt}=-\Delta U-(i\nu+\beta)V+\Omega W, \tag{3.32b}$$

$$\frac{dW}{dt}=-\Omega s_0 U-\Omega V-(i\nu+2\beta)W-\Omega u_0 S, \tag{3.32c}$$

$$\frac{dS}{dt}=\frac{iK}{2\nu}(s_0 U+V+u_0 S). \tag{3.32d}$$

We consider the case where β is much larger than $\frac{dS}{dt}$. U, V, and W relax to their steady state values much faster than S, and at any time the values of U, V, and W in terms of S can be approximated by setting $\frac{dU}{dt}$, $\frac{dV}{dt}$ and $\frac{dW}{dt}$ to zero

and solving

$$\begin{bmatrix} (i\nu+\beta) & -\Delta & -\Omega s_0 \\ \Delta & (i\nu+\beta) & -\Omega \\ \Omega s_0 & \Omega & (i\nu+2\beta) \end{bmatrix} \begin{bmatrix} U \\ V \\ W \end{bmatrix} = \begin{bmatrix} \Omega w_0 \\ 0 \\ -\Omega u_0 \end{bmatrix} S. \tag{3.33}$$

When these values for U and V are used in the equation for S we get

$$\frac{dS}{dt} = -(\alpha + i\gamma)S, \tag{3.34}$$

where α and γ are given by

$$\alpha = \frac{\hbar k^2 \Omega^2}{4m\nu} \left[\frac{D_1 N_1 - D_2 N_2}{D_1^2 + D_2^2} \right], \tag{3.35a}$$

$$\gamma = \frac{\hbar k^2 \Omega^2}{4m\nu} \left[\frac{D_2 N_1 + D_1 N_2}{D_1^2 + D_2^2} \right] + \frac{\hbar k^2 \Omega}{2m\nu} u_0, \tag{3.35b}$$

and N_1, N_2, D_1, and D_2 are given by

$$N_1 = 2\beta^2 w_0 s_0 - 2\beta\Delta w_0 + \beta\Omega u_0 - \nu^2 w_0 s_0, \tag{3.36a}$$

$$N_2 = \nu(\Omega u_0 - \Delta w_0 + 3\beta w_0 s_0), \tag{3.36b}$$

$$D_1 = \nu(5\beta^2 + \Delta^2 + \Omega^2 - \nu^2), \tag{3.36c}$$

$$D_2 = 2\beta(\beta^2 + \Delta^2 + \tfrac{1}{2}\Omega^2 - 2\nu^2). \tag{3.36d}$$

As can be seen α is again a decay constant for the amplitude of s_i and γ is a frequency shift. These expressions for α and γ are valid whenever they are much less than β and ν.

C. Numerical Results

The general equations (3.16) derived in section III.A were integrated numerically for a variety of initial values and frequencies using a fourth-order Runge-Kutta method (14). This allowed comparison to the analytical solutions derived

here for special cases. The Pascal programs used for this are listed in the Appendix.

With $\tau=\nu t$ equations (3.16) take the form

$$\frac{du}{d\tau}=-\frac{\beta}{\nu}u+\frac{\Delta}{\nu}v+\frac{\Omega}{\nu}ws, \tag{3.37a}$$

$$\frac{dv}{d\tau}=-\frac{\Delta}{\nu}u-\frac{\beta}{\nu}v+\frac{\Omega}{\nu}w, \tag{3.37b}$$

$$\frac{dw}{d\tau}=-\frac{\Omega}{\nu}(su+v)-\frac{2\beta}{\nu}(w-1), \tag{3.37c}$$

$$\frac{ds}{d\tau}=q, \tag{3.37d}$$

$$\frac{dq}{d\tau}=-\frac{K}{\nu^2}(su+v)-s. \tag{3.37e}$$

In all of the calculations k was assigned a value of $10^7 m^{-1}$ and m was assigned a value of 10^{-25}kg. These values were chosen because this k is typical for visible light, and 10^{-25}kg is about the mass of barium.

Figure 12 is a graph of s versus time for $\nu=10^5$, $\beta=10^5$, $\Delta=-10^5$, and $\Omega=5\times10^4$. Figure 13 is a graph of the natural log of the amplitude, $A=(s_{max}-s_{min})/2$, of s, versus time for the same values of ν, β, Δ, and Ω. In all cases the $Ln(A)$ versus time plots were linear, indicating exponential decay. A decay constant given by

$$\alpha=-\frac{\ln[A(t_2)]-\ln[A(t_1)]}{t_2-t_1} \tag{3.38}$$

was calculated.

Equation (3.27a) predicts a value for α when Ω is small. Figures 14, 15, and 16 compare α calculated from equation (3.27a) and α obtained from numerical integration of equations (3.37). Figure 14 is a plot of α versus Δ for $\nu=10^5$, $\beta=10^5$, and $\Omega=5\times10^4$. We see that the cooling rate is a maximum for $\Delta=-\nu$. Also, that

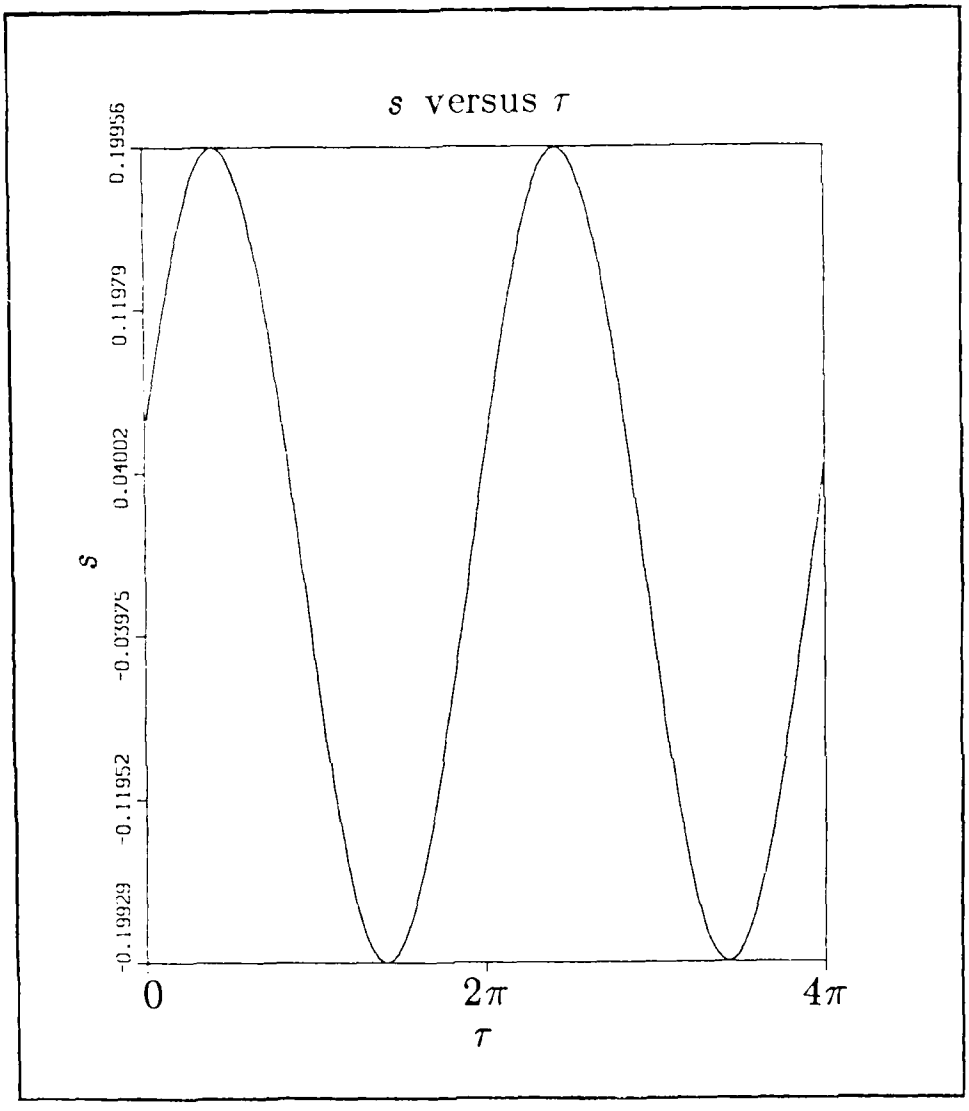

Figure 12. Plot of s versus normalized time, τ, from numerical integration of equations (3.37) for ν=10^6, β=10^5, Δ=-10^6, Ω=5x10^4.

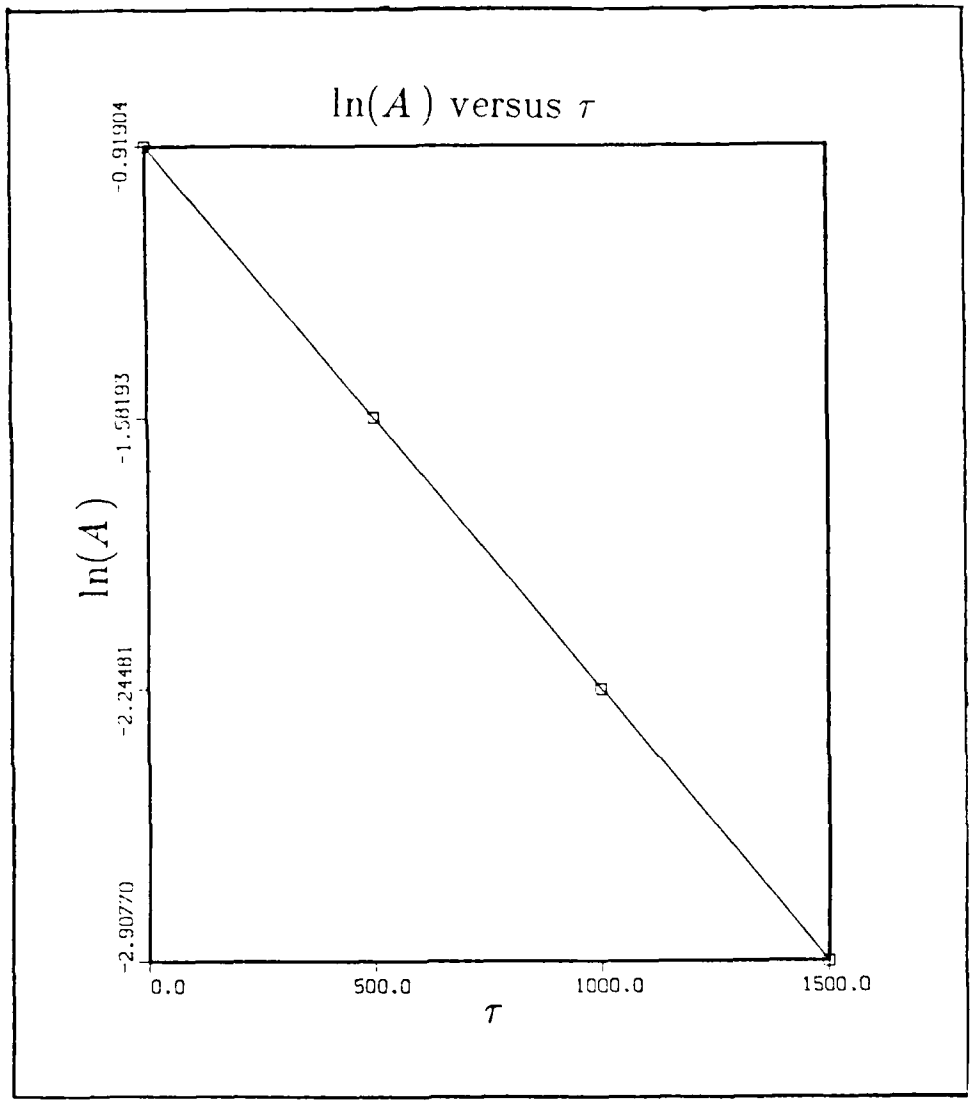

Figure 13. Plot of the natural logarithm of the amplitude of s versus τ from numerical integration of equations (3.37) for ν=10^5, β=10^5, Δ=-10^6, Ω=5x10^4.

the cooling rate becomes negative, which corresponds to heating, when $\Delta > 0$. Figure 15 is a plot of α versus $\mathcal{J}$ for $\nu=10^6$, $\Delta=-1.5\times10^5$, and $\Omega=5\times10^4$. Notice that maximum cooling occurs for $\mathcal{J}\approx\frac{1}{2}\nu$. Figure 16 is a plot of α versus Ω for $\nu=10^5$, $\mathcal{J}=10^6$, and $\Delta=-10^5$. The conditions under which equation (3.27a) is valid are that Ω be enough smaller than $\mathcal{J}$ so that w does not differ appreciably from -1. For the values of ν, Δ, and $\mathcal{J}$ used for this plot, there is good agreement for $\Omega<0.4\mathcal{J}$.

Equation (3.35a) gives a value for α when $\mathcal{J},\nu>>\alpha,\gamma$. Figures 17, 18, 19 compare α calculated from equation (3.35a) and α obtained from numerical integration of equations (3.37). Figure 17 is a plot of α versus Δ for $\nu=10^5$, $\mathcal{J}=10^7$, and $\Omega=10^5$. The cooling rate again becomes negative for positive Δ. Figure 18 is a plot of α versus $\mathcal{J}$ for $\nu=10^6$, $\Delta=-10^6$, and $\Omega=10^6$. Again maximum cooling occurs for $\mathcal{J}\approx\frac{1}{2}\nu$. Figure 19 is a plot of α versus Ω for $\nu=10^5$, $\mathcal{J}=10^7$, and $\Delta=-10^5$. For larger Ω the two curves again fail to agree, but the value for α calculated from equation (3.35a) does reach a maximum and begin to decrease. This general behavior agrees with that shown by the numerical integration. Equation (3.27a) does not exhibit this.

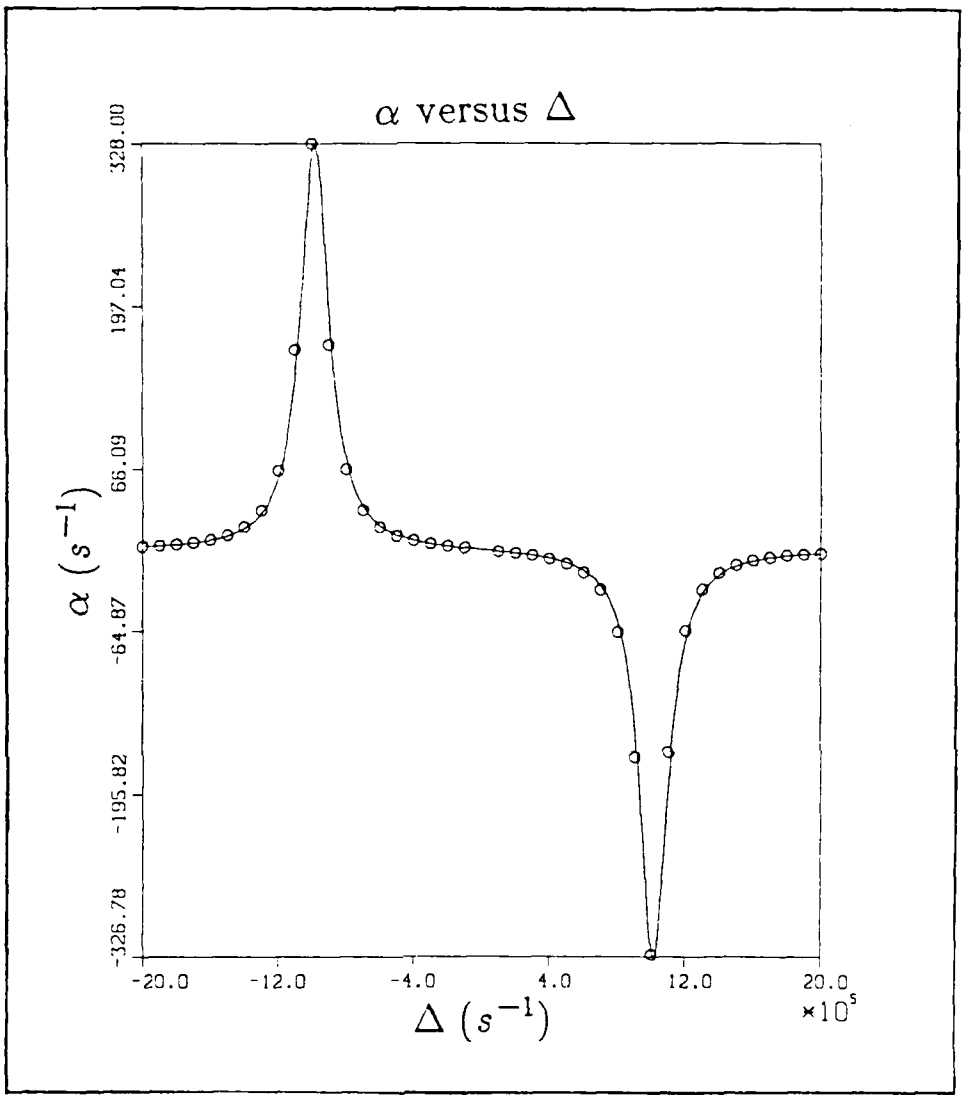

Figure 14. Plot of α versus Δ for ν=10^6, β=10^5, and Ω=5x10^4. The solid line represents the values of α calculated from equation (3.27a) and the circles are values of α calculated from numerical integration of equations (3.37).

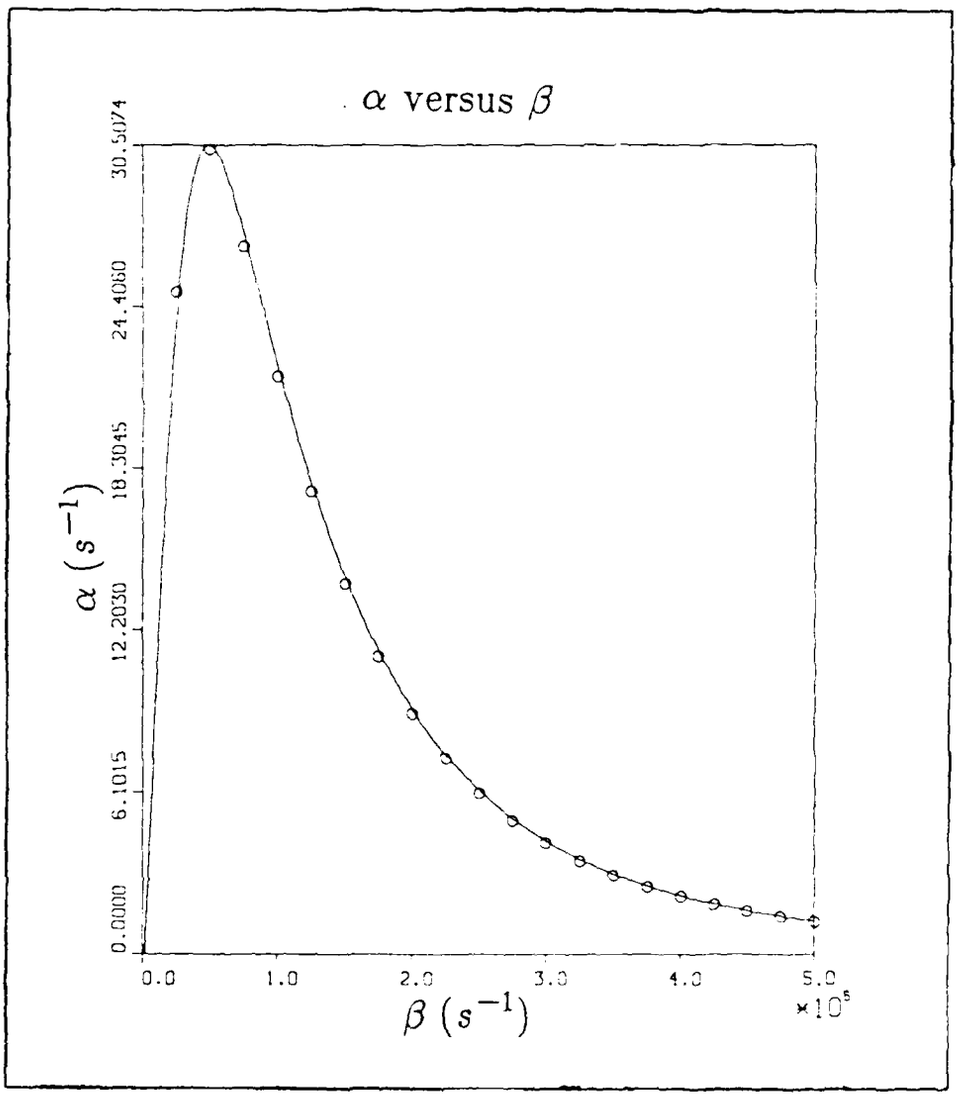

Figure 15. Plot of α versus β for ν=10^6, Δ=$-1.5\text{x}10^5$, and Ω=$5\text{x}10^4$. The solid line represents the values of α calculated from equation (3.27a) and the circles are values of α calculated from equation (3.37).

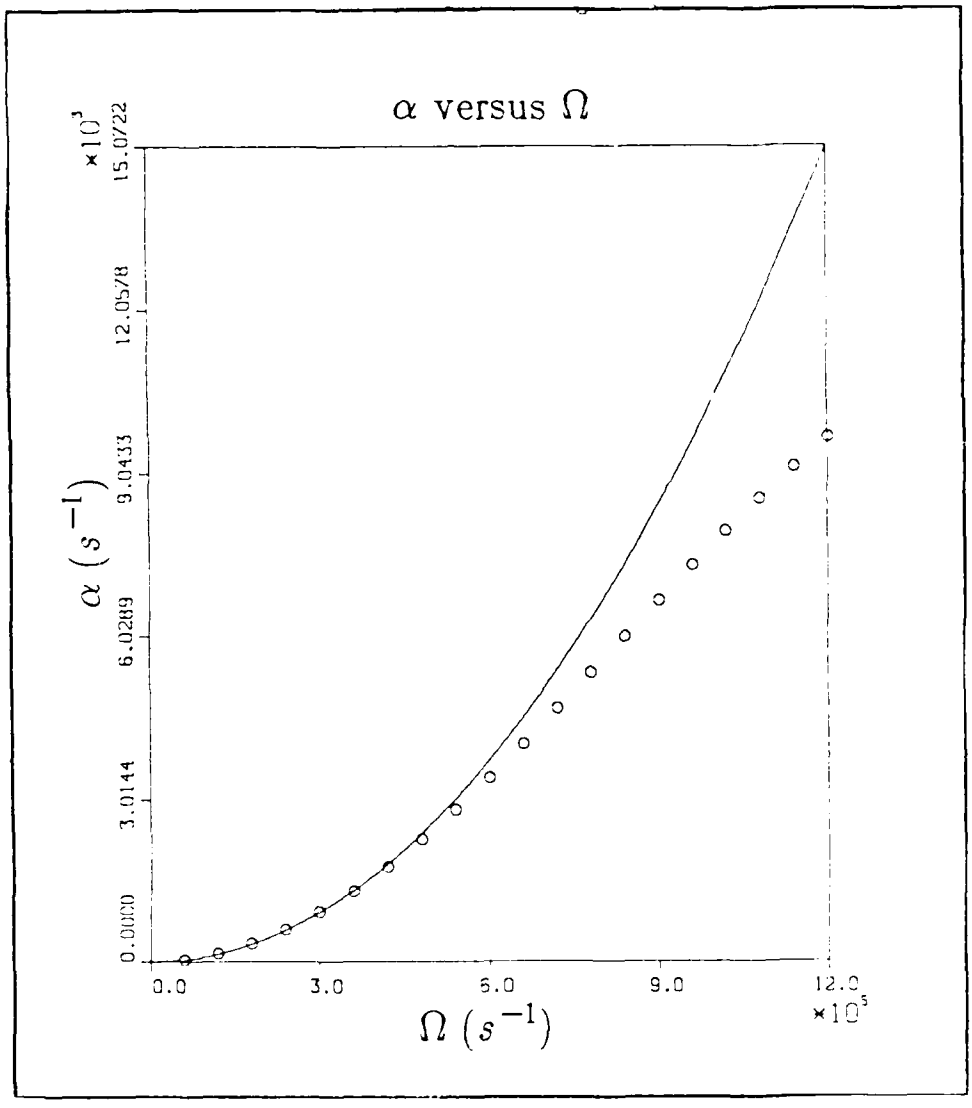

Figure 16. Plot of α versus β for ν=10^6, β=10^6, and Δ=-10^6. The solid line represents the values of α calculated from equation (3.27a) and the circles are values of α calculated from equation (3.37).

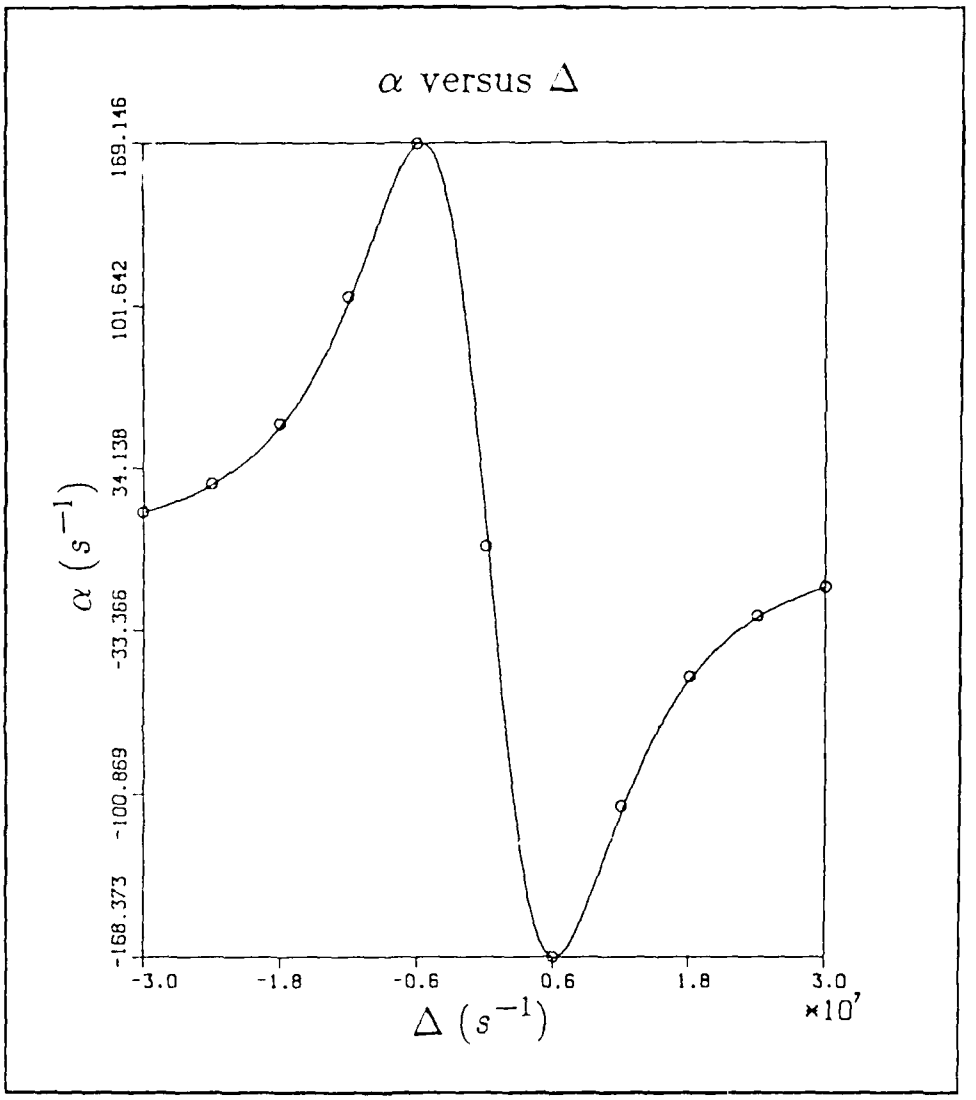

Figure 17. Plot of α versus Δ for ν=10^6, δ=10^7, and Ω=10^6. The solid line represents the values of α calculated from equation (3.35a) and the circles are values of α calculated from equation (3.37).

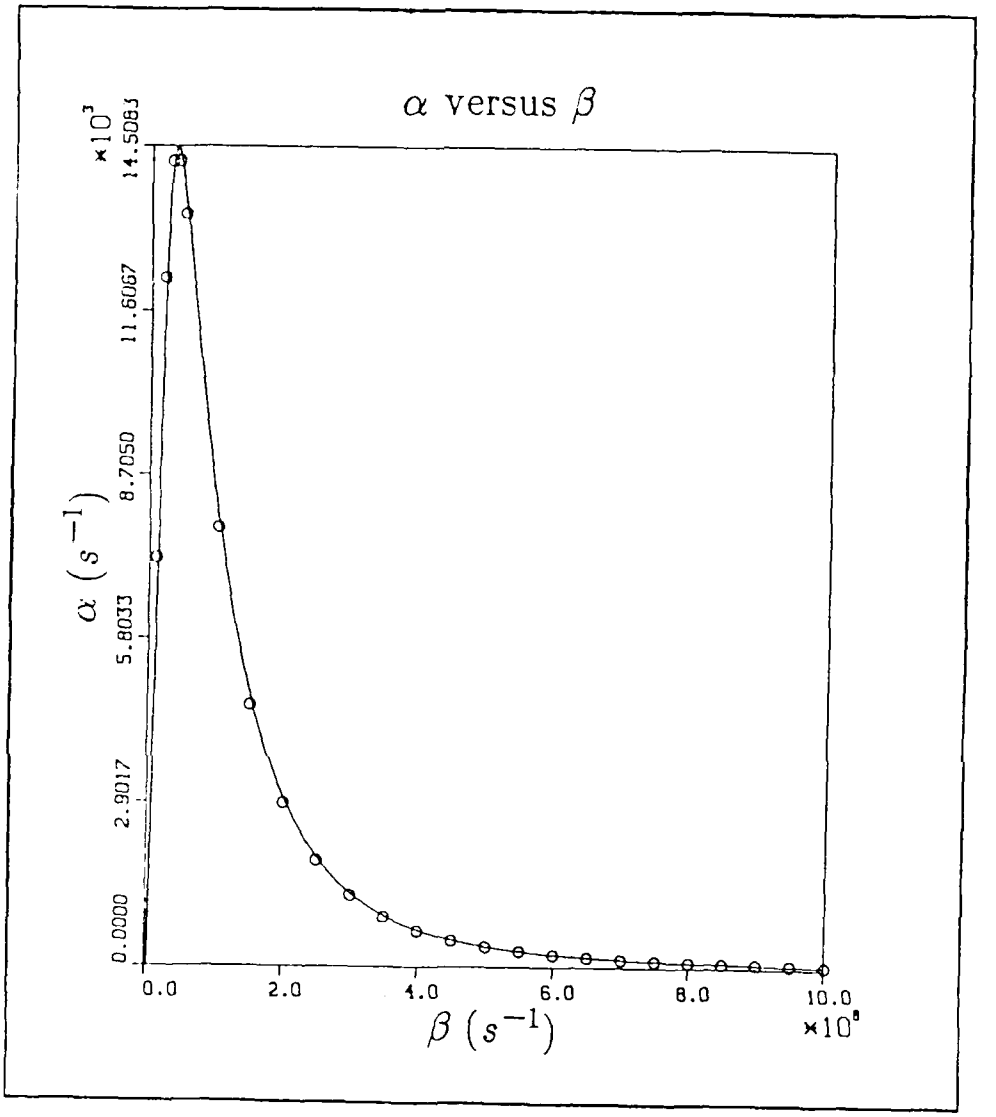

Figure 18. Plot of α versus β for ν=10^6, Δ=-10^6, and Ω=10^6. The solid line represents the values of α calculated from equation (3.35a) and the circles are values of α calculated from equation (3.37).

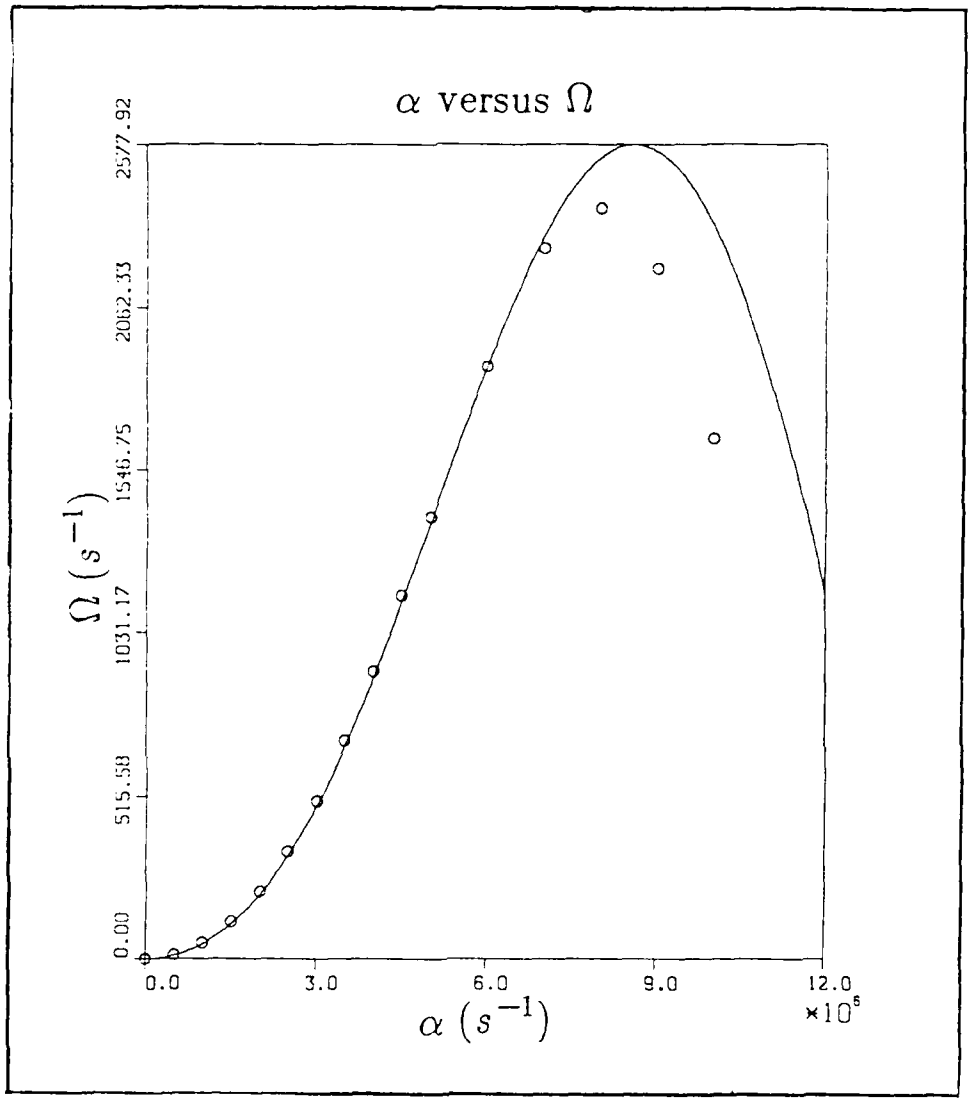

Figure 19. Plot of α versus Ω for $\nu=10^6$, $\beta=10^7$, and $\Delta=-10^6$. The solid line represents the values of α calculated from equation (3.35a) and the circles are values of α calculated from equation (3.37).

IV. Single Atom Spectroscopy: Ladder-Configuration

For the four-level system shown in Figure 2, the following assumptions about the Einstein A coefficients and the dipole transition moments between the various states will be made:

$$A_{30}=A_{31}=A_{20}=0, \tag{4.1a}$$

$$A_{21}<<A_{10},A_{32}, \tag{4.1b}$$

which imply

$$\mu_{30}=\mu_{31}=\mu_{20}=0, \tag{4.2a}$$

$$\mu_{21}<<\mu_{10},\mu_{32}. \tag{4.2b}$$

In addition, μ_{10}, μ_{21}, and μ_{32} will be taken to be real. The applied electric field is assumed to have the form

$$E(t)=E_1\cos\omega_1 t+E_2\cos\omega_2 t+E_3\cos\omega_3 t \tag{4.3}$$

with components at frequencies ω_1, ω_2, and ω_3 near to resonance with the three transition frequencies ω_{10}, ω_{21}, and ω_{32} respectively.

A. Dressed Atom Approach

A simple picture which shows some of the qualitative aspects of the ladder configuration is the dressed atom approach. Without spontaneous emission, the Hamiltonian matrix for this system in the rotating wave approximation is block diagonal (24) when the basis states are: 1) the atom in the ground state and n_1 photons of frequency ω_1, n_2 photons of frequency ω_2, and n_3 photons of frequency

ω_3, state $|0,n_1,n_2,n_3>$; 2) the atom in the first excited state and n_1-1 photons of frequency ω_1, etc., state $|1,n_1-1,n_2,n_3>$; 3) state $|2,n_1-1,n_2-1,n_3>$; and 4) state $|3,n_1-1,n_2-1,n_3-1>$. A representative block is

$$H_{ij}=\hbar(n_1\omega_1+n_2\omega_2+n_3\omega_3)\hat{I} \tag{4.4}$$

$$+\hbar\begin{bmatrix} 0 & \frac{1}{2}i\Omega_1 & 0 & 0 \\ -\frac{1}{2}i\Omega_1 & -\Delta_1 & \frac{1}{2}i\Omega_2 & 0 \\ 0 & -\frac{1}{2}i\Omega_2 & -\Delta_1-\Delta_2 & \frac{1}{2}i\Omega_3 \\ 0 & 0 & -\frac{1}{2}i\Omega_3 & -\Delta_1-\Delta_2-\Delta_3 \end{bmatrix}$$

where $\hat{I}$ is the identity matrix and

$$\Delta_1=\omega_1-\omega_{10}, \tag{4.5a}$$

$$\Delta_2=\omega_2-\omega_{21}, \tag{4.5b}$$

$$\Delta_3=\omega_3-\omega_{32} \tag{4.5c}$$

are the detunings on the various transitions, and

$$\Omega_1=\frac{\mu_{10}E_1}{\hbar}, \tag{4.6a}$$

$$\Omega_2=\frac{\mu_{21}E_2}{\hbar}, \tag{4.6b}$$

$$\Omega_3=\frac{\mu_{32}E_3}{\hbar} \tag{4.6c}$$

are the on-resonance Rabi frequencies for the three transitions being considered. This is a nearly degenerate system; the differences in energy between the states being just $\hbar$ times the appropriate Δ_i's. The dressed states are the states

obtained by diagonalizing the Hamiltonian. The dressed state energies are

$$E_i' = E_i - \hbar\lambda_i \tag{4.7}$$

where the λ_i are solutions of

$$\lambda(\lambda+\Delta_1)(\lambda-\Delta_1-\Delta_2)(\lambda+\Delta_1+\Delta_2+\Delta_3)-\frac{1}{4}\Omega_2^2\lambda(\lambda+\Delta_1+\Delta_2+\Delta_3) \tag{4.8}$$

$$-\frac{1}{4}\Omega_3^2\lambda(\lambda+\Delta_1)-\frac{1}{4}\Omega_1^2(\lambda+\Delta_1+\Delta_2)(\lambda+\Delta_1+\Delta_2+\Delta_3)+\frac{1}{16}\Omega_1^2\Omega_3^2=0$$

For $\Omega_2=0$ and Δ_1, $\Delta_3=0$ the solutions to equation (4.8) are

$$\lambda_1=-\tfrac{1}{2}\Omega_1 \tag{4.9a}$$

$$\lambda_2=+\tfrac{1}{2}\Omega_1 \tag{4.9b}$$

$$\lambda_3=-\tfrac{1}{2}\Omega_3 \tag{4.9c}$$

$$\lambda_4=+\tfrac{1}{2}\Omega_3 \tag{4.9d}$$

These λ's correspond to eigenstates for the characteristic block of the Hamiltonian matrix. The transformation matrix between the old states and these eigenstates is

$$T=\frac{1}{2^{\frac{1}{2}}}\begin{bmatrix} i & 1 & 0 & 0 \\ 1 & i & 0 & 0 \\ 0 & 0 & i & 1 \\ 0 & 0 & 1 & i \end{bmatrix} \tag{4.10}$$

This transformation diagonalizes the Hamiltonain when Δ_1, $\Delta_3=0$ and $\Omega_2=0$. When the Hamiltonian is diagonal, the basis states are stationary, that is there are no transitions between them. Figure 20 is an energy level diagram for the new states. If Ω_2 is turned on, there will be transitions between these states. In the old system, the transition frequency between state $|1,n_1-1,n_3\rangle$ and $|2,n_1-1,n_3\rangle$ was ω_{21}. There are four transition frequencies among the new states, shifted from ω_{21} by $\pm\frac{1}{2}(\Omega_1-\Omega_3)$ and $\pm\frac{1}{2}(\Omega_1+\Omega_3)$. Thus the dressed state approach provides quick, qualitative information about the four state system. To understand in more

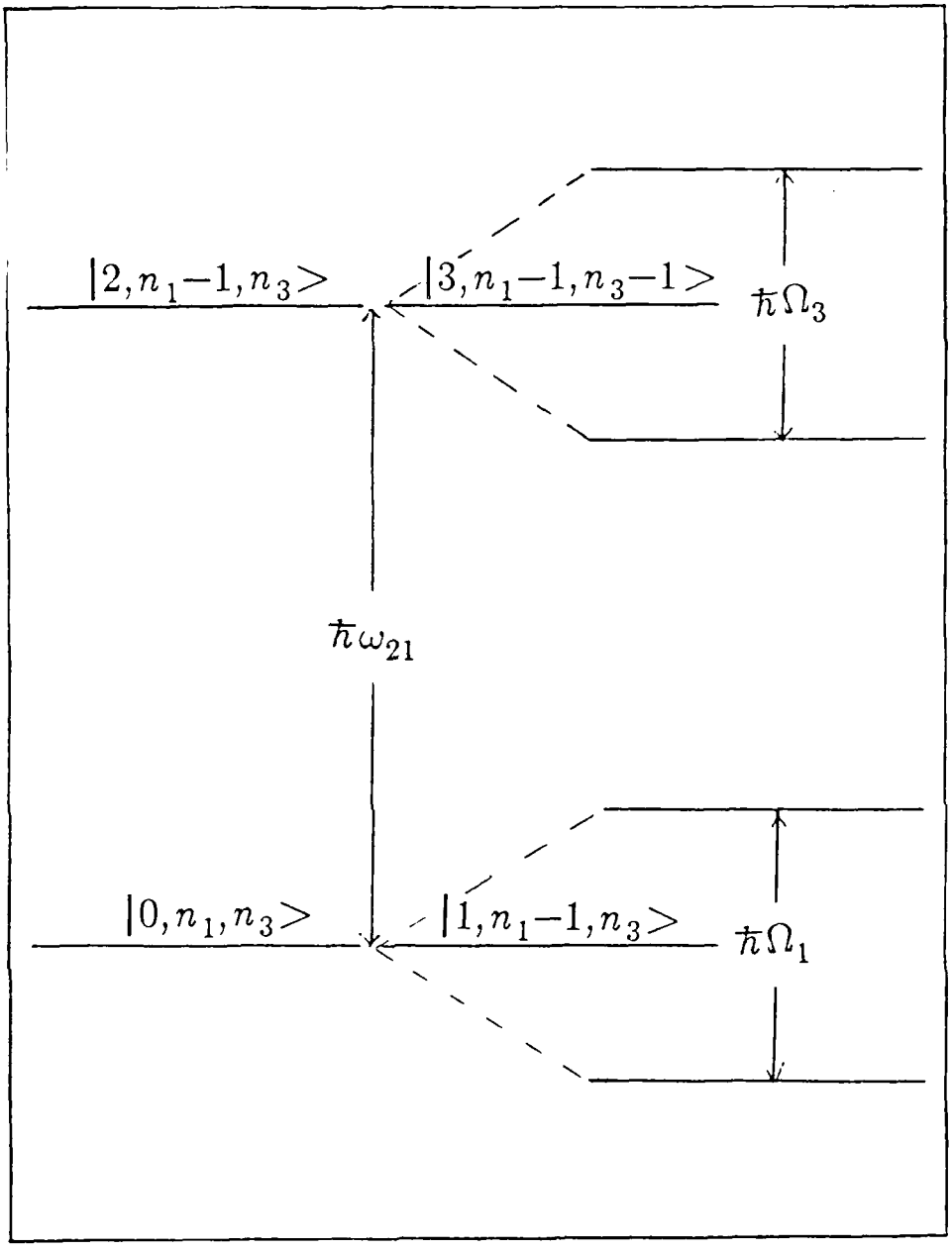

Figure 20. Energy Levels of Dressed States.

detail what the character of the fluorescence will be, it is helpful to turn to the optical Bloch equations.

B. Optical Bloch Equation Approach

The strategy we will use to extract numerical information about the fluorescence, such as the average dwell time in the upper two states, is similar to the approach taken in reference (23). Reference (23) deals with coherent excitation of the V configuration. In that paper the authors show that under certain general conditions, excitation of the weak transition can be treated as a rate process when viewed over coarse-grained intervals of time. Being able to treat the excitation of the weak transition as a rate process greatly simplifies the analysis of the statistics of the fluorescence. A similar proof will be given for the Ladder configuration.

1. Development of Optical Bloch Equations

The equations of motion for the components of the density-matrix, ρ_{nm}, of a coherently excited, multi-level system, in the electric dipole approximation are (27)

$$\frac{d\rho_{nn}}{dt}=\frac{dP_n}{dt}=-\sum_{r<n}A_{nr}P_n+\sum_{r>n}A_{rn}P_r+\frac{E(t)}{i\hbar}\sum_r(\rho_{nr}\mu_{rn}-\mu_{nr}\rho_{rn}) \qquad (4.11a)$$

for n = m, and

$$\frac{d\rho_{nm}}{dt}=-\left(i\omega_{nm}+\tfrac{1}{2}\sum_{r<n}A_{nr}+\tfrac{1}{2}\sum_{r<m}A_{mr}\right)\rho_{nm}+\frac{E(t)}{i\hbar}\sum_r\rho_{nr}\mu_{rm}-\mu_{nr}\rho_{rm}) \qquad (4.11b)$$

for $n \neq m$, where P_n is the probability to be in the nth state. The off-diagonal elements or coherences vary much more rapidly than the probabilities. It is on-

venient to work with the slowly varying coherences, σ_{ij}, defined by the equations

$$\rho_{01}=\sigma_{01}e^{i\omega_1 t}, \tag{4.12a}$$

$$\rho_{02}=\sigma_{02}e^{i(\omega_1+\omega_2)t}, \tag{4.12b}$$

$$\rho_{03}=\sigma_{03}e^{i(\omega_1+\omega_2+\omega_3)t}, \tag{4.12c}$$

$$\rho_{12}=\sigma_{12}e^{i\omega_2 t}, \tag{4.12d}$$

$$\rho_{13}=\sigma_{13}e^{i(\omega_2+\omega_3)t}, \tag{4.12e}$$

$$\rho_{23}=\sigma_{23}e^{i\omega_3 t}. \tag{4.12f}$$

We shall also work with the inversions

$$w_1=P_1-P_0, \tag{4.13a}$$

$$w_2=P_2-P_1, \tag{4.13b}$$

$$w_3=P_3-P_2, \tag{4.13c}$$

and the probabilities

$$P_-=P_0+P_1, \tag{4.14a}$$

$$P_+=P_2+P_3. \tag{4.14b}$$

Note that P_- is the probability to be in one of the lower two states and P_+ is the probability to be in one of the upper two states. Consider two cases: 1) when $P_-=1$ and $P_+=0$ we would expect to observe scattered light of frequency ω_1. 2) when $P_-=0$ and $P_+=1$ we expect to observe scattered light of frequency ω_3. During an actual experiment, the status of the system will be constantly monitored on a time scale which is short compared to the rate of change of P_- and P_- derived from the Schrodinger equation, so that case 1) or 2) will always apply, and the system will change abruptly between the two. This is what is meant by a

quantum jump.

The equations of motion for the inversions, the σ_{ij}'s, and the probabilities in the rotating wave approximation, are:

$$\frac{dw_1}{dt}=-\tfrac{1}{2}(A_{10}-\tfrac{1}{2}A_{21})-\tfrac{1}{2}(A_{10}-\tfrac{1}{2}A_{21})w_1-(A_{10}-\tfrac{1}{2}A_{21})w_2-\tfrac{1}{2}(A_{10}-\tfrac{1}{2}A_{21})w_3$$

$$-i\Omega_1(\sigma_{10}-\sigma_{01})-\tfrac{1}{2}i\Omega_2(\sigma_{21}-\sigma_{12}). \tag{4.15a}$$

$$\frac{dw_2}{dt}=\frac{1}{4}(A_{10}-2A_{21}-A_{32})-\frac{1}{4}(A_{10}-2A_{21}-A_{32})w_1$$

$$-\frac{1}{2}(A_{10}-2A_{21}-A_{32})w_2-\frac{1}{4}(A_{10}-2A_{21}-3A_{32})w_3 \tag{4.15b}$$

$$-i\Omega_2(\sigma_{21}-\sigma_{12})+\tfrac{1}{2}i\Omega_1(\sigma_{10}-\sigma_{01})+\tfrac{1}{2}i\Omega_3(\sigma_{32}-\sigma_{23}).$$

$$\frac{dw_3}{dt}=-\tfrac{1}{2}(A_{32}-\tfrac{1}{2}A_{21})-\tfrac{1}{2}(A_{32}-\tfrac{1}{2}A_{21})w_1-(A_{32}-\tfrac{1}{2}A_{21})w_2-\tfrac{1}{2}(3A_{32}-\tfrac{1}{2}A_{21})w_3$$

$$-i\Omega_3(\sigma_{32}-\sigma_{23})+i\tfrac{1}{2}\Omega_2(\sigma_{21}-\sigma_{12}). \tag{4.15c}$$

$$\frac{d\sigma_{01}}{dt}=-(\tfrac{1}{2}A_{10}+i\Delta_1)\sigma_{01}-\tfrac{1}{2}i\Omega_2\sigma_{02}+\tfrac{1}{2}i\Omega_1 w_1. \tag{4.15d}$$

$$\frac{d\sigma_{02}}{dt}=-(\tfrac{1}{2}A_{10}+i(\Delta_1+\Delta_2))\sigma_{02}-\tfrac{1}{2}i\Omega_2\sigma_{01}-\tfrac{1}{2}i\Omega_3\sigma_{03}+\tfrac{1}{2}i\Omega_1\sigma_{12}. \tag{4.15e}$$

$$\frac{d\sigma_{03}}{dt}=-(\tfrac{1}{2}A_{32}+i(\Delta_1+\Delta_2+\Delta_3))\sigma_{03}+\tfrac{1}{2}i\Omega_1\sigma_{13}-\tfrac{1}{2}i\Omega_3\sigma_{02}. \tag{4.15f}$$

$$\frac{d\sigma_{12}}{dt}=-(\tfrac{1}{2}(A_{10}-A_{21})+i\Delta_2)\sigma_{12}+\tfrac{1}{2}i\Omega_1\sigma_{02}+\tfrac{1}{2}i\Omega_2 w_2-\tfrac{1}{2}i\Omega_3\sigma_{13}. \tag{4.15g}$$

$$\frac{d\sigma_{13}}{dt}=-\tfrac{1}{2}(A_{10}-A_{32})-i(\Delta_2-\Delta_3)\sigma_{13}-\tfrac{1}{2}i\Omega_1\sigma_{23}-\tfrac{1}{2}i\Omega_2\sigma_{23}-\tfrac{1}{2}i\Omega_3\sigma_{12} \tag{4.15h}$$

$$\frac{d\sigma_{23}}{dt}=-\tfrac{1}{2}(A_{32}-A_{21})-i\Delta_3\sigma_{23}-\tfrac{1}{2}i\Omega_2\sigma_{13}-\tfrac{1}{2}i\Omega_3 w_3 \tag{4.15i}$$

$$\frac{dP_-}{dt}=-\frac{dP_+}{dt}=\tfrac{1}{2}A_{21}(P_+-w_3)+\tfrac{1}{2}i\Omega_2(\sigma_{21}-\sigma_{12}) \tag{4.15j}$$

2. Steady State Solutions of the Bloch Equations

We will first consider the steady state solutions to equations (4.15). For algebraic simplicity the detunings on the strong transitions, Δ_1 and Δ_3, will be set to zero. We will define the complex quantities, N_1, N_2, N_3, and N_4 as

$$N_1=A_{21}+2i\Delta_2, \tag{4.16a}$$

$$N_2=A_{32}+2i\Delta_2, \tag{4.16b}$$

$$N_3=A_{10}+A_{21}+2i\Delta_2, \tag{4.16c}$$

$$N_4=A_{10}+A_{32}+2i\Delta_2, \tag{4.16d}$$

The system that must be solved for the steady state solutions of the σ_{ij}'s in terms of the w_i's is

$$\begin{bmatrix} A_{10} & i\Omega_2 & 0 & 0 & 0 & 0 \\ i\Omega_2 & N_1 & i\Omega_3 & -i\Omega_1 & 0 & 0 \\ 0 & i\Omega_3 & N_2 & 0 & -i\Omega_1 & 0 \\ 0 & -i\Omega_1 & 0 & N_3 & i\Omega_3 & 0 \\ 0 & 0 & -i\Omega_1 & i\Omega_3 & N_4 & -i\Omega_2 \\ 0 & 0 & 0 & 0 & -i\Omega_2 & (A_{32}+A_{21}) \end{bmatrix} \begin{bmatrix} \sigma_{01} \\ \sigma_{02} \\ \sigma_{03} \\ \sigma_{12} \\ \sigma_{13} \\ \sigma_{23} \end{bmatrix} = i \begin{bmatrix} \Omega_1 w_1 \\ 0 \\ 0 \\ \Omega_2 w_2 \\ 0 \\ \Omega_3 w_3 \end{bmatrix} \tag{4.17}$$

The steady state solutions for the w_i's depend only on the imaginary parts of σ_{01},

σ_{12}, and σ_{32}. From equation (4.17) σ_{21}, σ_{12}, and σ_{32} are found to be

$$\sigma_{21}=\frac{i\Omega_1}{D}\Big[\Omega_1^2(A_{32}+A_{21})(\Omega_1^2-\Omega_3^2+N_2N_4)-\Omega_2^2(A_{32}-A_{21})(\Omega_3^2-\Omega_1^2+N_3N_4)$$

$$+\Omega_2^2(N_1N_2N_3-\Omega_1^2N_2-\Omega_3^2N_3) \tag{4.18a}$$

$$+(A_{32}+A_{21})N_1(N_2N_3N_4-\Omega_1^2N_3-\Omega_3^2N_2)\Big]w_1$$

$$-\Omega_2^2\Big[(A_{32}+A_{21})(\Omega_1^2-\Omega_3^2+N_2N_4)-\Omega_2^2N_2\Big]w_2-\Omega_3^2\Omega_2^2(N_2-N_3)w_3\Big]$$

$$\sigma_{12}=\frac{i\Omega_2}{D}\Big[\Omega_2^2(A_{32}+A_{21})(N_2N_4+\Omega_1^2)-\Omega_2^4N_2+\Omega_3^2A_{10}(A_{32}+A_{21})N_4-\Omega_3^2A_{10}\Omega_2^2$$

$$+A_{10}(A_{32}+A_{21})N_1(N_2N_4+\Omega_1^2)+\Omega_2^2A_{10}N_1N_2\Big]w_2 \tag{4.18b}$$

$$+\Omega_1^2\Big[(A_{32}+A_{21})(\Omega_1^2-\Omega_3^2+N_2N_4)+\Omega_2^2N_2\Big]w_1$$

$$+\Omega_3^2\Big[A_{10}(\Omega_3^2-\Omega_1^2+N_1N_2)+\Omega_2^2N_2\Big]w_3\Big]$$

$$\sigma_{23}=\frac{i\Omega_3}{D}\Big[\Omega_1^2A_{10}(\Omega_1^2-\Omega_3^2+N_2N_4)+\Omega_3^2A_{10}(\Omega_3^2-\Omega_1^2+N_3N_4)$$

$$+\Omega_2^2(N_2N_3N_4+\Omega_1^2N_3+\Omega_3^2N_2) \tag{4.18c}$$

$$+A_{10}N_1(N_2N_3N_4+\Omega_1^2N_3+\Omega_3^2N_2)\Big]w_3$$

$$-\Omega_1^2\Omega_2^2(N_2-N_3)w_1+\Omega_2^2\Big[A_{10}(\Omega_3^2-\Omega_1^2+N_1N_2)+\Omega_2^2N_2\Big]w_2\Big].$$

where D, the determinant of the matrix in equation (4.17), is

$$D=\Omega_2^4(N_2N_3-\Omega_2^2A_{10}(N_1N_2N_3-\Omega_1^2N_2-\Omega_3^2N_3)$$

$$+\Omega_2^2A_{32}(N_2N_3N_4+\Omega_1^2N_3-\Omega_3^2N_2)-\Omega_1^2A_{10}A_{32}(\Omega_1^2-\Omega_3^2+N_2N_4) \quad (4.19)$$

$$+\Omega_3^2A_{10}A_{32}(\Omega_3^2-\Omega_1^2+N_3N_4)+A_{10}A_{32}N_1(N_2N_3N_4-\Omega_1^2N_3-\Omega_3^2N_2)$$

In matrix form equations (4.18) are

$$\begin{bmatrix}\sigma_{01}\\ \sigma_{12}\\ \sigma_{23}\end{bmatrix}=\begin{bmatrix}z_{11} & z_{12} & z_{13}\\ z_{21} & z_{22} & z_{23}\\ z_{31} & z_{32} & z_{33}\end{bmatrix}\begin{bmatrix}w_1\\ w_2\\ w_3\end{bmatrix} \quad (4.20)$$

where the z_{ij}'s are defined by equations (4.18). Taking $y_{ij}=\mathrm{Im}(z_{ij})$, one may write the equations for the steady state values of the w_i's as

$$(-\tfrac{1}{2}A_{10}-2\Omega_1y_{11}+\Omega_2y_{21})w_1+(A_{10}-2\Omega_1y_{12}+\Omega_2y_{22})w_2$$

$$+(\tfrac{1}{2}A_{10}-2\Omega_1y_{13}+\Omega_2y_{23})w_3=\tfrac{1}{2}(A_{10}-\tfrac{1}{2}A_{21}) \quad (4.21a)$$

$$\left(\frac{1}{4}(A_{10}-2A_{21}+A_{32})+\Omega_1y_{11}-2\Omega_2y_{21}+\Omega_3y_{31}\right)w_1$$

$$+\left(\tfrac{1}{2}(-A_{10}-2A_{21}+A_{32})+\Omega_1y_{12}-2\Omega_2y_{22}+\Omega_3y_{32}\right)w_2 \quad (4.21b)$$

$$+\left(\frac{1}{4}(-A_{10}+2A_{21}+3A_{32})+\Omega_1y_{13}-2\Omega_2y_{23}+\Omega_3y_{33}\right)w_3=\tfrac{1}{2}(A_{21}-\tfrac{1}{2}A_{10}-A_{32})$$

$$(-\tfrac{1}{2}A_{32}-\Omega_2 y_{21}-2\Omega_3 y_{31})w_1+(-A_{32}-\Omega_2 y_{22}-2\Omega_3 y_{32})w_2$$

$$+(-\frac{3}{2}A_{32}-\Omega_2 y_{23}-2\Omega_3 y_{33})w_3=\tfrac{1}{2}(A_{32}-\tfrac{1}{2}A_{21}) \qquad (4.21c)$$

or in matrix form

$$\begin{bmatrix} a_{11} & a_{12} & a_{13} \\ a_{21} & a_{22} & a_{23} \\ a_{31} & a_{32} & a_{33} \end{bmatrix} \begin{bmatrix} w_1 \\ w_2 \\ w_3 \end{bmatrix} = \tfrac{1}{2} \begin{bmatrix} A_{10}-\tfrac{1}{2}A_{21} \\ A_{21}-\tfrac{1}{2}(A_{10}+A_{32}) \\ A_{32}-\tfrac{1}{2}A_{21} \end{bmatrix} \qquad (4.22)$$

where the a_{ij}'s are defined by equations (4.21). We define A as the determinant of the a_{ij} matrix. The solutions for the w_i's are

$$w_1=\frac{1}{2A}\Big[A_{10}(a_{22}a_{33}-a_{23}a_{32})-\tfrac{1}{2}(a_{13}a_{32}-a_{12}a_{33})$$

$$+A_{21}(a_{13}a_{32}-a_{12}a_{33})-\tfrac{1}{2}(a_{22}a_{33}-a_{23}a_{32})-\tfrac{1}{2}(a_{12}a_{23}-a_{13}a_{22}) \qquad (4.23a)$$

$$+A_{32}(a_{12}a_{23}-a_{13}a_{22})-\tfrac{1}{2}(a_{13}a_{32}-a_{12}a_{33})\Big]$$

$$w_2=\frac{1}{2A}\Big[A_{10}(a_{23}a_{31}-a_{21}a_{33})-\tfrac{1}{2}(a_{11}a_{33}-a_{13}a_{31})$$

$$+A_{21}(a_{11}a_{33}-a_{13}a_{31})-\tfrac{1}{2}(a_{23}a_{31}-a_{21}a_{33})-\tfrac{1}{2}(a_{13}a_{21}-a_{11}a_{23}) \qquad (4.23b)$$

$$+A_{32}(a_{13}a_{21}-a_{11}a_{23})-\tfrac{1}{2}(a_{11}a_{33}-a_{13}a_{31})\Big]$$

$$w_3=\frac{1}{2A}\Big[A_{10}(a_{21}a_{32}-a_{22}a_{31})-\tfrac{1}{2}(a_{12}a_{31}-a_{11}a_{32})$$

$$+A_{21}(a_{12}a_{31}-a_{11}a_{32})-\tfrac{1}{2}(a_{21}a_{32}-a_{22}a_{31})-\tfrac{1}{2}(a_{11}a_{22}-a_{12}a_{21}) \qquad (4.23c)$$

$$+A_{32}(a_{11}a_{22}-a_{12}a_{21})-\tfrac{1}{2}(a_{12}a_{31}-a_{11}a_{32})\Big]$$

Note that the steady state value of P_+ is given by

$$P_+=\tfrac{1}{2}(1+w_1+2w_2+w_3) \qquad (4.24)$$

Let us now consider the steady value of P_- as a function of Δ_2. Using the second Pascal program listed in the Appendix, P_- was calculated as a function of Δ_2 for various values of Ω_1, Ω_2, and Ω_3. Figure 21 is a plot of P_- versus Δ_2 for $A_{10}=10^5$, $A_{21}=1$, $A_{32}=1.25\times10^5$, $\Omega_1=10^7$, $\Omega_2=10^3$, and $\Omega_3=2\times10^7$. Note the peaks in the spectrum of P_- at $\Delta_2=\pm\frac{1}{2}(\Omega_1-\Omega_3)$ and $\Delta_2=\pm\frac{1}{2}(\Omega_1-\Omega_3)$ which agree with the dressed states results.

3. Adiabatic Solution of the Bloch Equations

A more useful approximation than the steady state solution is the adiabatic approximation. To determine the statistics of fluorescence, we are interested in how P_+ and P_- vary, not so much in how the coherences and inversions on the individual transitions vary. Note that in the equations for the time derivatives of w_1, w_3, σ_{01}, σ_{03}, σ_{12}, σ_{13}, and σ_{23} there are large self relaxation terms. The probabilities P_- and P_+ vary much more slowly than these other quantities. At this point it is difficult to tell how σ_{02} varies. It is reasonable to suppose that these quantities relax to their steady state values much faster than P_- and P_+ change. We begin by solving for the steady state solutions of σ_{01}, σ_{12}, and σ_{23} in terms of w_1, w_3, $U=\sigma_{20}+\sigma_{02}$, $V=i(\sigma_{20}-\sigma_{02})$, and $W=P_+-P_-$. The equation for σ_{01} can be solved by inspection. The solution is

$$\sigma_{01}=\frac{i}{A_{10}}(\Omega_1 w_1-\tfrac{1}{2}\Omega_2(U+iV))=r_{11}w_1+r_{13}U+r_{14}V \tag{4.25}$$

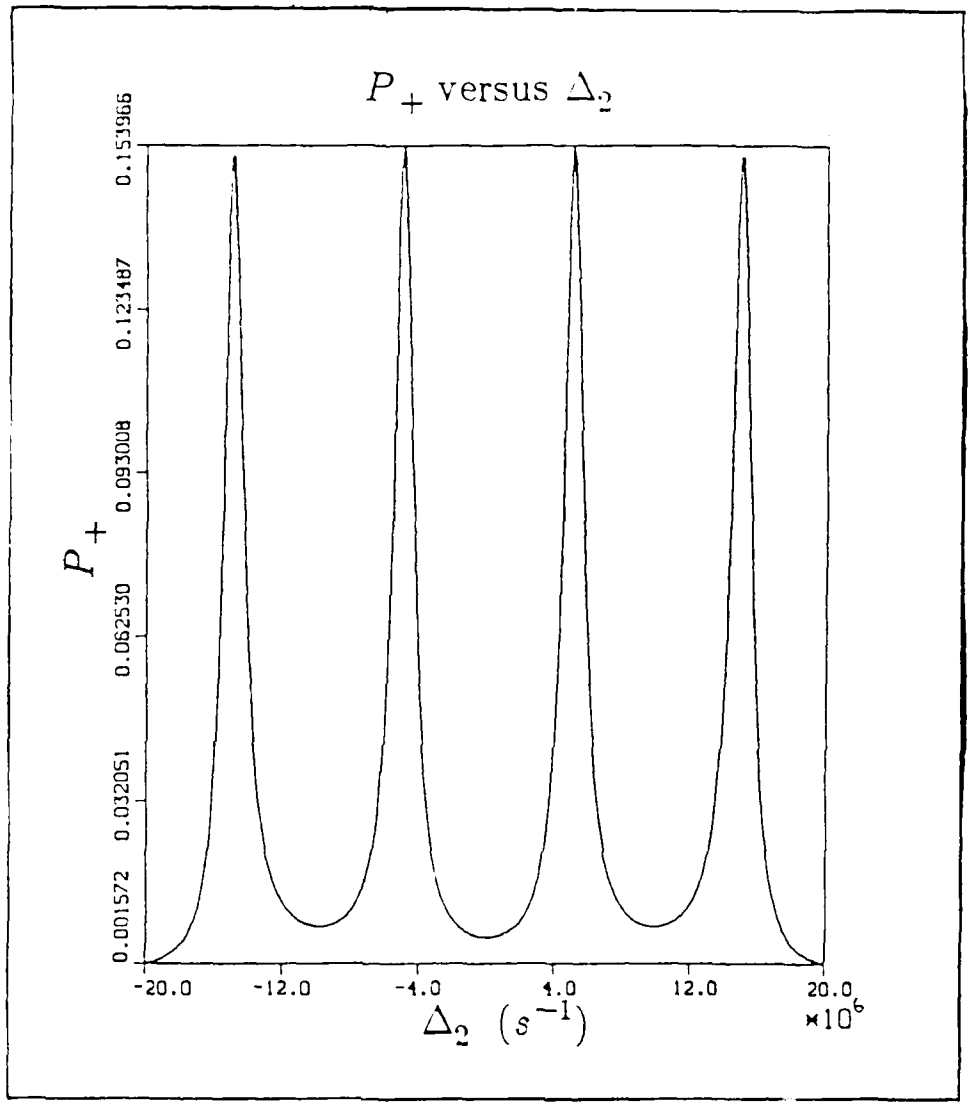

Figure 21. Plot of the steady state value of P_+ versus Δ_2 for A_{10}=10^5, A_{21}=1, A_{32}=1.25x10^6, Ω_1=10^7, Ω_2=10^3, Ω_3=2x10^7, and Δ_1=Δ_3=0.

The other σ_{ij}'s satify

$$\begin{bmatrix} N_2 & 0 & -i\Omega_1 & 0 \\ 0 & N_3 & i\Omega_3 & 0 \\ -i\Omega_1 & i\Omega_3 & N_4 & -i\Omega_2 \\ 0 & 0 & -i\Omega_2 & (A_{32}+A_{21}) \end{bmatrix} \begin{bmatrix} \sigma_{03} \\ \sigma_{12} \\ \sigma_{13} \\ \sigma_{23} \end{bmatrix}$$

$$= i \begin{bmatrix} -\Omega_3\sigma_{02} \\ \Omega_1\sigma_{02}+\Omega_2 w_2 \\ 0 \\ \Omega_3 w_3 \end{bmatrix} \tag{4.26}$$

The adiabatic solutions for σ_{12}, σ_{23}, and σ_{03} are

$$\sigma_{12}=\frac{i}{D_1}\Big[\Omega_1(A_{32}+A_{21})(\Omega_1^2-\Omega_3^2+N_2N_4)+\Omega_2^2N_2\sigma_{02}-\Omega_2\Omega_3^2N_2w_2$$

$$+\tfrac{1}{2}\Omega_2(A_{32}+A_{21})(N_2N_4+\Omega_1^2)+\Omega_2^2N_2(W-w_1-w_3)\Big] \tag{4.27a}$$

$$=r_{21}w_1+r_{22}w_3+r_{23}U+r_{24}V+r_{25}W$$

$$\sigma_{23}=\frac{i\Omega_3}{D_1}\Big[(N_2N_3N_4+\Omega_3^2N_2+\Omega_1^2N_3)w_3$$

$$+\tfrac{1}{2}\Omega_2^2N_2(W-w_1-w_3)+\Omega_1\Omega_2(N_2+N_3)\sigma_{02}\Big] \tag{4.27b}$$

$$=r_{31}w_1+r_{32}w_3+r_{33}U+r_{34}V+r_{35}W$$

$$\sigma_{03}=\frac{i\Omega_3}{D_1}\Big[(A_{32}+A_{21})(\Omega_1^2-\Omega_3^2-N_3N_4)-\Omega_2^2N_3\sigma_{02}-\Omega_1\Omega_2N_3w_2$$

$$+\tfrac{1}{2}\Omega_1\Omega_2(A_{32}+A_{21})(W-w_1-w_3)\Big] \tag{4.27c}$$

$$=r_{41}w_1+r_{42}w_3+r_{43}U+r_{44}V+r_{45}W$$

where D_1, the determinant of the matrix in equation (4.26) is

$$D_1=\Omega_2^2N_2N_3+(A_{32}+A_{21})(N_2N_3N_4+\Omega_1^2N_3+\Omega_3^2N_2) \tag{4.28}$$

Taking $s_{ij}=\mathrm{Re}(r_{ij})$ and $t_{ij}=\mathrm{Im}(r_{ij})$, the equations for w_1 and w_3 are

$$(A_{10}+2\Omega_1 t_{11}-\Omega_2 t_{21})w_1+(\tfrac{1}{2}A_{21}-\Omega_2 t_{22})w_3 \tag{4.29a}$$

$$=-\tfrac{1}{2}(A_{10}-\tfrac{1}{2}A_{21})+\tfrac{1}{2}(A_{10}+\tfrac{1}{2}A_{21}-2\Omega_2 t_{25})W+(\Omega_2 t_{23}-2\Omega_1 t_{13})U+(\Omega_2 t_{24}-2\Omega_1 t_{14})V$$

$$(2\Omega_3 t_{31}-\Omega_2 t_{21})w_1+(A_{32}+\tfrac{1}{2}A_{21}+2\Omega_3 t_{32}-\Omega_2 t_{22})w_3$$

$$=\tfrac{1}{2}(\tfrac{1}{2}A_{21}-A_{32})+(\frac{1}{4}A_{21}-\tfrac{1}{2}A_{32}-2\Omega_3 t_{35}-\Omega_2 t_{25})W \tag{4.29b}$$

$$+(\Omega_2 t_{23}-2\Omega_3 t_{33})U+(\Omega_2 t_{24}-2\Omega_3 t_{34})V$$

In matrix form this is

$$\begin{bmatrix} b_{11} & b_{12} \\ b_{21} & b_{22} \end{bmatrix}\begin{bmatrix} w_1 \\ w_3 \end{bmatrix}=\begin{bmatrix} \alpha_{10}+\alpha_{11}W+\alpha_{12}U+\alpha_{13}V \\ \alpha_{20}+\alpha_{21}W+\alpha_{22}U+\alpha_{23}V \end{bmatrix} \tag{4.30}$$

The steady state solutions for w_1 and w_3 are

$$w_1=\frac{1}{B}\Big[(b_{22}\alpha_{10}-b_{12}\alpha_{20})+(b_{22}\alpha_{11}-b_{12}\alpha_{21})W \tag{4.31a}$$

$$+(b_{22}\alpha_{12}-b_{12}\alpha_{22})U+(b_{22}\alpha_{13}-b_{12}\alpha_{23})V\Big]$$

$$=c_{10}+c_{11}W+c_{12}U+c_{13}V$$

$$w_3=\frac{1}{B}\Big[(b_{11}\alpha_{20}-b_{21}\alpha_{10})+(b_{11}\alpha_{21}-b_{21}\alpha_{11})W \tag{4.31b}$$

$$+(b_{11}\alpha_{22}-b_{21}\alpha_{12})U+(b_{11}\alpha_{23}-b_{21}\alpha_{13})V\Big]$$

$$=c_{20}+c_{21}W+c_{22}U+c_{23}V$$

We are now in a position to examine the time derivatives of U, V, and W. The

equations for these quantities are

$$\frac{dU}{dt}=-\tfrac{1}{2}A_{21}U-\Delta_2 V-\Omega_1\mathrm{Im}(\sigma_{12})-\Omega_2\mathrm{Im}(\sigma_{21})-\Omega_3\mathrm{Im}(\sigma_{23}) \tag{4.32a}$$

$$\frac{dV}{dt}=-\Delta_2 U-\tfrac{1}{2}A_{21}V+\Omega_1\mathrm{Re}(\sigma_{12})-\Omega_2\mathrm{Re}(\sigma_{21})-\Omega_3\mathrm{Re}(\sigma_{23}) \tag{4.32b}$$

$$\frac{dW}{dt}=-\tfrac{1}{2}A_{21}(1+W)+A_{21}w_3-\Omega_2\mathrm{Im}(\sigma_{12}) \tag{4.32c}$$

Putting the steady state solutions of w_1 and w_3 into the equations for the σ_{ij}'s and putting the expressions for the appropriate parts of the σ_{ij}'s into the equations for U, V, and W, we get

$$\frac{dU}{dt}=\eta_1-\tfrac{1}{2}\gamma_1 U+\delta_1 V-\xi_1 W \tag{4.33a}$$

$$\frac{dV}{dt}=\eta_2-\tfrac{1}{2}\gamma_2 V-\delta_2 U+\xi_2 W \tag{4.33b}$$

$$\frac{dW}{dt}=\eta_3-\tfrac{1}{2}\gamma_3 W-\delta_3 U+\xi_3 V \tag{4.33c}$$

where the constants are given by

$$\eta_1=-\Omega_1(t_{21}c_{10}-t_{22}c_{20})-\frac{\Omega_1\Omega_2}{A_{10}}c_{10}-\Omega_3(t_{41}c_{10}-t_{42}c_{20}) \tag{4.34a}$$

$$\eta_2=\Omega_1(s_{21}c_{10}+s_{22}c_{20})-\Omega_3(s_{41}c_{10}+s_{42}c_{20}) \tag{4.34b}$$

$$\eta_3=A_{21}(c_{20}-\tfrac{1}{2})-\Omega_2(t_{21}c_{10}-t_{22}c_{20}) \tag{4.34c}$$

$$\gamma_1 = A_{21} - 2\Omega_1(t_{23} + t_{21}c_{12} + t_{22}c_{22}) - \frac{\Omega_2}{A_{10}}(2\Omega_1 c_{12} - \Omega_2)$$

$$-2\Omega_3(t_{43} + t_{41}c_{12} + t_{42}c_{22}) \tag{4.34d}$$

$$\gamma_2 = A_{21} - 2\Omega_1(s_{24} + s_{21}c_{13} + s_{22}c_{23}) + \frac{\Omega_2^2}{A_{10}} \tag{4.34e}$$

$$+2\Omega_3(s_{44} + s_{41}c_{13} + s_{42}c_{23})$$

$$\gamma_3 = A_{21}(1 - 2c_{21}) - 2\Omega_2(t_{25} + t_{21}c_{11} + t_{22}c_{21}) \tag{4.34f}$$

$$\delta_1 = \Delta_2 - \Omega_1(t_{24} + t_{21}c_{13} + t_{22}c_{23}) + \frac{\Omega_1\Omega_2}{A_{10}}c_{13} + \Omega_3(t_{44} + t_{41}c_{13} + t_{42}c_{23}) \tag{4.34g}$$

$$\delta_2 = \Delta_2 - \Omega_1(s_{23} + s_{21}c_{12} + s_{22}c_{22}) + \Omega_3(s_{43} + s_{41}c_{12} + s_{42}c_{22}) \tag{4.34h}$$

$$\delta_3 = A_{21}c_{22} - \Omega_2(t_{23} + t_{21}c_{12} + t_{22}c_{22}) \tag{4.34i}$$

$$\xi_1 = -\Omega_1(t_{25} + t_{21}c_{11} + t_{22}c_{21}) + \frac{\Omega_1\Omega_2}{A_{10}}c_{11} + \Omega_3(t_{45} + t_{41}c_{11} + t_{42}c_{21}) \tag{4.34j}$$

$$\xi_2 = \Omega_1(s_{25} + s_{21}c_{11} + s_{22}c_{21}) - \Omega_3(s_{45} + s_{41}c_{11} + s_{42}c_{21}) \tag{4.34k}$$

$$\xi_3 = A_{21}c_{23} - \Omega_2(t_{24} + t_{21}c_{13} + t_{22}c_{23}) \tag{4.34l}$$

We will now look at the self relaxations terms for U, V, and W; specifically we will look at γ_1/γ_3 and γ_2/γ_3. We are interested in finding when these parameters are large, because then we can once again make an adiabatic approximation and use the steady state values of U and V in the equation for dW/dt.

Using the third Pascal program listed in the Appendix, γ_1/γ_3 and γ_2/γ_3 were calculated as functions of Δ_2 for constant Ω_1, Ω_2, and Ω_3, also, as functions of the Ω_i's for the other frequencies held constant. Figure 22 is a plot of γ_1/γ_3 versus Δ_2 for $A_{10}=10^5$, $A_{21}=1$, $A_{32}=1.25\times10^5$, $\Omega_1=10^7$, $\Omega_2=10^7$, and $\Omega_3=2\times10^7$. Figure 23 is a plot of γ_2/γ_3 versus Δ_2 for the same values of the other frequencies, and Figure 24 is, likewise, a plot of γ_3/γ_3 versus Δ_2. Note that $\gamma_1/\gamma_3 = \gamma_2/\gamma_3$ for all Δ_2. This is expected since U

and V are just twice the real and imaginary parts of the original variable τ_{21}. It can be seen that both γ_1 and γ_3 have resonances at $\Delta_2=0$, and $\Delta_2=\pm\frac{1}{2}\sqrt{\Omega_1^2-\Omega_2^2}$. However, γ_1 varies over several orders of magnitude, while γ_3 varies little from A_{21}. Figure 25 is a plot of γ_1 γ_3. The important thing to notice is that while there are resonances, even the off resonance values of γ_1 γ_3 are much larger 1. It was found that when either of the strong transitions is saturated, that is when $\Omega_1>>A_{10}$ or $\Omega_3>>A_{32}$, then γ_1 γ_3 and γ_2 γ_3 are much larger than 1. This means that the radiation applied to the strong transitions greatly increases the transverse relaxtion rate of the weak transition.

When these conditions are satisfied, we can use the steady state values of U and V in the equation for dW/dt. The equation for dW/dt is

$$\frac{dW}{dt}=\eta_3-4\frac{\delta_3(\delta_1\eta_2+\frac{1}{2}\gamma_2\eta_1)-\xi_3(\delta_2\eta_1-\frac{1}{2}\gamma_1\eta_2)}{\gamma_1\gamma_2+4\delta_1\delta_2}$$

$$-\left[\frac{1}{2}\gamma_3-4\frac{\delta_3(\delta_1\xi_2+\frac{1}{2}\gamma_2\xi_1)-\xi_3(\delta_2\xi_1-\frac{1}{2}\gamma_1\xi_2)}{\gamma_1\gamma_2+4\delta_1\delta_2}\right]W \qquad (4.35)$$

$$\equiv o-\upsilon W$$

Note that $1=P_++P_-$ and $W=P_+-P_-$. Also that $dW/dt=2dP_+/dt$, so that

$$\frac{dP_+}{dt}=-\frac{dP_-}{dt}=\frac{1}{2}o(P_++P_-)-\frac{1}{2}\upsilon(P_+-P_-)=-R_-P_++R_+P_- \qquad (4.36)$$

where R_+ and R_- are given by

$$R_-=\frac{1}{2}(\upsilon-o) \qquad (4.37a)$$

$$R_+=\frac{1}{2}(\upsilon+o) \qquad (4.37b)$$

Figure 26 is a plot of R_+ versus Δ_2 and Figure 27 is a plot of R_- versus Δ_2 for $A_{10}=10^6$, $A_{21}=1$, $A_{32}=1.25\times10^6$, $\Omega_1=10^7$, $\Omega_2=10^3$, and $\Omega_3=2\times10^7$. Again we see

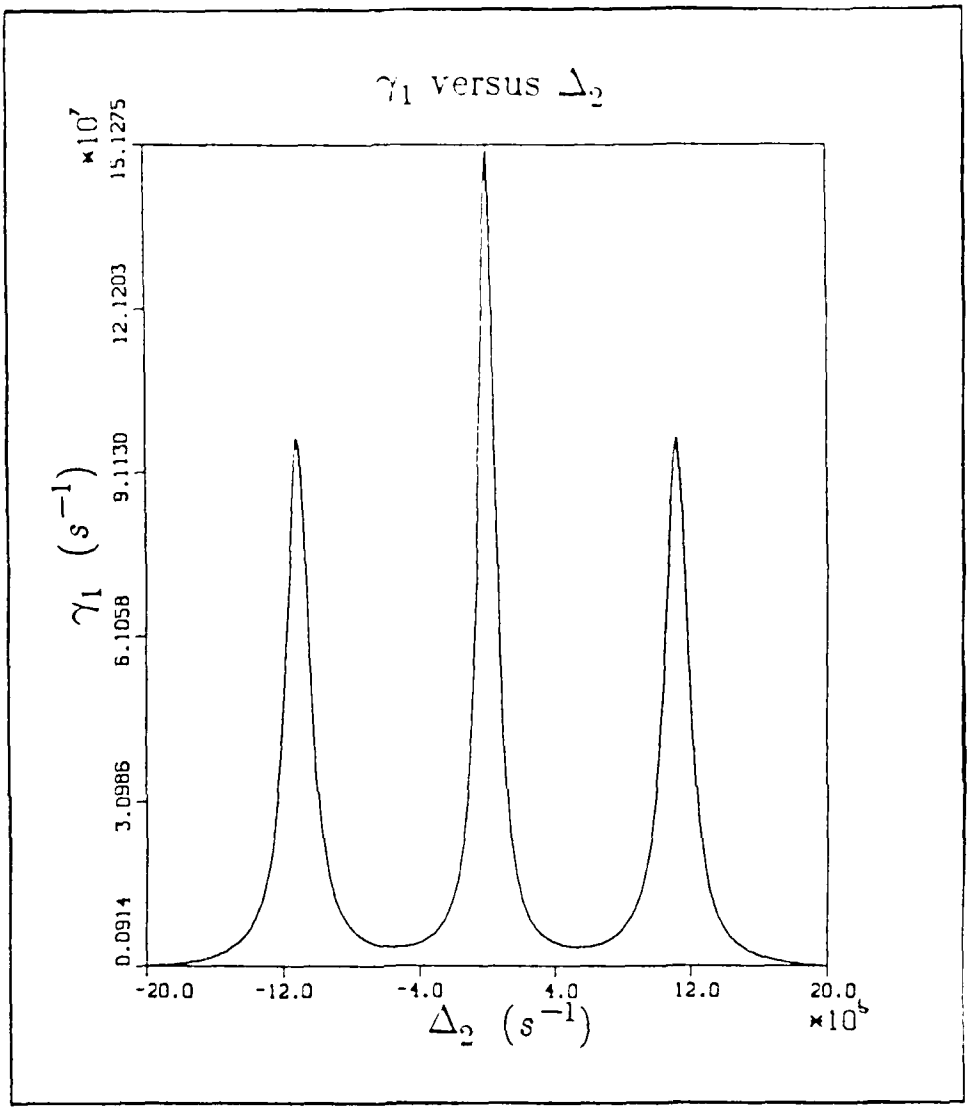

Figure 22. Plot of γ_1 versus Δ_2 for $A_{10}=10^6$, $A_{21}=1$, $A_{32}=1.25\times10^8$, $\Omega_1=10^7$, $\Omega_2=10^3$, $\Omega_3=2\times10^7$, and $\Delta_1=\Delta_3=0$.

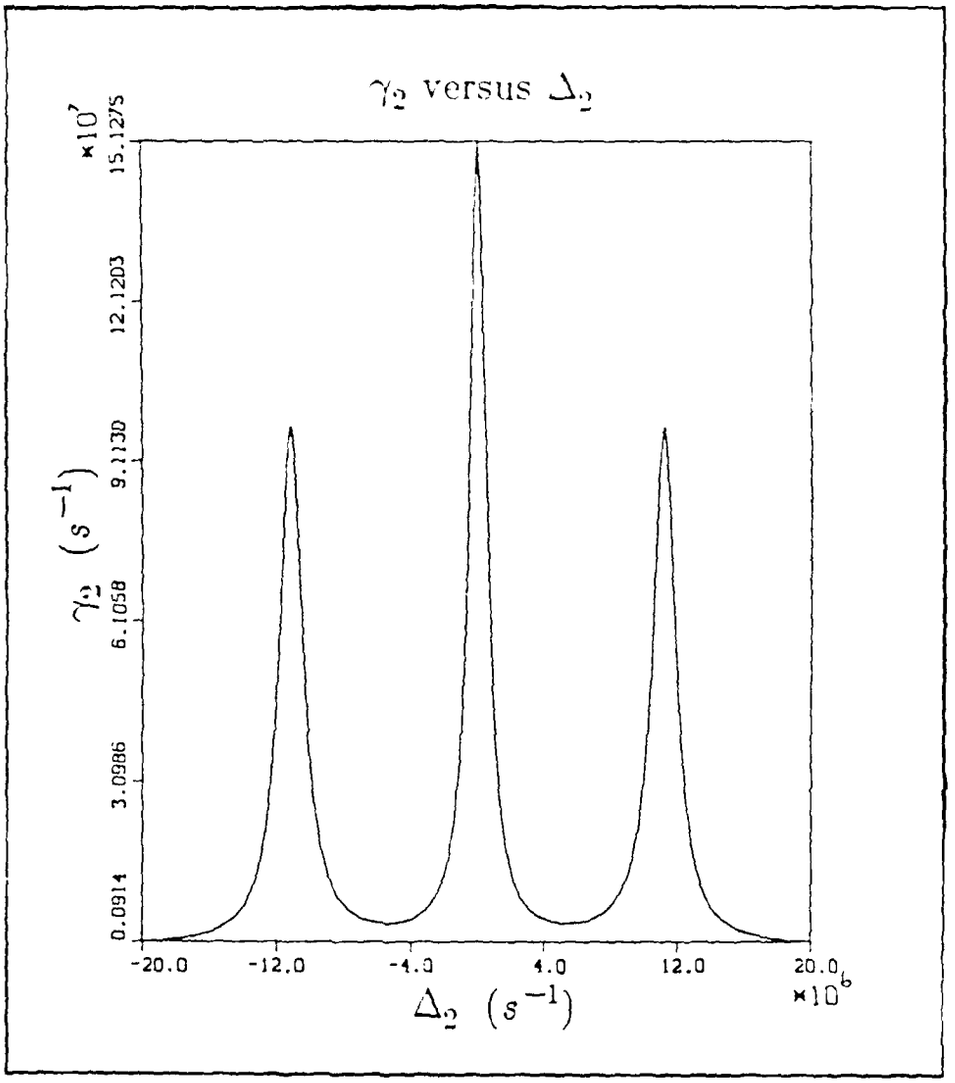

Figure 23. Plot of γ_2 versus Δ_2 for A_{10}=10^6, A_{21}=1, A_{32}=1.25×10^6, Ω_1=10^7, Ω_2=10^7, Ω_3=2×10^7, and Δ_1=Δ_3=0.

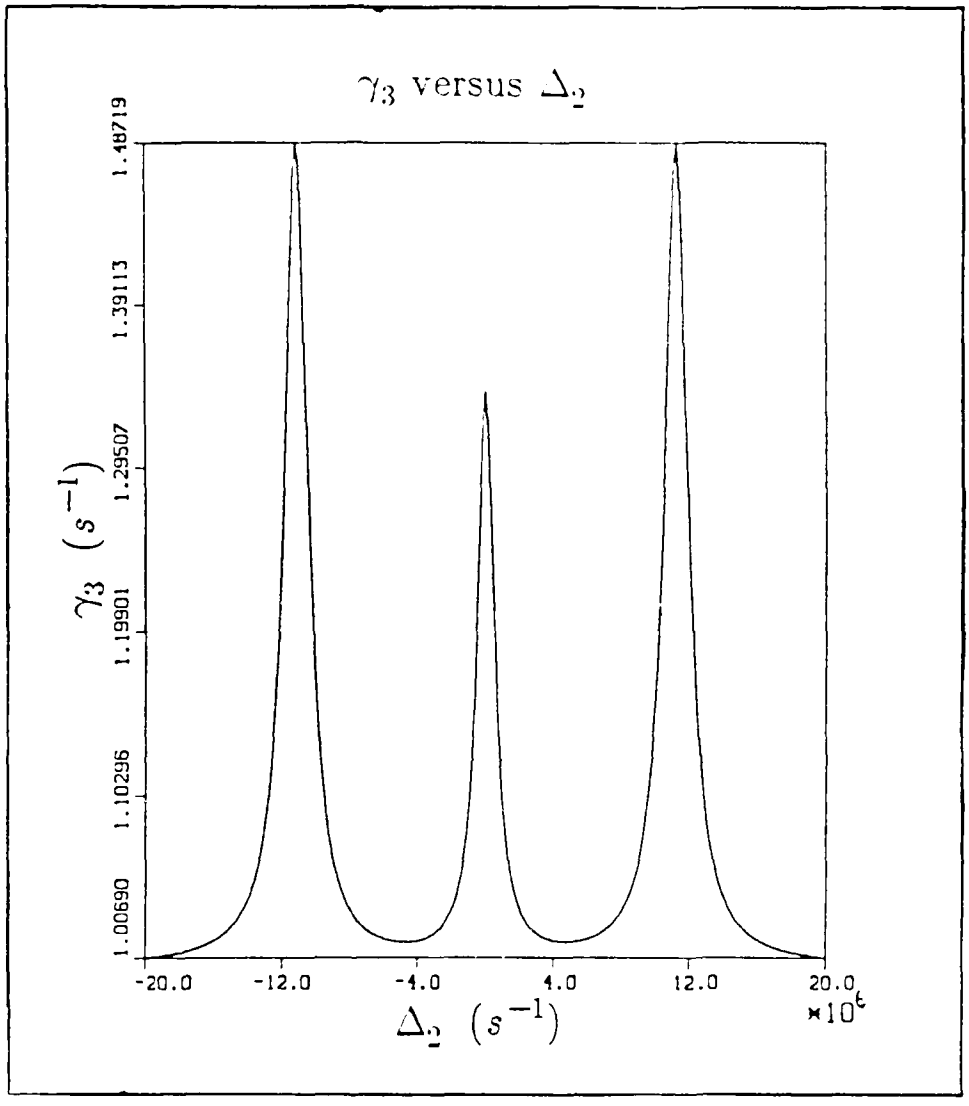

Figure 24. Plot of γ_3 versus Δ_2 for $A_{10}=10^6$, $A_{21}=1$, $A_{32}=1.25\times10^6$, $\Omega_1=10^7$, $\Omega_2=10^3$, $\Omega_3=2\times10^7$, and $\Delta_1=\Delta_3=0$.

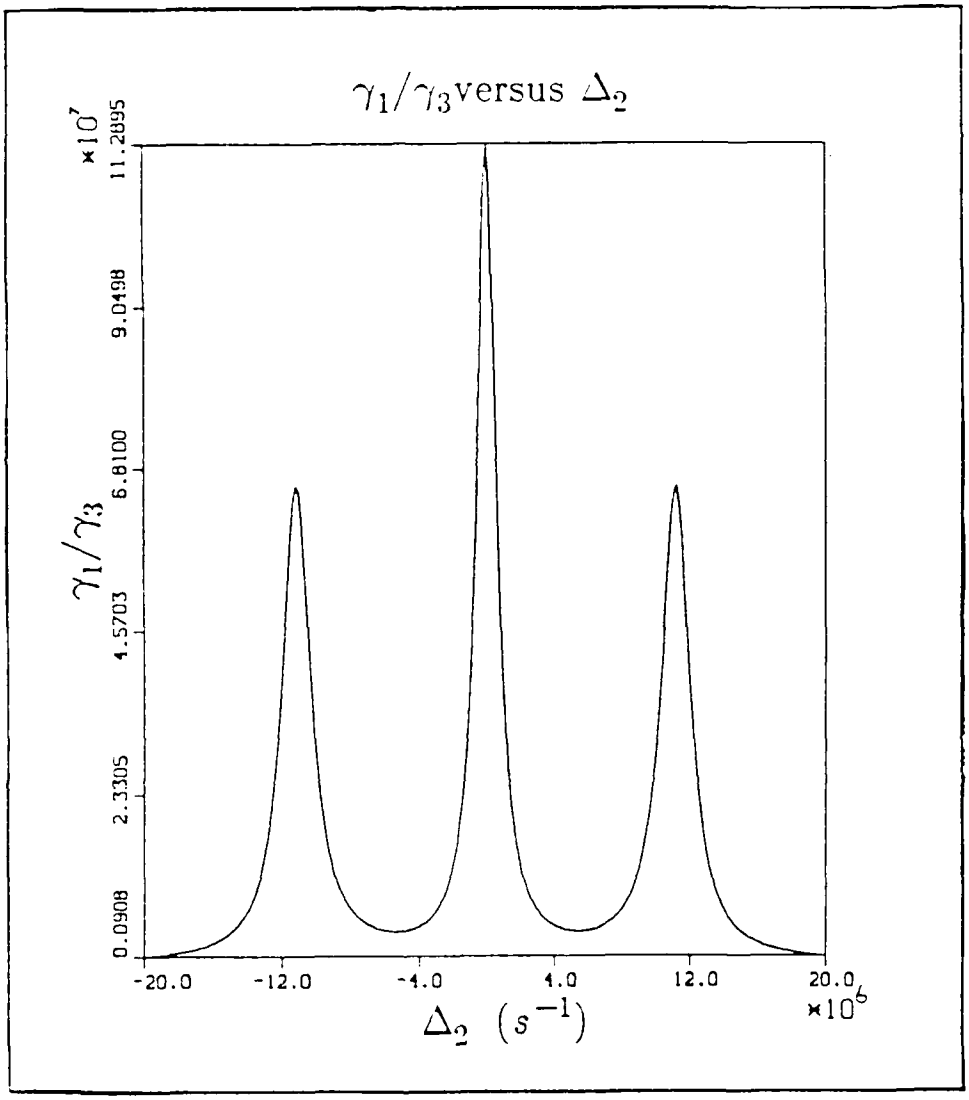

Figure 25. Plot of γ_1/γ_3versus Δ_2 for A_{10}=10^6, A_{21}=1, A_{32}= 1.25×10^6, Ω_1= 10^7, Ω_2 =10^7, Ω_3=2×10^7, and Δ_1=Δ_3=0.

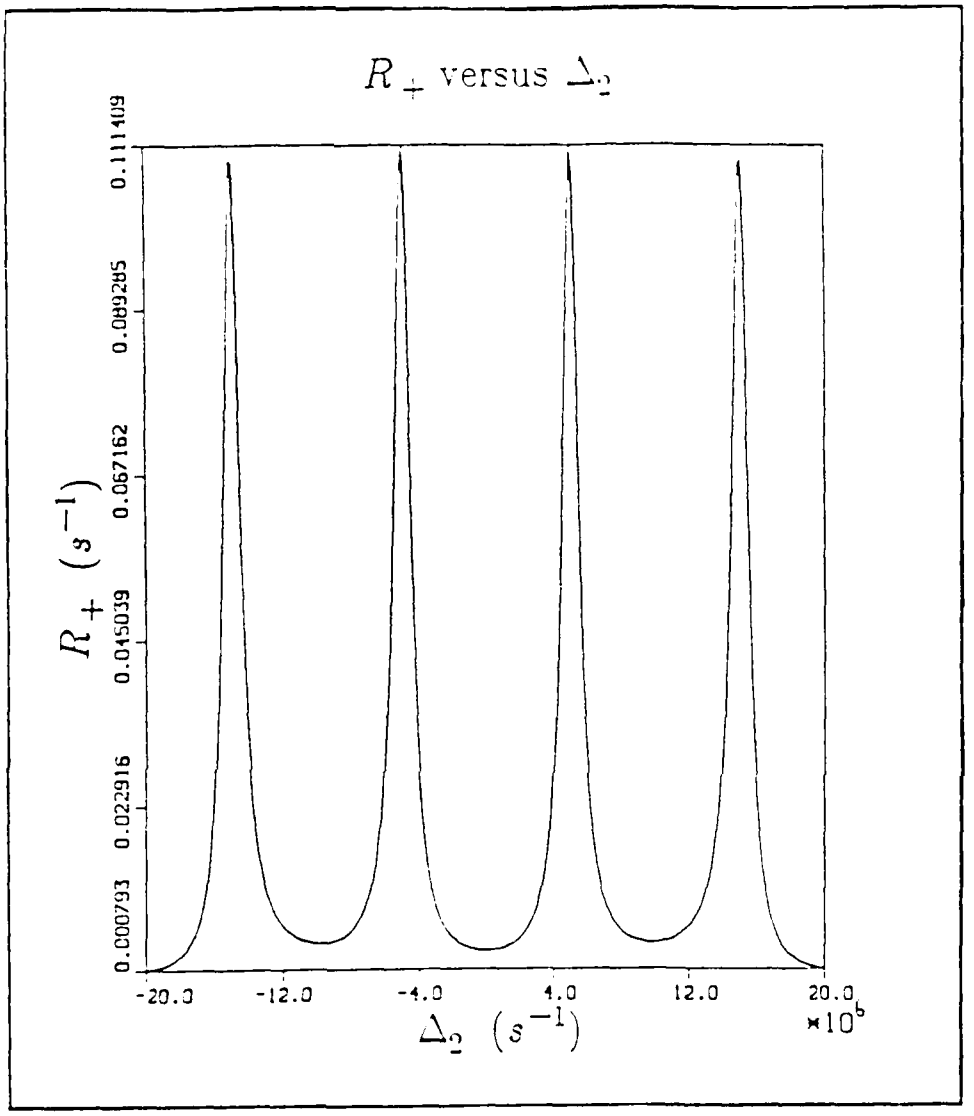

Figure 26. Plot of R_+ versus Δ_2 for A_{10}=10^6, A_{21}=1, A_{32}=1.25x10^5, Ω_1=10^7, Ω_2=10^3, Ω_3=2x10^7, and Δ_1=Δ_3=0.

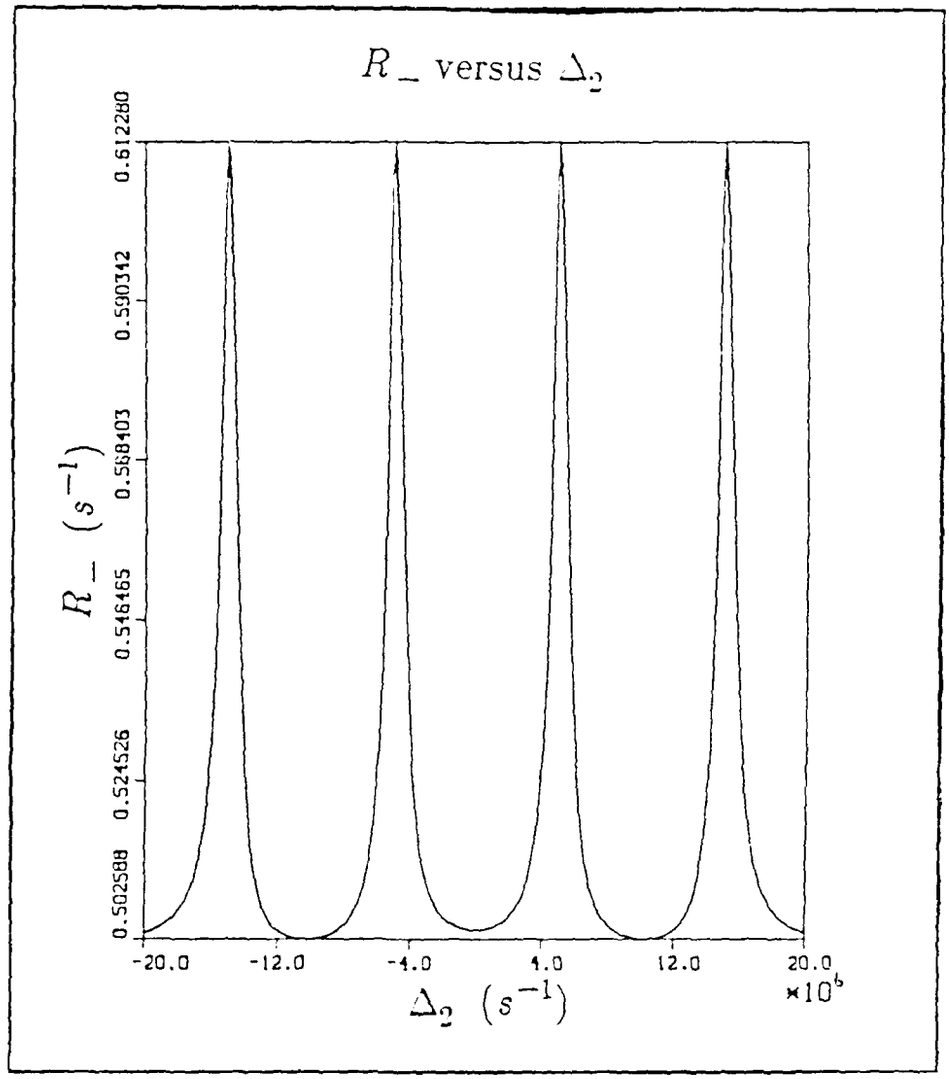

Figure 27. Plot of R_- versus Δ_2 for $A_{10}=10^6$, $A_{21}=1$, $A_{32}=1.25\times10^6$, $\Omega_1=10^7$, $\Omega_2=10^7$, $\Omega_3=2\times10^7$, and $\Delta_1=\Delta_3=0$.

resonances at $\Delta_2 = \pm\frac{1}{2}\Omega_1 - \Omega_2$, and $\Delta_3 = \pm\frac{1}{2}\Omega_1 - \Omega_3$.

Equation (4.37) is just a rate equation for P_- and P_+. We have thus shown that when either of the strong transitions is saturated, the excitation of the weak transition can be treated as a rate process over coarse-grained intervals of time.

C. Statistics of Fluorescence

The theory of a two level quantum system driven by rate processes is well understood (9). We define $\Gamma_1(\tau_1)$ as the probability density for durations τ_1 of fluorescence of frequency ω_1 and $\Gamma_3(\tau_3)$ as the probability density for durations τ_3 of fluorescence of frequency ω_3. The theory of referency (9) predicts that the distrubutions to have the form

$$\Gamma_1(\tau_1) = R_- e^{-R_-\tau_1} \tag{4.38a}$$

$$\Gamma_3(\tau_3) = R_+ e^{-R_+\tau_3} \tag{4.38b}$$

The mean length of fluorescence of frequency ω_1 is $1/R_-$, while the mean length of fluorescence of frequency ω_3 is $1/R_+$. Similarly, all other statistical information about weak transitions can be developed in an analogous manner to that used in reference (9) and (23).

I. Conclusion

A. Discussion of Results

In summary, the problem of laser cooling of a single ion or atom in a harmonic trap was considered. A simple theory of sideband cooling has been developed. In the limit that the particle's secular motion can be treated semiclassically, the theory allows the calculation of a logarithmic cooling rate either numerically or, for two special cases, analytically.

This theory of laser cooling differs from previous theories in that this theory predicts cooling rates, as opposed to minimum temperatures of cooling. Three advantages of this development are: 1) It provides a simple physical picture of the cooling process. 2) No assumptions needed to be made in the derivation of equations (3.16), the equations at the core of theory, about the relative magnitudes of the radiative decay constant β, the oscillation frequency in the trap ν, the detuning Δ, or the Rabi frequency Ω. That is the theory as whole is not a weak field ($\Omega << \beta$) theory or a strong trap ($\nu >> \beta$) theory, etc. 3) Calculating cooling rates for a set of parameters, even in a region where neither of the analytical solutions applies is a relatively simple numerical procedure.

As has been mentioned, other theories concentrate on determining minimum temperatures of cooling, not cooling rates. Itano and Wineland [18], however, use incoherent energy rate equations, among other methods, to determine the minimum temperatures. They make the weak field approximation, i.e., $\Omega << \beta$. It is interesting to compare the functional form of their energy rate equation

equation (19a) of reference (18), to equation (3.27a), the equation for α for the weak field case. Note that although α is the decay constant for the amplitude of the motion, the energy of a harmonic oscillator is proportional to the amplitude squared, so that the decay constant for the energy should be twice α. Their equation is

$$\frac{dE_z}{dt}=\gamma_s\left[\frac{-2(\omega_0-\omega)\hbar k^2<v_z^2>_v}{(\tfrac{1}{2}\gamma)^2+(\omega_0-\omega)^2}+R(1+f_{sz})\right] \tag{5.1}$$

In the notation of reference (18), γ is the natural linewidth, $\omega_0-\omega$ is $-\Delta$, $R=(\hbar k)^2/2M$, f_{sz} is the scattering coefficient, equal to 1/3 for isotropic scattering, and γ_s, the average scattering rate, is given by

$$\gamma_s=\frac{I}{\hbar\omega}<\sigma(\omega,\vec{v})>_v \tag{5.2}$$

where $\sigma(\omega,\vec{v})$ is the Doppler-shifted natural line shape. I is the intensity of the cooling laser which is proportional to the square of the Rabi frequency, Ω.

The first term in equation (5.1) describes cooling, while the second term, $\gamma_s R(1+f_{sz})$ corresponds to recoil heating. The energy of a harmonic oscillator is proportional to the average over one cycle of the velocity squared, so that the cooling term is linear in the energy, and corresponds to exponential cooling as predicted by the present theory. The resonant denominator is the same for both the weak field expression for α and the cooling term in equation (5.1). Also, the cooling term in equation (5.1) scales as Ω^2 as does α for small Ω. The dependence of α on β and ν differs from the cooling term presented by Itano and Wineland. In choosing α from equation (3.27a) or the expression presented by Wineland and Itano, we expect the expression for α to be the appropriate value for an energy decay constant when using laser cooling because it was derived using coherent radiation theory while Itano and Wineland used incoherent rate theory.

The present theory of laser cooling could be used to optimize the parameters of a cooling experiment. The parameters which can be varied are the oscillation frequency in the trap, ν; the detuning, Δ; the Rabi frequency (corresponding to laser intensity), Ω; and to some extent, by choosing appropriate transitions, the radiative decay constant, β. An appropriate transition for cooling would be between the ground state and some excited state, with no possible decay path back to the ground state except straight down, so that potential cooling time is not wasted with the atom sitting in intermediate levels. Such an ideal situation can be hard to come by in practice. The frequency of the cooling transition must also be accessible to a tunable laser. An additional consideration in selecting a transition is that the rate of cooling transitions per second is limited by β, so that it would seem that large β would be better. However, when β becomes large enough that the sidebands are no longer well separated from the central peak cooling is slowed by transitions between the sidebands. The maximum cooling rate occurs for $\beta \approx \frac{1}{2}\nu$. Once an appropriate transition has been chosen, ν should be adjusted as much as possible so that $\beta \approx \frac{1}{2}\nu$. This is not always possible; in the experiment performed by Neuhauser, et al (31), β was 2πx19MHz and ν was 2πx2.4MHz. For well separated sidebands, the value of Δ for the maximum cooling rate is just $-\nu$. If the sidebands are not well separated, the value of Δ corresponding to the maximum cooling rate is shifted toward zero. For given values of β and ν, plots of α versus Δ are easily generated, even in regions where neither analytical solution applies, and the best value of Δ can be taken from a graph. The same is true of Ω.

The spectroscopy of a single atom in the ladder configuration has been treated theoretically. A dressed atom approach was used to provide qualitative information about the system. It was shown that the weak transition is split into

four peaks, similarly to the Autler-Townes doublet for a three level system. The new transition frequencies are separted from the original transition frequency by $\pm\frac{1}{2}(\Omega_1-\Omega_3)$ and $\pm\frac{1}{2}(\Omega_1-\Omega_3)$.

The optical Bloch equations for the four level system in the rotating wave approximation were developed and solved for steady state. The steady state solution agreed with what was expected from the dressed atom development, i.e., the steady state probability to be in either of the upper states as a function of detuning on the weak transition, Δ_2, peaked sharply at $\Delta_2=\pm\frac{1}{2}(\Omega_1-\Omega_3)$ and $\Delta_2=\pm\frac{1}{2}(\Omega_1+\Omega_3)$.

The Bloch equations were solved in the adiabatic approximation. It was shown that the statistics of the weak transition can be described as a rate process whenever either of the strong transitions is saturated. Upward and downard transition rates were extracted from this treatment. The upward transition rate was shown to be sharply peaked at the four resonant frequencies listed above.

B. Recommendations for Further Study

Fluctuations have not been introduced into the simple theory of cooling. If this could be done, it would greatly add to the theory's utility by making it possible to calculate a minimum temperature of cooling.

One of the criticisms made about Kimble, Cook, and Wells' (24) treatment of intermittent atomic fluorescence or the "V" configuration was that intermittent fluorescence was assumed at the beginning and the statistics of that fluorescence developed from that assumption. That same criticism could be made about the treatment of the ladder configuration presented here. It should be possible to

prove that the fluorescence changes abruptly between frequencies ω_1 and ω_3 using an approach similar to Cohen-Tannoudji and Dalibard (4), and that calculation should be done.

Bibliography

1. Arrecchi, F. T., A. Schenzle, R. G. DeVoe, K. Jungmann, and R. G. Brewer. "Comment on the Ultimate Single-Ion Laser-Frequency Standard." Physical Review A, 33: 2124-2126 (March 1986).

2. Ashkin, A. and J. P. Gordon. "Cooling and Trapping of Ions by Resonance Radiation Pressure." Optics Letters, 4: 161-163 (June 1979).

3. Bergquist, J. C., R. G. Hulet, W. M. Itano, and D. J. Wineland. "Observation of Quantum Jumps In a Single Atom." Physical Review Letters, 57: 1699-1702 (October 1986).

4. Cohen-Tannoudji, C. and J. Dalibard. "Single Atom Laser Spectroscopy. Looking for Dark Periods in Fluorescence Light." Europhysics Letters 1: 441-448 (May 1986).

5. Cook, R. J. "Theory of Atomic Motion in a Resonant Electromagnetic Wave," Physical Review Letters, 41: 1788-1791 (December 1978).

6. Cook, R. J. "Theory of Resonance Radiation Pressure," Physical Review A, 22: 1078-1098 (September 1980).

7. Cook, R. J. "Quantum-Mechanical Fluctuations of the Resonance Radiation Force." Physical Review Letters, 44: 976-979 (14 April 1980).

8. Cook, R. J. "Atomic Motion in Resonant Radiation: An Application of Ehrenfest's Theorem." Physical Review A, 20: 224-228 (July 1979).

9. Cook, R. J. and H. J. Kimble. "Possibility of Direct Observation of Quantum Jumps." Physical Review Letters, 54: 1023-1026 (March 1985).

10. Cook, R. J., D. G. Shankland, and A. L. Wells. "Quantum Theory of Particle Motion in a Rapidly Oscillating Field." Physical Review A, 31: 564-567 (February 1985).

11. Dehmelt, H. G. "Radio Frequency Spectroscopy of Stored Ions I: Storage." Advances in Atomic and Molecular Physics, Volume 3, edited by D. R. Bates. New York: Academic Press, 1967.

12. Dehmelt, H. G. "Stored Ion Spectroscopy." Advances in Laser Spectroscopy, edited by F. T. Arecchi, F. Strumia, and H. Walther. New York: Plenum Press, 1983.

13. Dehmelt, H. G. Bulletin of the American Physical Society, 20: 60 (1975).

14. Finn, M. A., G. W. Greenless, and D. A. Lewis. "Experimental Evidence for Quantum Jumps in Three-Level Systems," : Optics Communications, 60: 149-153 (November 1986).

15. Gerald, C. F. and P. O. Wheatley, Applied Numerical Analysis (Addison-Wesley Publishing Company, Reading, Massachusetts, 1984), pp. 306-312.

16. Gordon, J. P. and A. Ashkin. "Motion of Atoms in a Radiation Trap," Physical Review A, 21: 1606-1617 (May 1980).

17. Hansch, T. W. and A. L. Schawlow. "Cooling of Gases by Laser Radiation," Optics Communications, 13: 68-69 (January 1975).

18. Itano, W. M. and D. J. Wineland. "Laser Cooling of Ions Stored in Harmonic and Penning Traps," Physical Review A, 25: 35-54 (January 1982).

19. Javanainen, J. "Light-Induced Motion of Trapped Ions I: Low-Intensity Limit," Journal of Physics B, 14: 2519-2534 (1981).

20. Javanainen, J. "Light-Induced Motion of Trapped Ions II: "Arbitrary Intensity," Journal of Physics B, 14: 4191-4205 (1981).

21. Javanainen, J., M. Lindberg, and S. Stenholm. "Laser Cooling of Trapped Ions: Dynamics of the Final Stages," Journal of the Optical Society of America B, 1: 111-115 (March 1984).

22. Javanainen, J. "Possibility of Quantum Jumps in a Three-Level System," Physical Review A, 33: 2121-2123 (March 1986).

23. Kimble, H. J., R. J. Cook, and A. L. Wells. "Intermittent Atomic Fluorescence," Physical Review A, 34: 3190-3195 (October 1986).

24. Knight, P. L. and P. W. Milonni. "The Rabi Frequency in Optical Spectra," Physics Reports, 66: 23-107 (December 1980).

25. Letokhov, V. S. and V. G. Minogin. Applied Physics, 17: 99 (1978).

26. Migdall, A. L., J. V. Prodan, W. D. Phillips, T. H. Bergeman, and H. J. Metcalf. "First Observation of Magnetically Trapped Neutral Atoms," Physical Review Letters, 54: 2596-2599 (June 1985).

27. Milonni, P. W. "Semiclassical and Quantum-Electrodynamical Approaches in Nonrelativistic Radiation Theory," Physics Reports (1976).

28. Nagourney, W., J. Sandberg, and H. Dehmelt. "Shelved Optical Electron Amplifier: Observation of Quantum Jumps," Physical Review Letters, 56: 2797-2799 (June 1986).

29. National Bureau of Standards. National Bureau of Standards Technical Note 1086: Trapped Ions and Laser Cooling. Washington: Government Printing Office, 1985.

30. Neuhauser, W., M. Hohenstatt, P. Toschek, and H. Dehmelt. "Optical-Sideband Cooling of Visible Atom Cloud Confined in Parabolic Well," Physical Review Letters, 41: 233-236 (24 July 1978).

31. Neuhauser, W., M. Hohenstatt, P. Toschek, and H. Dehmelt. "Localized Visible Ba^+ Mono-Ion Oscillator," Physical Review A, 22: 1137-1140 (September 1980).

32. Pegg, D. T., R. Loudon, and P. L. Knight. "Correlations in Light Emitted by Three-Level Atoms," Physical Review A, 33: 4085-4091 (June 1986).

33. Sauter, T., W. Neuhauser, R. Blatt, and P. E. Toschek. "Observation of Quantum Jumps," Physical Review Letters, 57: 1696-1698 (October 1986).

34. Schenzle, A. and R. G. Brewer. "Macroscopic Quantum Jumps in a Single Atom," Physical Review A, 34: 3127-3142 (October 1986).

35. Schenzle, A., R. G. DeVoe, and R. G. Brewer. "Possibility of Quantum Jumps," Physical Review A, 33: 2127-2130 (March 1986).

36. Stenholm, S. "The Semiclassical Theory of Laser Cooling," Reviews of Modern Physics, 58: 699-738 (July 1986).

37. Wells, Capt A. L. Quantum Theory of Ion Motion and Laser Motion in a Radio Frequency Quadrupole Trap. MS Thesis AFIT/GEP/PH/84D-12. School of Engineering, Air Force Institute of Technology (AU), Wright-Patterson AFB, OH, December 1984.

38. Wineland, D. J. and H. Dehmelt. "Proposed $10^{14}\Delta\nu\ \nu$ Laser Fluorescence Spectroscopy on Tl^{+} Mono-Ion Oscillator III," Bulletin of the American Society, 20: 637 (1975).

39. Wineland, D. J. and W. M. Itano. "Laser Cooling of Atoms," Physical Review A, 20: 1521-1540 (October 1979).

40. Wineland, D. J., W. M. Itano, J. C. Bergquist, and R. G. Hulet. "Laser-Cooling Limits and Single-Ion Spectroscopy," Physical Review A, 36: 2220-2232 (September 1987).

Appendix: Programs Used for Numerical Calculations

I. Numerical Integration of Equations 3.37

```
    Program PNEW2;
{$U+}
{$I GRAPH.P}

LABEL 1,2;

CONST
  N:integer=100;
  hbar=1.055E-34;
  mass=1E-25;
  k=1E+07;
  nu=1E+06;
  beta=10;
  delta=-1;
{  omega=1; }
  dt=0.05;

TYPE
  BUFF=ARRAY[0..406] OF BYTE;
  number=array[1..250] of real;
  gob=array[1..250] of integer;
  rungekutta=array['u'..'y'] of real;
  title=string[15];

VAR
  BUFFER:BUFF;
  SAMPLE:BYTE;
  I,J,LOLA:INTEGER;
  DATA:text;
  AU,AV,AW,AX,C,M:number;
  U,V,W,X,Y,KAPPA,omega:real;
  K1,K2,K3,K4:rungekutta;

PROCEDURE RUNGE(u,v,w,x,y,kappa:real; VAR rk:rungekutta);
  BEGIN
```

```
  rk[1]:= lt*(-beta*u-delta*v-omega*w*x);
  rk[2]:=dt*(-delta*u-beta*v-omega*w);
  rk[3]:=dt*(-omega* x*u-v-2*beta*w-1);
  rk[4]:=dt*y;
  rk[5]:=dt*(-kappa* x*u-v)-x);
  END;

PROCEDURE MINIMUM(num:number; L:integer; VAR min:real);
  BEGIN
  min:=num[1];
  FOR I:=2 to L DO
    BEGIN
    IF num[I] < min THEN min:=num[I];
    END;
  END;

PROCEDURE MAXIMUM(num:number; L:integer; VAR max:real);
  BEGIN
  max:=num[1];
  FOR I:=2 to L DO
    BEGIN
    IF num[I] > max THEN max:=num[I];
    END;
  END;

PROCEDURE SCALE(min,max:real; num:number; L:integer; VAR mark:gob);
  VAR s:real;
  BEGIN
  s:=(max-min)/180;
  FOR I:=1 to L DO
    BEGIN
    mark[I]:=round((num[I]-min)/s);
    END;
  END;

PROCEDURE PRINT(num:number; L,flag:integer; Title: VAR part:real);
  VAR min,max:real; mark:gob;
  BEGIN
  GRAPHMODE;
  DRAW(10,190,260,190,3);
  DRAW(10,190,10,10,3);
  DRAW(260,190,260,10,3);
  DRAW(10,10,260,10,3);
```

```
FOR I:=1 TO 9 DO
  BEGIN
  J:=190-I*18:
  DRAW(10,J,13,J,3):
  END:

FOR I:=1 TO 9 DO
  BEGIN
  J:=10+I*25:
  DRAW(J,190,J,187,3):
  END:

MINIMUM(num,L,min):
MAXIMUM(num,L,max):
IF flag=0 THEN par:=0:
IF flag=2 THEN par:=(num[L]-num[1])*nu/(dt*3*(N*1E-02+250)):
IF flag=1 THEN par:=-LN((max-min)/2):
GOTOXY(1,25):
WRITE(min:10,'  ',max:10,'  ',(max-min):10):
GOTOXY(1,1):
WRITE(((max+min)/2):10,'  ',T):
IF flag=2 THEN WRITE('  ',par):
SCALE(min,max,num,L,mark):
PLOT(11,190-mark[1],3):
IF flag>1 THEN CIRCLE(11,190-mark[1],3,3):
J:=ROUND(250/(L-1)):

FOR I:=1 TO (L-1) DO
  BEGIN
  PLOT(11+(I*J),190-mark[I+1],3):
  IF flag>1 THEN CIRCLE(11+(I*J),190-mark[I+1],3,3):
  IF flag<3 THEN DRAW(11+(I-1)*J,190-mark[I],11+I*J,190-mark[I+1],3):
  END;

IF flag>1 THEN
  BEGIN

FOR I:=1 to 80 DO
  BEGIN
  GETPIC(BUFFER,4*(I-1),0,4*(I-1),200):
  WRITE(LST,#27,'@',#27,'1'):
  WRITE(LST,#27,#75,#201,#0):
  FOR J:=1 to 201 DO
    BEGIN
```

```
      SAMPLE:=BUFFER[J-1-6];
      WRITE(LST,CHR SAMPLE[1]);
      END;
    END;

  WRITELN(LST,#11,#11,#11,#10,10,#27,'@');
  END;
  END;

FUNCTION KUTTA(rk1,rk2,rk3,rk4:real):real;
  BEGIN
  KUTTA:=(1/6)*(rk1+2*rk2+2*rk3+rk4);
  END;

BEGIN

 FOR LOLA:=1 to 5 DO
  BEGIN
  omega:=LOLA*10;
  U:=0;
  V:=0;
  W:=-1;
  X:=0.2;
  Y:=0.2;
  KAPPA:=hbar*sqr(k)*omega/(nu*2*mass);
  writeln(lst,'nu=  ',nu);
  writeln(lst,'beta=  ',beta*nu);
  writeln(lst,'delta=  ',delta*nu);
  writeln(lst,'omega=  ',omega*nu);
  writeln(lst,'dtau=  ',dt);
  writeln(lst,N,'x100');
  writeln(lst,#10,#10);

  FOR I:=1 to 100 DO
    BEGIN
      RUNGE(U,V,W,X,Y,KAPPA,K1);
      RUNGE(U+0.5*K1['u'],V+0.5*K1['v'],W+0.5*K1['w'],X+0.5*K1['x'],
      Y+0.5*K1['y'],KAPPA,K2);
      RUNGE(U+0.5*K2['u'],V+0.5*K2['v'],W+0.5*K2['w'],X+0.5*K2['x'],
      Y+0.5*K2['y'],KAPPA,K3);
      RUNGE(U+K3['u'],V+K3['v'],W+K3['w'],X+K3['x'],Y+K3['y'],KAPPA,K4);
      U:=U+KUTTA(K1['u'],K2['u'],K3['u'],K4['u']);
      V:=V+KUTTA(K1['v'],K2['v'],K3['v'],K4['v']);
      W:=W+KUTTA(K1['w'],K2['w'],K3['w'],K4['w']);
```

```
      X:=X+KUTTA(K1['x'],K2['x'],K3['x'],K4['x']);
      Y:=Y+KUTTA(K1['y'],K2['y'],K3['y'],K4['y']);
    END; {End of Outside Loop}


FOR I:=1 to 250 DO
  BEGIN
    RUNGE(U,V,W,X,Y,KAPPA,K1);
    RUNGE(U+0.5*K1['u'],V+0.5*K1['v'],W+0.5*K1['w'],X+0.5*K1['x'],
    Y+0.5*K1['y'],KAPPA,K2);
    RUNGE(U+0.5*K2['u'],V+0.5*K2['v'],W+0.5*K2['w'],X+0.5*K2['x'],
    Y+0.5*K2['y'],KAPPA,K3);
    RUNGE(U+K3['u'],V+K3['v'],W+K3['w'],X+K3['x'],Y+K3['y'],KAPPA,K4);
    U:=U+KUTTA(K1['u'],K2['u'],K3['u'],K4['u']);
    V:=V+KUTTA(K1['v'],K2['v'],K3['v'],K4['v']);
    W:=W+KUTTA(K1['w'],K2['w'],K3['w'],K4['w']);
    X:=X+KUTTA(K1['x'],K2['x'],K3['x'],K4['x']);
    Y:=Y+KUTTA(K1['y'],K2['y'],K3['y'],K4['y']);
  AU[I]:=U;
  AV[I]:=V;
  AW[I]:=W;
  AX[I]:=X;
  END; {End of Outside Loop}

PRINT(AX,250,1,'S1',C'1');

FOR I:=1 to N DO
  BEGIN
  FOR J:=1 to 100 DO
    BEGIN
    RUNGE(U,V,W,X,Y,KAPPA,K1);
    RUNGE(U+0.5*K1['u'],V+0.5*K1['v'],W+0.5*K1['w'],X+0.5*K1['x'],
    Y+0.5*K1['y'],KAPPA,K2);
    RUNGE(U+0.5*K2['u'],V+0.5*K2['v'],W+0.5*K2['w'],X+0.5*K2['x'],
    Y+0.5*K2['y'],KAPPA,K3);
    RUNGE(U+K3['u'],V+K3['v'],W+K3['w'],X+K3['x'],Y+K3['y'],KAPPA,K4);
    U:=U+KUTTA(K1['u'],K2['u'],K3['u'],K4['u']);
    V:=V+KUTTA(K1['v'],K2['v'],K3['v'],K4['v']);
    W:=W+KUTTA(K1['w'],K2['w'],K3['w'],K4['w']);
    X:=X+KUTTA(K1['x'],K2['x'],K3['x'],K4['x']);
    Y:=Y+KUTTA(K1['y'],K2['y'],K3['y'],K4['y']);
    END; {End of Inside Loop}
  END; {End of Outside Loop}
```

```
FOR I:=1 to 250 DO
  BEGIN
    RUNGE(U,V,W,X,Y,KAPPA,K1):
    RUNGE(U+0.5*K1['u'],V+0.5*K1['v'],W+0.5*K1['w'],X+0.5*K1['x'],
    Y+0.5*K1['y'],KAPPA,K2):
    RUNGE(U+0.5*K2['u'],V+0.5*K2['v'],W+0.5*K2['w'],X+0.5*K2['x'],
    Y+0.5*K2['y'],KAPPA,K3):
    RUNGE(U+K3['u'],V+K3['v'],W+K3['w'],X+K3['x'],Y+K3['y'],KAPPA,K4 :
    U:=U+KUTTA(K1['u'],K2['u'],K3['u'],K4['u']):
    V:=V+KUTTA(K1['v'],K2['v'],K3['v'],K4['v']):
    W:=W+KUTTA(K1['w'],K2['w'],K3['w'],K4['w']):
    X:=X+KUTTA(K1['x'],K2['x'],K3['x'],K4['x']):
    Y:=Y+KUTTA(K1['y'],K2['y'],K3['y'],K4['y']):
  AU[I]:=U:
  AV[I]:=V:
  AW[I]:=W:
  AX[I]:=X:
  END: {End of Outside Loop}

PRINT(AX,250,1,'S2',C[2]):

FOR I:=1 to N DO
  BEGIN
  FOR J:=1 to 100 DO
    BEGIN
    RUNGE(U,V,W,X,Y,KAPPA,K1):
    RUNGE(U+0.5*K1['u'],V+0.5*K1['v'],W+0.5*K1['w'],X+0.5*K1['x'],
    Y+0.5*K1['y'],KAPPA,K2):
    RUNGE(U+0.5*K2['u'],V+0.5*K2['v'],W+0.5*K2['w'],X+0.5*K2['x'],
    Y+0.5*K2['y'],KAPPA,K3):
    RUNGE(U+K3['u'],V+K3['v'],W+K3['w'],X+K3['x'],Y+K3['y'],KAPPA,K4 :
    U:=U+KUTTA(K1['u'],K2['u'],K3['u'],K4['u']):
    V:=V+KUTTA(K1['v'],K2['v'],K3['v'],K4['v']):
    W:=W+KUTTA(K1['w'],K2['w'],K3['w'],K4['w']):
    X:=X+KUTTA(K1['x'],K2['x'],K3['x'],K4['x']):
    Y:=Y+KUTTA(K1['y'],K2['y'],K3['y'],K4['y']):
    END: {End of Inside Loop}
  END: {End of Outside Loop}

FOR I:=1 to 250 DO
  BEGIN
    RUNGE(U,V,W,X,Y,KAPPA,K1):
    RUNGE(U+0.5*K1['u'],V+0.5*K1['v'],W+0.5*K1['w'],X+0.5*K1['x'],
    Y+0.5*K1['y'],KAPPA,K2):
```

AD-A189 576 THEORY OF LASER COOLING AND SPECTROSCOPY OF HARMONICALLY TRAPPED SINGLE ATOMS(U) AIR FORCE INST OF TECH WRIGHT-PATTERSON AFB OH SCHOOL OF ENGINEERING 2/2

UNCLASSIFIED A L WELLS DEC 87 AFIT/DS/PH/87-5 F/G 7/4 NL

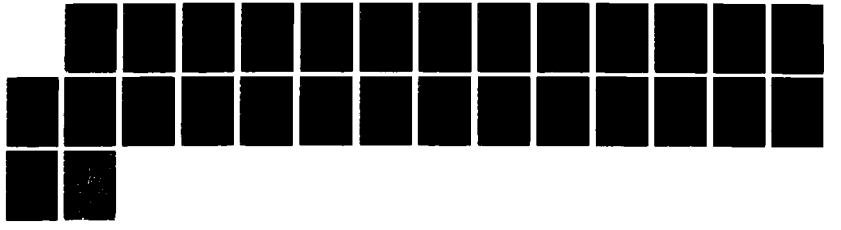

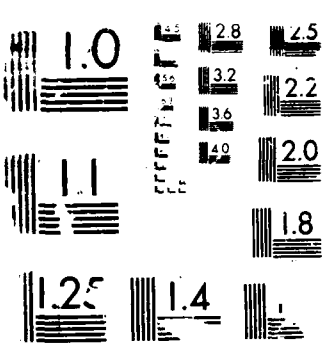
1.0
1.1
1.25
1.4
2.8
3.2
3.6
4.0
2.5
2.2
2.0
1.8

```
      RUNGE(U+0.5*K2['u'],V+0.5*K2['v'],W+0.5*K2['w'],X+0.5*K2['x'],
      Y+0.5*K2['y'],KAPPA,K3);
      RUNGE(U+K3['u'],V+K3['v'],W+K3['w'],X+K3['x'],Y+K3['y'],KAPPA,K4);
      U:=U+KUTTA(K1['u'],K2['u'],K3['u'],K4['u']);
      V:=V+KUTTA(K1['v'],K2['v'],K3['v'],K4['v']);
      W:=W+KUTTA(K1['w'],K2['w'],K3['w'],K4['w']);
      X:=X+KUTTA(K1['x'],K2['x'],K3['x'],K4['x']);
      Y:=Y+KUTTA(K1['y'],K2['y'],K3['y'],K4['y']);
    AU[I]:=U;
    AV[I]:=V;
    AW[I]:=W;
    AX[I]:=X;
    END; {End of Outside Loop}

PRINT(AX,250,1,'S3',C[3]);

FOR I:=1 to N DO
    BEGIN
    FOR J:=1 to 100 DO
      BEGIN
      RUNGE(U,V,W,X,Y,KAPPA,K1);
      RUNGE(U+0.5*K1['u'],V+0.5*K1['v'],W+0.5*K1['w'],X+0.5*K1['x'],
      Y+0.5*K1['y'],KAPPA,K2);
      RUNGE(U+0.5*K2['u'],V+0.5*K2['v'],W+0.5*K2['w'],X+0.5*K2['x'],
      Y+0.5*K2['y'],KAPPA,K3);
      RUNGE(U+K3['u'],V+K3['v'],W+K3['w'],X+K3['x'],Y+K3['y'],KAPPA,K4);
      U:=U+KUTTA(K1['u'],K2['u'],K3['u'],K4['u']);
      V:=V+KUTTA(K1['v'],K2['v'],K3['v'],K4['v']);
      W:=W+KUTTA(K1['w'],K2['w'],K3['w'],K4['w']);
      X:=X+KUTTA(K1['x'],K2['x'],K3['x'],K4['x']);
      Y:=Y+KUTTA(K1['y'],K2['y'],K3['y'],K4['y']);
      END; {End of Inside Loop}
    END; {End of Outside Loop}

FOR I:=1 to 250 DO
    BEGIN
      RUNGE(U,V,W,X,Y,KAPPA,K1);
      RUNGE(U+0.5*K1['u'],V+0.5*K1['v'],W+0.5*K1['w'] X+0.5*K1['x'],
      Y+0.5*K1['y'],KAPPA,K2);
      RUNGE(U+0.5*K2['u'],V+0.5*K2['v'],W+0.5*K2['w'],X+0.5*K2['x'],
      Y+0.5*K2['y'],KAPPA,K3);
      RUNGE(U+K3['u'],V+K3['v'],W+K3['w'],X+K3['x'],Y+K3['y'],KAPPA,K4);
      U:=U+KUTTA(K1['u'],K2['u'],K3['u'],K4['u']);
      V:=V+KUTTA(K1['v'],K2['v'],K3['v'],K4['v']);
```

```
        W:=W+KUTTA(K1['w'],K2['w'],K3['w'],K4['w']);
        X:=X+KUTTA(K1['x'],K2['x'],K3['x'],K4['x']);
        Y:=Y+KUTTA(K1['y'],K2['y'],K3['y'],K4['y']);
      AU[I]:=U;
      AV[I]:=V;
      AW[I]:=W;
      AX[I]:=X;
      END; {End of Outside Loop}

    PRINT(AX,250,1,'S4',C[4]);
    PRINT(C,4,2,'LnA',M[LOLA]);

    END;

  PRINT(M,LOLA,8,'Alpha vs. omega',C[5]);

    TEXTMODE(2);
    END.
```

II. Calculation of Steady State Values from Section IV.B.2.

```
    Program STEDSTAT:
{$U+}
{$I GRAPH.P}

LABEL 1,2;

CONST
  a10=1.25E+06;
  a21=1E+04;
  a32=1E+06;
  omega1=2E+07;
  omega2=1000;
  omega3=1E+07;
  d1=-2E+07;
  d2=2E+07;

TYPE
  complex=array [1..2] of real;
  buff=array[0..406] OF BYTE;
  number=array[1..250] of real;
  gob=array[1..250] of integer;
  title=string[20];

VAR
  BUFFER:buff;
  SAMPLE:byte;
  W1,W2,W3,PMIN,PPLUS,W,P0,P1,P2,P3:number;
  T:title;
  J,L,flag:integer;
  N1,N2,N3,N4,DET,
  ZE11,ZE12,ZE13,ZE21,ZE22,ZE23,ZE31,ZE32,ZE33:complex;
  M,DD,DELTA,
  Y11,Y12,Y13,Y21,Y22,Y23,Y31,Y32,Y33,
  AL11,AL12,AL13,AL21,AL22,AL23,AL31,AL32,AL33,
  D:real;

  I,IT1,IT2,IT3,IT4,IT5,IT6,IT7,ITS:complex;
  RT1,RT2,RT3,RT4,RT5,RT6,RT7,RTS:real;

PROCEDURE rkeyin (x:REAL;VAR z:COMPLEX);
 BEGIN
  z[1]:=x;
```

```
 z[2]:=0.0;
END;

PROCEDURE ikeyin (x:REAL;VAR z:COMPLEX);
BEGIN
 z[1]:=0.0;
 z[2]:=x;
END;

PROCEDURE keyin (z1:COMPLEX; VAR z2:COMPLEX);

BEGIN
 z2[1]:=z1[1];
 z2[2]:=z1[2];
END;

PROCEDURE negate(y:COMPLEX;VAR z:COMPLEX);
BEGIN
 z[1]:=-y[1];
 z[2]:=-y[2];
END;

PROCEDURE conjugate(y:COMPLEX;VAR z:COMPLEX);
BEGIN
 z[1]:=y[1];
 z[2]:=-y[2];
END;

FUNCTION modulus(y:COMPLEX):REAL;
BEGIN
 modulus:=SQR(y[1])+SQR(y[2]);
END;

PROCEDURE invert(y:COMPLEX;VAR z:COMPLEX);
VAR mag:REAL;
 BEGIN
  mag:=modulus(y);
  z[1]:=y[1]/mag;
  z[2]:=-y[2]/mag;
 END;

PROCEDURE add(y1,y2:COMPLEX;VAR z:COMPLEX);
BEGIN
 z[1]:=y1[1]+y2[1];
```

```
 z[2]:=y1[2]+y2[2];
END;

PROCEDURE subtract(y1,y2:COMPLEX;VAR z:COMPLEX);
 BEGIN
  z[1]:=y1[1]-y2[1];
  z[2]:=y1[2]-y2[2];
 END;

PROCEDURE multiply(y1,y2:COMPLEX;VAR z:COMPLEX);
 BEGIN
  z[1]:=y1[1]*y2[1]-y1[2]*y2[2];
  z[2]:=y1[1]*y2[2]+y1[2]*y2[1];
 END;

PROCEDURE divide(y1,y2:COMPLEX;VAR z:COMPLEX);
 VAR mag:REAL;w1,w2:COMPLEX;
  BEGIN
   mag:=modulus(y2);
   conjugate(y2,w1);
   multiply(y1,w1,w2);
   z[1]:=w2[1]/mag;
   z[2]:=w2[2]/mag;
  END;

PROCEDURE scalarmult(x:real;y:complex;VAR z:COMPLEX);
  BEGIN
   z[1]:=x*y[1];
   z[2]:=x*y[2];
  END;

PROCEDURE MINIMUM(num:number; VAR min:real);
   BEGIN
   min:=num[1];
   FOR J:=1 to 250 DO
     BEGIN
     IF num[J] < min THEN min:=num[J];
     END;
   END;

PROCEDURE MAXIMUM(num:number; VAR max:real);
   BEGIN
   max:=num[1];
   FOR J:=1 to 250 DO
```

```
    BEGIN
    IF num[J] > max THEN max:=num[J];
    END;
  END;

PROCEDURE SCALE(min,max,dx:real; num:number; VAR mark:gob);
  VAR s:real;
  BEGIN
  s:=(max-min)/180;
  FOR J:=1 to 250 DO
    BEGIN
    mark[J]:=round((num[J]-min)/s);
    END;
  END;

PROCEDURE PRINT(num:number; dx:real; T:title; VAR par:real);
  VAR min,max:real; mark:gob;
  BEGIN
  GRAPHMODE;
  DRAW(10,190,260,190,3);
  DRAW(10,190,10,10,3);
  DRAW(260,190,260,10,3);
  DRAW(10,10,260,10,3);

  FOR J:=1 TO 9 DO
    BEGIN
    L:=190-J*18;
    DRAW(10,L,13,L,3);
    END;

  FOR J:=1 TO 9 DO
    BEGIN
    L:=10+J*25;
    DRAW(L,190,L,187,3);
    END;

  MINIMUM(num,min);
  MAXIMUM(num,max);
  SCALE(min,max,dx,num,mark);
  GOTOXY(1,25);
  WRITE(min:10,'  ',max:10,'  ',(max-min):10);
  GOTOXY(1,1);
  WRITE(((max+min)/2):10,'    ',T);
```

```
    FOR J:=1 TO 249 DO
      BEGIN
      DRAW(10+J,190-mark[J],11+J,190-mark[J+1],3);
      END;

  READ(M);
  IF M=1 THEN
   BEGIN
    FOR J:=1 to 80 DO
     BEGIN
      GETPIC(BUFFER,4*(J-1),0,4*(J-1),200);
      WRITE(LST,#27,'@',#27,'1');
      WRITE(LST,#27,#75,#201,#0);
      FOR L:=1 to 201 DO
       BEGIN
        SAMPLE:=BUFFER[(L-1)+6];
        WRITE(LST,CHR(SAMPLE));
       END;
     END;

    WRITELN(LST,#11,#11,#11,#11,#11,#10,#10,#10,#10,#27,'@');
   END;

    END;

  BEGIN
   DD:=(d2-d1)/250;
   DELTA:=d1;

   WRITELN(LST,'d1=',d1,'  d2=',d2,'  deldel=',DD);
   WRITELN(LST,'Omega1=',omega1,'  Omega2=',omega2,'  Omega3=',omega3 :
   WRITELN(LST,'A10=',a10,'  A21=',a21,'  A32=',a32);
   WRITELN(LST,#11);

   IKEYIN(1,I);

   RT1:=omega1*omega1;
   RT2:=omega2*omega2;
   RT3:=omega3*omega3;

   N1[1]:=a21;
   N2[1]:=a32;
   N3[1]:=a10;
   N4[1]:=a10+a32;
```

```
FOR J:=1 to 250 DO
 BEGIN

 DELTA:=DELTA+DD:

 N1[2]:=2*DELTA;
 N2[2]:=2*DELTA;
 N3[2]:=2*DELTA;
 N4[2]:=2*DELTA:

 SCALARMULT(RT2*RT2,N2,IT1);
 MULTIPLY(IT1,N3,IT8);
                    {first term in DET}
 MULTIPLY(N1,N2,IT1);
 MULTIPLY(IT1,N3,IT2);

 SCALARMULT(RT1,N2,IT1);
 ADD(IT1,IT2,IT3);

 SCALARMULT(RT3,N3,IT1);
 ADD(IT1,IT3,IT2);

 SCALARMULT(RT2*a10,IT2,IT7);

 ADD(IT8,IT7,IT6);
                    {1st and 2nd terms in DET}
 MULTIPLY(N2,N3,IT1);
 MULTIPLY(IT1,N4,IT2);

 SCALARMULT(RT1,N3,IT1);
 ADD(IT1,IT2,IT3);

 SCALARMULT(RT3,N2,IT1);
 ADD(IT1,IT3,IT2);

 SCALARMULT(RT2*a32,IT2,IT7);

 ADD(IT6,IT7,IT8);
                    {1st, 2nd, and 3rd terms in DET}
 RKEYIN(RT1-RT3,IT1);
 MULTIPLY(N2,N4,IT2);
 ADD(IT1,IT2,IT3);
 SCALARMULT(RT1*a10*a32,IT3,IT7);
```

```
ADD(IT8,IT7,IT6);
                    {1st, 2nd, 3rd, and 4th terms in DET}
RKEYIN(RT3-RT1,IT1);
MULTIPLY(N3,N4,IT2);
ADD(IT1,IT2,IT3);
SCALARMULT(RT3*a10*a32,IT3,IT7);

ADD(IT6,IT7,IT8);
                    {1st,2nd,3rd,4th, and 5th terms in DET}
MULTIPLY(N2,N3,IT1);
MULTIPLY(IT1,N4,IT2);

SCALARMULT(RT1,N3,IT1);
ADD(IT1,IT2,IT3);

SCALARMULT(RT3,N2,IT2);
ADD(IT3,IT2,IT1);

SCALARMULT(a10*a32,N1,IT2);
MULTIPLY(IT1,IT2,IT3);

ADD(IT8,IT3,DET);           {DET}

RKEYIN(RT1-RT3,IT1);
MULTIPLY(N2,N4,IT2);
ADD(IT1,IT2,IT3);
SCALARMULT(RT1*a32,IT3,IT8);

RKEYIN(RT3-RT2,IT1);
MULTIPLY(N3,N4,IT2);
ADD(IT1,IT2,IT3);
SCALARMULT(RT3*a32,IT3,IT7);

ADD(IT8,IT7,IT6);

MULTIPLY(N1,N2,IT1);
MULTIPLY(IT1,N3,IT2);
SCALARMULT(RT1,N2,IT3);
ADD(IT2,IT3,IT1);
SCALARMULT(RT3,N3,IT2);
ADD(IT1,IT2,IT3);
SCALARMULT(RT2,IT3,IT7);
```

```
ADD(IT6,IT7,IT8);

MULTIPLY(N2,N3,IT1);
MULTIPLY(IT1,N4,IT2);
SCALARMULT(RT1,N3,IT1);
ADD(IT1,IT2,IT3);
SCALARMULT(RT3,N2,IT2);
ADD(IT2,IT3,IT1);
SCALARMULT(a32,N1,IT2);
MULTIPLY(IT1,IT2,IT7);

ADD(IT8,IT7,IT6);

SCALARMULT(omega1,I,IT1);
MULTIPLY(IT1,IT6,IT2);
DIVIDE(IT2,DET,ZE11);
Y11:=ZE11[2];                          {ZE11}

RKEYIN(RT1-RT3,IT1);
MULTIPLY(N2,N4,IT2);
ADD(IT1,IT2,IT3);
SCALARMULT(a32,IT3,IT1);
SCALARMULT(RT2,N2,IT2);
ADD(IT1,IT2,IT3);

SCALARMULT(omega1*RT2,I,IT1);
MULTIPLY(IT3,IT1,IT2);
DIVIDE(IT2,DET,ZE12);
Y12:=ZE12[2];                          {ZE12}

ADD(N2,N3,IT1);
MULTIPLY(I,IT1,IT2);
SCALARMULT(omega1*RT2*RT3,IT2,IT1);
DIVIDE(IT1,DET,ZE13);
Y13:=ZE13[2];                          {ZE13}

SCALARMULT(RT2,N2,IT8);
RKEYIN(RT1-RT3,IT1);
MULTIPLY(N2,N4,IT2);
ADD(IT1,IT2,IT3);
SCALARMULT(a32,IT3,IT1);
ADD(IT1,IT8,IT7);
MULTIPLY(I,IT7,IT8);
SCALARMULT(RT1*omega2,IT8,IT7);
```

```
DIVIDE(IT7,DET,ZE21);
Y21:=ZE21[2];                          {ZE21}

MULTIPLY(N2,N4,IT1);
SCALARMULT(a32,IT1,IT2);
RKEYIN(RT1*a32,IT1);
ADD(IT1,IT2,IT3);
SCALARMULT(RT2,N2,IT2);
ADD(IT3,IT2,IT1);
SCALARMULT(RT2,IT1,IT8);

SCALARMULT(a32,N4,IT1);
RKEYIN(RT2,IT2);
ADD(IT1,IT2,IT3);
SCALARMULT(RT3*a10,IT3,IT7);

ADD(IT8,IT7,IT6);

RKEYIN(RT1*a32,IT1);
SCALARMULT(RT2,N2,IT2);
ADD(IT1,IT2,IT3);
MULTIPLY(N2,N4,IT2);
SCALARMULT(a32,IT2,IT1);
ADD(IT1,IT3,IT2);
SCALARMULT(a10,N1,IT1);
MULTIPLY(IT1,IT2,IT7);

ADD(IT6,IT7,IT8);

SCALARMULT(omega2,I,IT1);
MULTIPLY(IT8,IT1,IT2);
DIVIDE(IT2,DET,ZE22);
Y22:=ZE22[2];                          {ZE22}

RKEYIN(RT3-RT1,IT1);
MULTIPLY(N1,N2,IT2);
ADD(IT1,IT2,IT3);
SCALARMULT(a10,IT3,IT2);
SCALARMULT(RT2,N2,IT1);
ADD(IT1,IT2,IT3);
SCALARMULT(omega2*RT3,I,IT2);
MULTIPLY(IT3,IT2,IT1);
DIVIDE(IT1,DET,ZE23);
Y23:=ZE23[2];                          {ZE23}
```

```
ADD(N2,N3,IT1);
SCALARMULT(-RT1*RT2*omega3.I,IT2);
MULTIPLY(IT1,IT2,IT3);
DIVIDE(IT3,DET,ZE31);
Y31:=ZE31[2];                          {ZE31}

RKEYIN(RT3-RT1,IT1);
MULTIPLY(N1,N2,IT2);
ADD(IT1,IT2,IT3);
SCALARMULT(a10,IT3,IT2);
SCALARMULT(RT2,N2,IT1);
ADD(IT1,IT2,IT3);
SCALARMULT(RT2*omega3.I,IT2);
MULTIPLY(IT3,IT2,IT1);
DIVIDE(IT1,DET,ZE32);
Y32:=ZE32[2];                          {ZE32}

RKEYIN(RT1-RT3,IT1);
MULTIPLY(N2,N4,IT2);
ADD(IT1,IT2,IT3);
SCALARMULT(RT1*a10,IT3,IT8);

RKEYIN(RT3-RT1,IT1);
MULTIPLY(N3,N4,IT2);
ADD(IT1,IT2,IT3);
SCALARMULT(RT3*a10,IT3,IT7);

ADD(IT8,IT7,IT6);

MULTIPLY(N2,N3,IT1);
MULTIPLY(IT1,N4,IT2);
SCALARMULT(RT1,N3,IT3);
ADD(IT2,IT3,IT1);
SCALARmult(RT3,N2,IT2);
ADD(IT1,IT2,IT3);
SCALARMULT(RT2,IT3,IT7);

ADD(IT6,IT7,IT8);

MULTIPLY(N2,N3,IT1);
MULTIPLY(IT1,N4,IT2);
SCALARMULT(RT1,N3,IT1);
ADD(IT1,IT2,IT3);
```

```
SCALARMULT(RT3,N2,IT2);
ADD(IT3,IT2,IT1);
MULTIPLY(IT1,N1,IT2);
SCALARMULT(a10,IT2,IT7);

ADD(IT8,IT7,IT6);

MULTIPLY(I,IT6,IT7);
SCALARMULT(omega3,IT7,IT8);
DIVIDE(IT8,DET,ZE33);
Y33:=ZE33[2];                          {ZE33}

AL11:=-a10/2+a21/4-2*omega1*Y11+omega2*Y21;
AL12:=a10+a21/2-2*omega1*Y12+omega2*Y22;
AL13:=a10/2-a21/4-2*omega1*Y13+omega2*Y23;

AL21:=(a10-2*a21+a32)/4-2*omega2*Y21+omega1*Y11+omega3*Y31;
AL22:=(-a10+2*a21+a32)/2-2*omega2*Y22+omega1*Y12+omega3*Y32;
AL23:=(-a10+2*a21+3*a32)/4-2*omega2*Y23+omega1*Y13+omega3*Y33;

AL31:=-a32/2+a21/4-2*omega3*Y31+omega2*Y21;
AL32:=-a32+a21/2-2*omega3*Y32+omega2*Y22;
AL33:=-3*a32/2-a21/4-2*omega3*Y33+omega2*Y23;

D:=AL11*(AL22*AL33-AL23*AL32)
  +AL12*(AL23*AL31-AL21*AL33)
  +AL13*(AL21*AL32-AL22*AL31);

W1[J]:=((a10-a21/2)*(AL22*AL33-AL23*AL32)
      +AL12*(AL23*(a32-a21/2)-(a21-a10/2-a32/2)*AL33)
      +AL13*((a21-a10/2-a32/2)*AL32-AL22*(a32-a21/2)))/(2*D);

W2[J]:=(AL11*((a21-a10/2-a32/2)*AL33-AL23*(a32-a21/2))
      +(a10-a21/2)*(AL23*AL31-AL21*AL33)
      +AL13*(AL21*(a32-a21/2)-(a21-a10/2-a32/2)*AL31))/(2*D);

W3[J]:=(AL11*(AL22*(a32-a21/2)-(a21-a10/2-a32/2)*AL32)
      +AL12*((a21-a10/2-a32/2)*AL31-AL21*(a32-a21/2))
      +(a10-a21/2)*(AL21*AL32-AL22*AL31))/(2*D);

PMIN[J]:=(1-W1[J]-2*W2[J]-W3[J])/2;

PPLUS[J]:=(1+W1[J]+2*W2[J]+W3[J])/2;
```

```
    W[J]:=PPLUS[J]-PMIN[J];

    P0[J]:=(1-3*W1[J]-2*W2[J]-W3[J])/4;
    P1[J]:=(1+W1[J]-2*W2[J]-W3[J])/4;
    P2[J]:=(1+W1[J]+2*W2[J]-W3[J])/4;
    P3[J]:=(1+W1[J]+2*W2[J]+3*W3[J])/4;

   END;

 PRINT(W1,DD,'W1 vs. Delta',M);
 PRINT(W2,DD,'W2 vs. Delta',M);
 PRINT(W3,DD,'W3 vs. Delta',M);

 PRINT(PMIN,DD,'Pminus vs. Delta',M);
 PRINT(PPLUS,DD,'Pplus vs. Delta',M);
 PRINT(W,DD,'W vs. Delta',M);

PRINT(P0,DD,'P0 vs. Delta',M);
PRINT(P1,DD,'P1 vs. Delta',M);
PRINT(P2,DD,'P2 vs. Delta',M);
PRINT(P3,DD,'P3 vs. Delta',M);


  TEXTMODE(2);
END.
```

III. Calculation of Adiabatic Variables from Section IV.B.3.

```
    Program ADIAB;
{$U+}
{$I GRAPH.P}

LABEL 1,2;

CONST
  a10=1E+06;
  a21=1;
  a32=1.25E+06;
  omega1=1E+07;
  omega2=1E+03;
  omega3=2E+07;
  d1=-2E+07;
  d2=2E+07;

TYPE
  complex=array [1..2] of real;
  buff=array[0..406] OF BYTE;
  number=array[1..250] of real;
  gob=array[1..250] of integer;
  title=string[20];

VAR
  BUFFER:buff;
  SAMPLE:byte;
  GAMMA1,GAM1GAM3,GAMMA2,GAM2GAM3,GAMMA3,ETA1,ETA2,ETA3,
     DELTA1,DELTA2,DELTA3,XI1,XI2,XI3,PSI,PHI,RP,RM,
     PP,PM,TEST:number;
  T:title;
  J,L,flag:integer;
  N1,N2,N3,N4,DET,
  R11,R13,R14,R21,R22,R23,R24,R25,R31,R32,R33,R34,R35,
     R41,R42,R43,R44,R45:complex;
  M,DD,DELTA,
  AL10,AL11,AL12,AL13,AL20,AL21,AL22,AL23,
  B11,B12,B21,B22,B,C10,C11,C12,C13,C20,C21,C22,C23,
  D:real;

  I,IT1,IT2,IT3,IT4,IT5,IT6,IT7,IT8:complex;
  RT1,RT2,RT3,RT4,RT5,RT6,RT7,RT8:real;
```

```
PROCEDURE rkeyin (x:REAL;VAR z:COMPLEX);
 BEGIN
  z[1]:=x;
  z[2]:=0.0;
 END;

PROCEDURE ikeyin (x:REAL;VAR z:COMPLEX);
 BEGIN
  z[1]:=0.0;
  z[2]:=x;
 END;

PROCEDURE keyin (z1:COMPLEX; VAR z2:COMPLEX);

 BEGIN
  z2[1]:=z1[1];
  z2[2]:=z1[2];
 END;

PROCEDURE negate(y:COMPLEX;VAR z:COMPLEX);
 BEGIN
  z[1]:=-y[1];
  z[2]:=-y[2];
 END;

PROCEDURE conjugate(y:COMPLEX;VAR z:COMPLEX);
 BEGIN
  z[1]:=y[1];
  z[2]:=-y[2];
 END;

FUNCTION modulus(y:COMPLEX):REAL;
 BEGIN
  modulus:=SQR(y[1])+SQR(y[2]);
 END;

PROCEDURE invert(y:COMPLEX;VAR z:COMPLEX);
 VAR mag:REAL;
  BEGIN
   mag:=modulus(y);
   z[1]:=y[1]/mag;
   z[2]:=-y[2]/mag;
  END;
```

```
PROCEDURE add(y1,y2:COMPLEX;VAR z:COMPLEX);
 BEGIN
  z[1]:=y1[1]-y2[1];
  z[2]:=y1[2]+y2[2];
 END;

PROCEDURE subtract(y1,y2:COMPLEX;VAR z:COMPLEX);
 BEGIN
  z[1]:=y1[1]-y2[1];
  z[2]:=y1[2]-y2[2];
 END;

PROCEDURE multiply(y1,y2:COMPLEX;VAR z:COMPLEX);
 BEGIN
  z[1]:=y1[1]*y2[1]-y1[2]*y2[2];
  z[2]:=y1[1]*y2[2]+y1[2]*y2[1];
 END;

PROCEDURE divide(y1,y2:COMPLEX;VAR z:COMPLEX);
 VAR mag:REAL;w1,w2:COMPLEX;
  BEGIN
   mag:=modulus(y2);
   conjugate(y2,w1);
   multiply(y1,w1,w2);
   z[1]:=w2[1]/mag;
   z[2]:=w2[2]/mag;
  END;

PROCEDURE scalarmult(x:real;y:complex;VAR z:COMPLEX);
  BEGIN
   z[1]:=x*y[1];
   z[2]:=x*y[2];
  END;

PROCEDURE MINIMUM(num:number; VAR min:real);
   BEGIN
   min:=num[1];
   FOR J:=1 to 250 DO
      BEGIN
      IF num[J] < min THEN min:=num[J];
      END;
   END;

PROCEDURE MAXIMUM(num:number; VAR max:real);
```

```
  BEGIN
  max:=num[1];
  FOR J:=1 to 250 DO
    BEGIN
    IF num[J] > max THEN max:=num[J];
    END;
  END;

PROCEDURE SCALE(min,max,dx:real; num:number; VAR mark:gob);
  VAR s:real;
  BEGIN
  s:=(max-min)/180;
  IF s=0 THEN s:=1;
  FOR J:=1 to 250 DO
    BEGIN
    mark[J]:=round((num[J]-min)/s);
    END;
  END;

PROCEDURE PRINT(num:number; dx:real; T:title; VAR par:real);
  VAR min,max:real; mark:gob;
  BEGIN
  GRAPHMODE;
  DRAW(10,190,260,190,3);
  DRAW(10,190,10,10,3);
  DRAW(260,190,260,10,3);
  DRAW(10,10,260,10,3);

  FOR J:=1 TO 9 DO
    BEGIN
    L:=190-J*18;
    DRAW(10,L,13,L,3);
    END;

  FOR J:=1 TO 9 DO
    BEGIN
    L:=10+J*25;
    DRAW(L,190,L,187,3);
    END;

  MINIMUM(num,min);
  MAXIMUM(num,max);
  SCALE(min,max,dx,num,mark);
  GOTOXY(1,25);
```

```
    WRITE(min:10,'  ',max:10,'  ',(max-min):10);
    GOTOXY(1,1);
    WRITE(((max-min)/2):10,'  ',T);

    FOR J:=1 TO 249 DO
      BEGIN
      DRAW(10+J,190-mark[J],11+J,190-mark[J+1],3);
      END;

  READ(M);
  IF M=1 THEN
   BEGIN
    FOR J:=1 to 80 DO
     BEGIN
      GETPIC(BUFFER,4*(J-1),0,4*(J-1),200);
      WRITE(LST,#27,'@',#27,'1');
      WRITE(LST,#27,#75,#201,#0);
      FOR L:=1 to 201 DO
       BEGIN
        SAMPLE:=BUFFER[(L-1)+6];
        WRITE(LST,CHR(SAMPLE));
       END;
     END;

    WRITELN(LST,#11,#11,#11,#11,#11,#10,#10,#10,#10,#27,'@');
   END;

    END;

  BEGIN
   DD:=(d2-d1)/250;
   DELTA:=d1;

   WRITELN(LST,'ADIAB');
   WRITELN(LST,'d1=',d1,'  d2=',d2,'  deldel=',DD);
   WRITELN(LST,'Omega1=',omega1,'  Omega2=',omega2,'  Omega3=',omega3);
   WRITELN(LST,'A10=',a10,'  A21=',a21,'  A32=',a32);
   WRITELN(LST,#11);

   IKEYIN(1,I);

   RT1:=omega1*omega1;
   RT2:=omega2*omega2;
   RT3:=omega3*omega3;
```

```
N1[1]:=a21:
N2[1]:=a32:
N3[1]:=a10-a21:
N4[1]:=a10-a32:

FOR J:=1 to 250 DO
 BEGIN

 DELTA:=DELTA+DD;

 N1[2]:=2*DELTA:
 N2[2]:=2*DELTA:
 N3[2]:=2*DELTA:
 N4[2]:=2*DELTA:

 RKEYIN(omega1/a10,IT1):
 MULTIPLY(IT1,I,R11);

 RKEYIN(-omega2/(2*a10),IT1):
 MULTIPLY(IT1,I,R13):

 MULTIPLY(R13,I,R14):

 MULTIPLY(N2,N3,IT1):
 MULTIPLY(IT1,N4,IT2):
 SCALARMULT(RT1,N3,IT3):
 ADD(IT2,IT3,IT1):
 SCALARMULT(RT3,N2,IT2):
 ADD(IT1,IT2,IT3):
 SCALARMULT(a32-a21,IT3,IT1):
 MULTIPLY(N2,N3,IT2):
 SCALARMULT(RT2,IT2,IT3):
 ADD(IT1,IT3,DET):

 MULTIPLY(N2,N4,IT1):
 RKEYIN(RT1,IT2):
 ADD(IT1,IT2,IT3):
 SCALARMULT(a32+a21,IT3,IT1):
 SCALARMULT(RT2,N2,IT2):
 ADD(IT1,IT2,IT3):
 SCALARMULT(-omega2/2,IT3,IT2):
 MULTIPLY(I,IT2,IT1):
 DIVIDE(IT1,DET,R21):
```

```
SCALARMULT(omega2*RT3,N2,IT1);
MULTIPLY(I,IT1,IT2);
DIVIDE(IT2,DET,IT3);
ADD(IT3,R21,R22);

SCALARMULT(-1,R21,R25);

MULTIPLY(N2,N4,IT1);
RKEVIN(RT1-RT3,IT2);
ADD(IT1,IT2,IT3);
SCALARMULT(a32-a21,IT3,IT1);
SCALARMULT(RT2,N2,IT2);
ADD(IT1,IT2,IT3);
SCALARMULT(omega1/2,IT3,IT1);
MULTIPLY(I,IT1,IT2);
DIVIDE(IT2,DET,R23);

MULTIPLY(I,R23,R24);

SCALARMULT(-RT2*omega3/2,N2,IT1);
MULTIPLY(I,IT1,IT2);
DIVIDE(IT1,DET,R31);

SCALARMULT(-1,R31,R35);

MULTIPLY(N2,N3,IT1);
MULTIPLY(IT1,N4,IT2);
SCALARMULT(RT3,N2,IT1);
ADD(IT1,IT2,IT3);
SCALARMULT(RT1,N3,IT2);
ADD(IT3,IT2,IT1);
SCALARMULT(omega3,IT1,IT2);
MULTIPLY(I,IT2,IT1);
DIVIDE(IT1,DET,IT2);
ADD(IT2,R31,R32);

ADD(N2,N3,IT1);
SCALARMULT(omega1*omega2*omega3/2,IT1,IT2);
MULTIPLY(I,IT2,IT1);
DIVIDE(IT1,DET,R33);

MULTIPLY(I,R33,R34);
```

```
RKEYIN(-omega1*omega2*omega3*(a21-a32)/2,IT1);
MULTIPLY(I,IT1,IT2);
DIVIDE(IT2,DET,R41);

SCALARMULT(-1,R41,R45);

SCALARMULT(-omega1*omega2*omega3,N3,IT1);
MULTIPLY(I,IT1,IT2);
DIVIDE(IT2,DET,IT1);
ADD(IT1,R41,R42);

MULTIPLY(N3,N4,IT1);
RKEYIN(RT3-RT1,IT2);
ADD(IT1,IT2,IT3);
SCALARMULT((a32+a21)/2,IT3,IT1);
SCALARMULT(RT2/2,N3,IT3);
ADD(IT1,IT3,IT2);
SCALARMULT(-omega3,IT2,IT1);
MULTIPLY(I,IT1,IT2);
DIVIDE(IT2,DET,R43);

MULTIPLY(I,R43,R44);

B11:=a10+2*omega1*R11[2]-omega2*R21[2];
B12:=a21/2-omega2*R22[2];
B21:=2*omega3*R31[2]-omega2*R21[2];
B22:=a32+a21/2+2*omega3*R32[2]-omega2*R22[2];

AL10:=-(a10-a21/2)/2;
AL20:=-(a32-a21/2)/2;
AL11:=(a10+a21/2+2*omega2*R25[2])/2;
AL21:=-a32/2+a21/4-2*omega3*R35[2]+omega2*R25[2];
AL12:=omega2*R23[2]-2*omega1*R13[2];
AL22:=omega2*R23[2]-2*omega3*R33[2];
AL13:=omega2*R24[2];
AL23:=omega2*R24[2]-2*omega3*R34[2];

B:=B11*B22-B12*B21;

C10:=(B22*AL10-B12*AL20)/B;
C20:=(B11*AL20-B21*AL10)/B;
C11:=(B22*AL11-B12*AL21)/B;
C21:=(B11*AL21-B21*AL11)/B;
C12:=(B22*AL12-B12*AL22)/B;
```

```
C22:=(B11*AL22-B21*AL12)/B:
C13:=(B22*AL13-B12*AL23)/B:
C23:=(B11*AL23-B21*AL13)/B:

GAMMA1[J]:=a21-2*omega1*(R23[2]+R21[2]*C12-R22[2]*C22
  -(omega2/a10)*(2*omega1*C12-omega2)
  -2*omega3*(R43[2]+R41[2]*C12-R42[2]*C22);

GAMMA2[J]:=a21-2*omega1*(R24[1]+R21[1]*C13-R22[1]*C23)
  +(RT2/a10)+2*omega3*(R44[1]-R41[1]*C13+R42[1]*C23);

GAMMA3[J]:=a21*(1-2*C21)-2*omega2*(R25[2]-R21[2]*C11-R22[2]*C21);

GAM1GAM3[J]:=GAMMA1[J]/GAMMA3[J];

GAM2GAM3[J]:=GAMMA2[J]/GAMMA3[J];

ETA1[J]:=-omega1*(R21[2]*C10+R22[2]*C20)+(omega1*omega2/a10)*C10
    +omega3*(R41[2]*C10+R42[2]*C20);

ETA2[J]:=omega1*(R21[1]*C10+R22[1]*C20)-omega3*(R41[1]*C10-R42[1]*C20);

ETA3[J]:=a21*(C20-0.5)-omega2*(R21[2]*C10+R22[2]*C20);

DELTA1[J]:=DELTA-omega1*(R24[2]+R21[2]*C13+R22[2]*C23)
    +(omega1*omega2/a10)*C13+omega3*(R44[2]+R41[2]*C13-R42[2]*C23);

DELTA2[J]:=DELTA-omega1*(R23[1]+R21[1]*C12+R22[1]*C22)
    +omega3*(R43[1]+R41[1]*C12+R42[1]*C22);

DELTA3[J]:=a21*C22-omega2*(R23[2]+R21[2]*C12+R22[2]*C22);

XI1[J]:=-omega1*(R25[2]+R21[2]*C11+R22[2]*C21)
    +(omega1*omega2/a10)*C11+omega3*(R45[2]+R41[2]*C11-R42[2]*C21);

XI2[J]:=omega1*(R25[1]+R21[1]*C11+R22[1]*C21)
    -omega3*(R45[1]+R41[1]*C11+R42[1]*C21);

XI3[J]:=a21*C23-omega2*(R24[2]+R21[2]*C13+R22[2]*C23);

RT5:=4/(GAMMA1[J]*GAMMA2[J]+4*DELTA1[J]*DELTA2[J]);

PHI[J]:=ETA3[J]
      +RT5*(DELTA3[J]*(0.5*GAMMA2[J]*ETA1[J]+DELTA1[J]*ETA2[J]
```

```
                -XI3[J]*(0.5*GAMMA1[J]*ETA2[J]-DELTA2[J]*ETA1[J]) :

PSI[J]:=0.5*GAMMA3[J]
        -RT5*(DELTA3[J]*(0.5*GAMMA2[J]*XI1[J]-DELTA1[J]*XI2[J])
            -XI3[J]*(0.5*GAMMA1[J]*XI2[J]-DELTA2[J]*XI1[J])):

RT4:=GAMMA1[J]*GAMMA2[J]*GAMMA3[J]/8-XI2[J]*DELTA1[J]*DELTA3[J]
   +XI1[J]*DELTA2[J]*XI3[J]-GAMMA2[J]*XI1[J]*DELTA3[J]/2
   -DELTA1[J]*DELTA2[J]*GAMMA3[J]/2-GAMMA1[J]*XI2[J]*XI3[J]/2:

   RM[J]:=0.5*(PSI[J]-PHI[J]):
   RP[J]:=0.5*(PSI[J]-PHI[J]):

   PP[J]:=RP[J]/(RP[J]-RM[J]):
   PM[J]:=RM[J]/(RP[J]-RM[J]):

TEST[J]:=PP[J]-PM[J]:

  END:

 PRINT(GAMMA1.DD,'GAMMA1 VS. Delta',M):
 PRINT(GAMMA2.DD,'GAMMA2 VS. Delta',M):
 PRINT(GAMMA3.DD,'GAMMA3 VS. Delta',M):
 PRINT(GAM1GAM3.DD,'GAM1/GAM3 VS. Delta',M):
 PRINT(GAM2GAM3.DD,'GAM2/GAM3 VS. Delta',M):
 PRINT(DELTA1.DD,'Delta1 VS. Delta',M):
 PRINT(DELTA2.DD,'Delta2 VS. Delta',M):
 PRINT(PHI.DD,'PHI VS. Delta',M):
 PRINT(PSI.DD,'PSI VS. Delta',M):
 PRINT(RM.DD,'RM VS. Delta',M):
 PRINT(RP.DD,'RP VS. Delta',M):
 PRINT(PM.DD,'PM VS. Delta',M):
 PRINT(PP.DD,'PP VS. Delta',M):
 PRINT(ETA3.DD,'ETA3 VS. Delta',M):
 PRINT(DELTA3.DD,'DELTA3 VS. Delta',M):
 PRINT(TEST.DD,'TEST VS. Delta',M):

  TEXTMODE(2):
END.
```

Vita

Ann Laurie Wells was born on 21 December 1957 in Opelika, Alabama, the daughter of Claude and Diana Conn. She graduated from high school in LaFayette, Alabama in 1976. She attended Auburn University in Auburn, Alabama on a four year AFROTC Scholarship and a four year National Merit Scholarship. She received a Bachelor of Science in Physics with high honors and was commissioned in the Air Force on 6 June 1980. She was a Distinguished Graduate of Auburn's AFROTC program. She was assigned to the Air Force Weapons Laboratory, Kirtland AFB, New Mexico where she worked with the Particle Beam Group, part of the Advanced Concepts Branch. In June 1983 she entered the Air Force Institute of Technology and received a Master of Science in Engineering Physics in December of 1984. She was a Distinguished Graduate of the AFIT Master's program.

UNCLASSIFIED
SECURITY CLASSIFICATION OF THIS PAGE

AD-A189 576

REPORT DOCUMENTATION PAGE

Form Approved
OMB No. 0704-0188

1a. REPORT SECURITY CLASSIFICATION: UNCLASSIFIED	1b. RESTRICTIVE MARKINGS
2a. SECURITY CLASSIFICATION AUTHORITY	3. DISTRIBUTION/AVAILABILITY OF REPORT: Approved for public release; distribution unlimited.
2b. DECLASSIFICATION/DOWNGRADING SCHEDULE	
4. PERFORMING ORGANIZATION REPORT NUMBER(S): AFIT/DS/PH/87-5	5. MONITORING ORGANIZATION REPORT NUMBER(S)
6a. NAME OF PERFORMING ORGANIZATION: Air Force Inst. of Tech. WPAFB, OH 45433-6583 / 6b. OFFICE SYMBOL (If applicable): AFIT/ENP	7a. NAME OF MONITORING ORGANIZATION
6c. ADDRESS (City, State, and ZIP Code)	7b. ADDRESS (City, State, and ZIP Code)
8a. NAME OF FUNDING/SPONSORING ORGANIZATION / 8b. OFFICE SYMBOL (If applicable)	9. PROCUREMENT INSTRUMENT IDENTIFICATION NUMBER
8c. ADDRESS (City, State, and ZIP Code)	10. SOURCE OF FUNDING NUMBERS: PROGRAM ELEMENT NO. / PROJECT NO. / TASK NO / WORK UNIT ACCESSION NO.

11. TITLE (Include Security Classification): See Box 19

12. PERSONAL AUTHOR(S): Ann Laurie Wells, B.S., M.S., Capt, USAF

13a. TYPE OF REPORT	13b. TIME COVERED	14. DATE OF REPORT (Year, Month, Day)	15. PAGE COUNT
PhD Dissertation	FROM _____ TO _____	1987 December	111

16. SUPPLEMENTARY NOTATION

17. COSATI CODES			18. SUBJECT TERMS (Continue on reverse if necessary and identify by block number)
FIELD	GROUP	SUB-GROUP	Quantum Physics, Trapping, Ion Trapping, Laser Cooling, Lamb-Dicke Limit, Quadrupole Trap
20	10		

19. ABSTRACT (Continue on reverse if necessary and identify by block number)

Title: THEORY OF LASER COOLING AND SPECTROSCOPY OF HARMONICALLY TRAPPED SINGLE ATOMS

Research Chairman: Richard J. Cook, Major, USAF

Approved for public release: IAW AFR 190-1
LYNN E. Wolaver 31 Dec 87
Dean for Research and Professional Development
Air Force Institute of Technology (AU)
Wright-Patterson AFB OH 45433-6583

20. DISTRIBUTION/AVAILABILITY OF ABSTRACT	21. ABSTRACT SECURITY CLASSIFICATION
☐ UNCLASSIFIED/UNLIMITED ☒ SAME AS RPT. ☐ DTIC USERS	UNCLASSIFIED

22a. NAME OF RESPONSIBLE INDIVIDUAL	22b. TELEPHONE (Include Area Code)	22c. OFFICE SYMBOL
Won B. Roh	(513) 255-4498	AFIT/ENP

DD Form 1473, JUN 86 — Previous editions are obsolete. — SECURITY CLASSIFICATION OF THIS PAGE: UNCLASSIFIED

Abstract

The problem of laser cooling of a single ion or atom in a harmonic trap was considered. A simple theory of sideband cooling has been developed. In the limit that the particle's secular motion can be treated semiclassically, the theory allows the calculation of a logarithmic cooling rate either numerically or, for two special cases, analytically. The theory could be used to optimize the parameters of a cooling experiment.

The spectroscopy of a single atom in the ladder configuration has been treated theoretically. A dressed atom approach was used to provide qualitative information about the system. The optical Bloch equations for the four level system in the rotating wave approximation were developed and solved for steady state. The Bloch equations were also solved in the adiabatic approximation and upward and downward transition rates were extracted from this treatment.

END

DATE

3-88

DTIC